Regulation of the Gene Encoding Thrombin-Activable Fibrinolysis Inhibitor in Non-Hepatic Cells

By

JOELLEN HSUAN-HSIEN LIN

A thesis submitted to the Graduate Program in Biochemistry

in the Department of Biomedical & Molecular Sciences

in conformity with the requirements for the

Degree of Doctor of Philosophy

Queen's University

Kingston, Ontario, Canada

September, 2011

For my wonderful family,

Tom Lin, Sophie Chuang, Sandy Lin and Mathieu Garand

Tomorrow, we continue sailing forward.

Abstract

Thrombin-activable fibrinolysis inhibitor (TAFI) is a carboxypeptidase B-like pro-enzyme that, once activated, attenuates fibrinolysis. TAFIa also possesses anti-inflammatory properties. Although liver is the main source of plasma TAFI, platelet-derived TAFI has also been reported. An alternatively spliced TAFI variant resulted from the skipping of exon 6 and a 52-base deletion in exon 10 of *CPB2* mRNA (Δ6+10) was described to be brain specific. This TAFI variant is reputed to possess a secretase-like activity that cleaves β-amyloid precursor protein to form β-amyloid, a process involved in the onset of Alzheimer's disease.

In this thesis, we report the identification of *CPB2* mRNA and TAFI protein in various vascular and inflammatory cells. Specifically, we describe the expression of *CPB2* mRNA in the megakaryocytic cell lines MEG-01 and Dami, the monocytic cell line THP-1, and peripheral blood mononuclear cells. TAFI protein was detected in differentiated Dami and THP-1 cells.

We next describe the effect of external stimuli such as phorbol myristate acetate (PMA) on *CPB2* expression in Dami and THP-1 cells. We found that PMA treatment increases both *CPB2* mRNA abundance and promoter activity in Dami cells, and decreases both *CPB2* mRNA abundance and promoter activity in THP-1 cells. Deletion analysis of the *CPB2* promoter indicated cell-type specific regulation of *CPB2* gene expression.

Finally, we evaluated the expression of alternatively spliced *CPB2* mRNA variants in hepatic and non hepatic cells. We found that exon 6 skipping variants are expressed in all cell types of interest. The variant previously reported to be brain specific was also found to be expressed in platelets. We found that the alternatively spliced TAFI variants accumulated inside the cells in a non-secretable, hypoglycosylated form and showed no carboxypeptidase activity.

Taken together, this thesis provides further evidence supporting the hypothesis that platelet-derived TAFI is originated from *CPB*2 gene expression in megakaryocytes. Moreover, our data imply a potential for site-specific anti-inflammatory control provided by macrophage-derived TAFI. Alternative splicing of the *CPB2* mRNA may give rise to variants with an intracellular role, perhaps as a peptidase chaperone, and may modulate the synthesis of secretable TAFI.

Acknowledgements

I would like to express my sincere gratitude to my supervisors Drs. Marlys L. Koschinsky and Michael B. Boffa for giving me the opportunity to work in their laboratories, first at Queen's University in Kingston then at the University of Windsor in Windsor, throughout the course of my almost 8 years of research training. I will always remember Dr. Koschinsky being open-minded about new ideas, embracing our individualities, encouraging creativity, and having high tolerance for differences in opinion--key ingredients in making science fun and meaningful. Drs. Colin Funk and Bruce Hill and Diane Sommerfeld have also provided advice and encouragement over the years. I would also like to thank Dr. Lev Becker for inspiration in the early stage of my career, past MLK and MBB lab members, particularly Dr. Taewoo Cho, Dr. John Tra, Steven Schadinger, Dainn Andrews, Sue Johnston, and Curtis Noordhof for fruitful discussions and great times in and outside of the lab. Furthermore, I would like to thank our assistant Branislava Zagorac for her incredible hard work, so we can go full throttle in completing projects with tight deadlines. Big thanks to other members of MLK/MBB lab, Andrew Craig, Nicole Feric, Tanya Marar, Dragana Novakovic, Rocco Romagunolo, and Corey Scipione for advice and support during difficult times, and for making MLK/MBB lab the craziest and the funniest lab my husband and I have ever been part of. Thanks to David, Skye, Kisely and Carter Barbic for their friendships. This work would be impossible without the care from my husband Dr. Mathieu Garand, who always makes sure that I am well fed, well rested and well prepared for any challenges ahead. Finally, to my parents and sister, Tom Lin, Sophie Chuang and Sandy Lin, thank you for always being there for me and Mat.

Table of Contents

List of Figures

Chapter 1: General introduction

Chapter 2: Identification of human thrombin-activatable fibrinolysis inhibitor in vascular and inflammatory cells

Chapter 3: Regulation of *CPB2* gene expression in megakaryocytes, platelets, and monocyte /macrophage cells

Chapter 4: *CPB2* mRNA undergoes alternative splicing event in a variety of cell types

Chapter 5: General Discussion

List of Tables

Chapter 2: Identification of human thrombin-activatable fibrinolysis inhibitor in vascular and inflammatory cells

Chapter 3: Regulation of *CPB2* gene expression in megakaryocytes, platelets, and monocyte /macrophage cells

Chapter 4: *CPB2* mRNA undergoes alternative splicing events in a variety of cell types

List of Abbreviations

3'UTR	3'-Untranslated Region
6-FAM	6-carboxyfluorescein
APC	activated Protein C
APP	β-amyloid precursor protein
ATCC	American Type Culture Collection
ATIII	antithrombin III
BCA assay	Bicinchoninic Acid assay
BD	Becton, Dickinson and company
BHK	Baby Hamster Kidney cells
BM	Bone Marrow
BMMNC	Bone Marrow Mononuclear Cells
BSA	Bovine Serum Albumin
C/EBP	CCAAT/enhancer-binding protein
CAD	Coronary Artery Disease
CFTB	Calcium-free Tyrode's Buffer
CPB2	Carboxypeptidase B2
CPR	Carboxypeptidase R (arginine)
CPU	'Unstable' Carboxypeptidase
DAPI	4', 6-diamidino-2-phenylindole
Desafib X	minimally Degraded fibrin
DNA	Deoxyribonucleic Acid

ECM	Extracellular Matrix
EDTA	Ethylenediaminetetraacetic Acid
EGM-2	Endothelial cell Growth Medium-2
EGM-2 MV	Microvascular Endothelial cell Growth Medium-2
EGTA	Ethylene Glycol Tetraacdtic Acid
EMSA	Electrophoretic Mobility Shift Assay
ER	Endoplasmic Reticulum
FBS	Fetal Bovine Serum
FDPs	Fibrin Degradation Products
Fluo-Pg	Fluorescein-labeled Plasminogen
FOG-1	Friend of GATA-1
GE	General Electric company
GPIIb	Glycoprotein IIb
GR	Glucocorticoid Receptor
GRE	Glucocorticoid Response Element
HBCPB	Human Brain carboxypeptidase B
HBS	HEPES-buffered saline
HBSS	Hanks' Balanced Salt Solution
HCAEC	primary Human Coronary Artery Endothelial Cells
HEPES	4-(2-Hydroxyethyl)-1-Piperazineethanesulfonic acid
HNF-1	Hepatic Nuclear Factor-1
HTB	HEPES-Tyrode's Buffer
HUVECs	Human Umbilical Vein Endothelial Cells
IFN-γ	Interferon-γ

II	Prothrombin
IIa	Thrombin
IL	Interleukin
ISFP	International Congress on Fibrinolsysis and Proteolysis
LPS	Lipopolysaccharide
MI	Myocardial Infarction
MMPs	Matrix Metalloproteinases
NET	NaCl-EDTA-Tris buffer
NF-Y	Nuclear Factor-Y
NF-κB	Nuclear Factor kapa-light-chain-enhancer of activated B cells
NMD	Nonsense-Mediated mRNA Decay
Opn	Osteopontin
ORF	Open Reading Frame
PAI-1	Plasminogen Activator Inhibitor-1
PBMNC	Peripheral Blood Mononuclear Cells
PBS	Phosphate-Buffered Saline
PC	Protein C
PCR	polymerase chain reaction
PF4	Platelet Factor 4
PIPES	Piperazine-N,N'-bis 2-Ethanesulfonic acid
PMA	Phorbol Myristate Acetate
PNGase F	N-Glycosidase F
PPAck	D-Phe-Pro-Arg-chloromethylketone
pTAFI	plasma TAFI

PTCI	Potato Tuber Carboxypeptidase Inhibitor
PVDF	Polyvinylidene Fluoride
qRT-PCR	real-time quantitative RT-PCR
RFU	Relative Fluorescence Units
RNA	Ribonucleic Acid
RPMI	Roswell Park Memorial Institute medium
rTAFI	recombinant TAFI
RT-PCR	reverse transcription polymerase chain reaction
SDS-PAGE	Sodium Dodecyl-Sulfate Polyacrylamide Gel Electrophoresis
SMCs	(primary human coronary artery) Smooth Muscle Cells
SmGM-2	Smooth muscle Growth Medium-2
SNPs	Single Nucleotide Polymorphisms
SRCR	Scavenger Receptor Cyctein-Rich
T3	Triiodothyronine
TAFI	Thrombin Activable Fibrinolysis Inhibitor
TAFIa	activated Thrombin Activable Fibrinolysis Inhibitor
TAFIai	inactivated TAFIa
TBSS	Tris Buffered Saline Solution
TCI	Tick Carboxypeptidase Inhibitor
TF	Tissue Factor
TFPI	Tissue Factor Pathway Inhibitor
TM	Thrombomodulin
TNFα	Tissue Necrosis Factor α
tPA	tissue-type Plasminogen Activator

TPO	thrombopoietin
TR	Thyroid Hormone Receptor
TRE	Thyroid Hormone Response Element
uPA	urokinase-type Plasminogen Activator
Va	activated Factor V
VIIa	activated Factor VII
vWf	von Willebrand factor
Xa	activated Factor X

Preface

This thesis was written in manuscript format, according to the regulations outlined in the Queen's University School of Graduate Studies and Research Guideline. Chapter two has been published in the *Thrombosis and Haemostasis*. Parts of Chapter three (Figures 11-12, Table 3) have been published in the *Journal of Thrombosis and Haemostasis*. Chapter four is currently being prepared for submission. The contributions of others in each study are outlined in the statement of co-authorship preceding each chapter.

Chapter 1: General introduction

1.1 TAFI as a molecular link between hemostasis, fibrinolysis, and inflammation

Hemostasis is a tightly regulated process that possesses the ability to induce the rapid and localized formation of a hemostatic plug at the site of vascular injury (1), while maintaining the fluidity of blood at sites remote from the injury. Normal hemostasis is controlled by the balance between coagulant and fibrinolytic mechanisms to prevent inappropriate clotting. Thrombin activable fibrinolysis inhibitor (TAFI) is a carboxypeptidase B-like pro-enzyme that, upon activation by thrombin (IIa) or the thrombin/thrombomodulin complex (IIa/TM), attenuates fibrinolysis; therefore, TAFI serves as a molecular link between coagulation and fibrinolysis (2).

Plasma TAFI antigen levels vary significantly between individuals. Moreover, this variation has been associated with risk of myocardial infarction, ischemic stroke, and venous thromboembolism. Therefore, TAFI has been implicated as a risk factor for thrombotic and atherothrombotic disorders. Since genetic factors such as single nucleotide polymorphisms (SNPs) account for only 25% of the total variation (3), there is clearly an important role for external stimuli in affecting *CPB2* gene regulation. TAFI was first described as a blood plasma protein; like most plasma proteins, particularly those factors involved in coagulation and fibrinolysis, the liver has been implicated as the source. However, emerging data from our laboratory and others has challenged the initial dogma of TAFI as being restricted to a role in regulating the balance between coagulation and fibrinolysis. Indeed, TAFI has also been identified in human hippocampus and platelets; TAFI mRNA has been detected in the Dami (megakaryoblastic) cell line, human umbilical vein endothelial cells (HUVECs), and adipocytes of patients with type 2 diabetes (4-6). Thus, evidence is emerging that TAFI may be expressed in

cell types other than hepatocytes, and these findings in turn suggest novel functions for the TAFI pathway in addition to the regulation of fibrin deposition. Interactions between coagulation and inflammation are also important when facing acute challenges such as severe infection or trauma. TAFI has been suggested to play a role in the vascular response to inflammation as TAFIa inactivates pro-inflammatory mediators such as IIa-cleaved Osteopontin (Opn), and activates the anti-inflammatory chemoattractant, plasmin-cleaved chemerin (7). Thus, it is becoming apparent that TAFI plays a broader role in host defence. The work in this thesis is aimed at enhancing our understanding of this role through discovery of novel sites of TAFI synthesis and elucidation of the factors that regulate expression of the gene encoding TAFI.

1.1.1 Cell-based model of hemostasis

The function of hemostasis is to prevent excessive blood loss by forming appropriately localized blood clots while maintaining the fluidity of blood at sites away from the injury. The coagulation system consists of two cascades of zymogen to enzyme conversions that converge at the step of prothrombin activation by a prothrombinase complex of Factor Xa, Factor Va, Ca^{2+} ions, and positively charged phospholipids. While the traditional "cascade" model based on *in vitro* data has served to improve our understanding of coagulation since its development in the 1960s, it does not explain many *in vivo* observations. For example, the classical model does not explain why the activation of factor X by the "extrinsic" pathway cannot compensate for a deficiency of Factor VIII or Factor IX from the "intrinsic" pathway, resulting in haemophilia A or B, respectively. Similarly, patients lacking factor VII from the "extrinsic" pathway have a bleeding tendency despite the fact that their "intrinsic" system is intact (1;8).

Recently, a cell-based model of hemostasis was proposed to better explain the clinical data, emphasizing that the localized cell surface plays an important role in controlling coagulation (8). In this model, coagulation occurs in three overlapping steps: initiation, amplification and propagation (Fig.1). Initiation phase starts with the exposure of tissue factor (TF) from the TF bearing cells, which are typically found outside of the vasculature, to the blood. Factor VII is activated when bound to TF. The TF/VIIa complex then activates a small amount of Factor IX and X to become Factor IXa and Xa, respectively. Factor Xa subsequently activates Factor V and form a Xa/Va complex on the surface of the TF bearing cells and converts a small amount of prothrombin (II) to IIa. The formation of IIa sets the stage for the amplification phase.

During the amplification phase, the small amount of IIa generated from the initiation phase activates platelets, which then have the ability to increase their adhesion on the endothelial cells and expose binding sites and receptors for clotting factors. In addition, the small amount of IIa produced starts the formation of fibrin by cleavage of fibrinogen molecules. At the same time, IIa activates Factor V, VIII and XI. Von Willebrand Factor (vWF) is also cleaved by IIa to help the formation of Factor VIIIa. At the end of the amplification phase, activated platelets have Factor Va, VIIIa, and Xa bound to their surfaces. Factor IXa, generated either from the initiation phase or from XIa on the platelet surface, forms a complex with Factor VIIIa to generate Factor Xa. Factor Xa then form a complex with its co-factor Va on the platelet surface to convert II to IIa (Fig. 1) (1;8). The propagation phase occurs on the surface of platelets and is characterized by the burst of IIa production that helps consolidate the fibrin clot through a variety of mechanisms including the activation of Factor XIII, which catalyses the formation of isopeptide bond cross-links between fibrin strands, as well as the activation of TAFI.

1.1.2 Anticoagulant and fibrinolytic systems

Coagulation needs to be tightly controlled in order to prevent inappropriate propagation that can abrogate proper circulation. Anticoagulant systems including TF pathway inhibitor (TFPI), activated protein C (APC)/protein S complex, and antithrombin III (ATIII) are in place to keep coagulation under control (1;8). TFPI binds and inhibits the TF-FVIIa complex, thereby inhibiting coagulation in the vicinity of the intact endothelium (8). ATIII is a protease inhibitor that inhibits activated coagulation factors IIa, IXa, and Xa (1). Thrombomodulin (TM) is an endothelial membrane protein that, when bound to IIa, changes the substrate specificity of IIa such that it no longer recognizes fibrinogen (2), but instead cleaves protein C to form the anticoagulant enzyme APC. APC forms a complex with its cofactor protein S and down-regulates further IIa production by cleaving and inactivating factor Va and VIIIa (2). In addition to its anticoagulant activity, APC was demonstrated both *in vitro* and *in vivo* to possess pro-fibrinolytic activity. However, further analysis of this phenomenon by Bajzar and Nesheim demonstrated that APC does not possess intrinsic profibrinolytic properties, but rather, through its anticoagulant function, down-regulates the activation of an anti-fibrinolytic factor in plasma, which in turn results in enhanced fibrinolysis (9). This anti-fibrinolytic factor was ultimately found to be TAFI.

In addition to anti-coagulants that slow down the clot formation, there exists another system, the fibrinolytic system, that removes clots once the repair of damaged tissue occurs and helps to maintain the fluidity of blood. The fibrinolytic system has evolved to lyse fibrin clots to form soluble fibrin degradation products (FDPs), thereby preventing undesirable thrombotic events (Fig. 1). The formation of fibrin by IIa allows the binding of tissue-type plasminogen activator (tPA) and plasminogen to fibrin as a ternary complex, consequently enhancing the activation of plasminogen to form plasmin. Plasmin then lyses the blood clot by converting fibrin

to soluble FDPs (2). As such, fibrin is not only the ultimate substrate of the fibrinolytic system; it is also an essential cofactor in this system. In the absence of fibrin, activation of plasminogen by tPA does not occur at a physiologically relevant rate. Partial degradation of fibrin by plasmin yields a form of fibrin (fibrin') that contains newly-exposed carboxyl-terminal lysine residues. This fibrin' possesses 3-fold better cofactor activity for plasminogen activation than native fibrin (2). Thus, the formation of fibrin' by plasmin creates a positive feedback loop in the fibrinolytic cascade. Plasminogen can also be activated by urokinase-type plasminogen activator (uPA). The ability of tPA, but not uPA, to bind to fibrin makes tPA the major activator of plasminogen in the fibrinolytic cascade.

Activated TAFI (TAFIa) attenuates fibrinolysis by removing the carboxyl-terminal lysine residues from fibrin' to form fibrin". This form of fibrin has a cofactor activity for tPA-mediated plasminogen activation that is several orders of magnitude below that of even native fibrin (2). Hence, TAFIa attenuates fibrinolysis by suppressing fibrin cofactor activity and positive feedback in fibrinolysis. TAFI is activated by the terminal product of the coagulation cascade (IIa/TM complex) and TAFIa directly acts on fibrin' to attenuate fibrinolysis; thus, TAFI functions as a direct molecular link between the two systems, and plays a key role in the balance between the deposition and removal of the fibrin clot (2;9).

1.2 The *CPB2* gene and the properties of TAFI

1.2.1 The *CPB2* gene

The human gene encoding TAFI, *CPB2*, is located on chromosome 13 (13q14.11) and contains 11 exons and 10 introns spanning 48 kb in length (10-12) (Fig. 2). A total of 19 single

nucleotide polymorphisms (SNPs) have been reported with ten in the 5'-flanking region, six in the coding region and three in the 3' flanking region of the gene (10). Four major haplotypes represent the segregation of these polymorphisms as they occurr in the population. All four haplotypes have different *CPB2* mRNA stabilities with H1 being the most stable, followed by H3, H2, and H4 (13). Ten potential liver transcription factor binding sites in the proximal region of human TAFI promoter have also been identified (14) (Fig. 3). Several potential mechanisms for the regulation of hepatic *CPB2* gene expression are discussed in section 1.5 below.

1.2.2. The properties of TAFI

TAFI is a basic carboxypeptidase precursor that, once activated, removes carboxyl-terminal arginine and lysine residues from proteins and peptide substrates (15). The catalytic domain of TAFI has 48% sequence identity with the B-type carboxypeptidases and less conserved activation peptides (~20%) (16). TAFI was first functionally characterized by Bajzar *et al.* (17), and was also independently discovered by three other groups. As such, TAFI is also known as plasma carboxypeptidase B (15), pro-carboxypeptidase R (for arginine) or U (for unstable) (18;19). As described above, activated TAFI (TAFIa) attenuates fibrinolysis by removing the carboxyl-terminal lysine residues from fibrin' to form fibrin". This modification decreases the fibrin cofactor activity for the tPA-mediated positive feedback loop of plasminogen activation, thus, attenuating fibrinolysis (2). Fibrin' also increases the conversion of Glu-plasminogen to Lys-plasminogen, the latter form being 20-fold better substrate for tPA-mediated activation. Therefore, TAFIa has another way to attenuate fibrinolysis, through the fibrin' to fibrin" modification, and the subsequent decreased formation of Lys-plasminogen. Along the

same line, when plasmin binds to fibrin or fibrin', it confes protection from circulating α2-antiplasmin; removal of carboxyl-terminal lysine residues by TAFIa diminish plasmin-fibrin interaction, hence reduced protection of plasmin from α2-antiplasmin.

The inactivity of the zymogen, TAFI, is thought to be the result of steric interference by the activation peptide (16). Some carboxypeptidases have zymogen activity against small substrates because the active site is pre-formed. Indeed, TAFIa cleaves furylacryloyl azoformyl-lysine/arginine. In 2007, Valnickova and coworkers (20) reported that TAFI zymogen is an active enzyme exhibiting an 18-fold lower k_{cat}/K_m ratio than that of the TAFIa, and that TAFI zymogen is capable of significantly down regulating fibrinolysis. This claim generated much discussion in the field with two opposite views. Foley and coworkers (21), in the subsequent year, provided evidence against the claim of Valnickova and coworkers by showing that potato tuber carboxypeptidase inhibitor (PTCI) has no effect on TAFI zymogen and that TAFI zymogen has no effect on the FDPs-based TAFIa assay (22). The authors concluded that even though the TAFI zymogen is effective in cleaving small peptide substrates, it is not able to cleave macromolecules such as fibrin degradation products. As such, the TAFI zymogen does not play a significant role in attenuating fibrinolysis (21). The TAFI zymogen activity detected by Valnickova and coworkers was likely due to the small but significant activation of TAFI that can be mediated by IIa in the absence of TM.

The plasma TAFI zymogen is composed of 401 amino acids with a theoretical molecular mass of ~48 kDa that migrates on a SDS-PAGE with an apparent molecular mass of ~60 kDa due to glycosylation (Fig. 2) (17). Upon activation, TAFIa migrates on SDS-PAGE with a molecular mass of ~35 kDa due to the loss of the N-terminal peptide containing four N-linked oligosaccharides (Fig. 2) (23). There are a total of five potential N-glycosylation sites in human

TAFI with four located in the activation peptide (Asn22, Asn51, Asn63, Asn86) and one in the catalytic domain (Asn219) (23). The glycosylation site Asn219 is in close proximity to the proposed substrate binding site (Arg214, Arg217, Lys218) and both glycosylated (4 different types of glycans) and unglycosylated forms were purified. Thus, the authors suspected that the glycosylation pattern in this region may play a role in regulating the binding of substrates to TAFIa (glycosylation depicted in Fig.2) (23). In addition, Valnickova and coworkers identified a small percentage of glycosylated TAFI species that contained bisecting N-acetylglucosamne (GlcNAc) groups. Attachment of the bisecting GlcNAc is catalyzed by the enzyme β-D-mannoside β-1,4 N-acetylglucosaminyltransferase III (GnT-III) and it serves as a stop signal for further addition of glycans by other glycosyltransferases. However, only a very low amount of GnT-III is expressed in the liver (24), suggesting that the bisecting GlcNac form of TAFI found in plasma most likely originated from cell types other than hepatocytes (23). The crystal structure of TAFI was published by Marx *et al.* (Fig. 2) in 2008 (16). Contrary to the finding of Valnickova *et al.* (23), Marx *et al.* argued that the Asn219 is most likely not glycosylated as the site is completely buried within the catalytic domain and glycosylation at this position is incompatible with the TAFI structure (16).

TAFI can be activated by thrombin (IIa), plasmin and the thrombin-thrombomodulin complex (IIa/TM) with a cleavage at Arg92 resulting in an apparent molecular weight of 19 kDa for the N-linked glycosylated activation peptide and ~35 kDa for the TAFIa moiety (10). IIa/TM is at least 1000 times more effective in activating TAFI than IIa alone, IIa/TM has therefore a major role as a physiological activator of TAFI (25). Additionally, it has been hypothesized that IIa alone could activate TAFI to an extent that would be sufficient in order to observe a down-regulation of fibrinolysis (26). Moreover, TAFIa is intrinsically unstable and the stability is

temperature-dependent with a half-life approximately 10 minutes at 37 °C (27). Since no naturally-occurring inhibitor of TAFIa has been found in plasma to date, inactivation through the temperature-sensitive conformational change resulting in TAFIai (inactivated TAFIa) may serve as the main mechanism for the regulation of TAFIa activity *in vivo* (27). Furthermore, TAFIai can be further cleaved at Arg302 by IIa and plasmin, resulting in the generation of 210-and-99-amino-acid-long fragments (10).

1.2.3 The structure of TAFI, the basis for intrinsic TAFI zymogen activity, and the TAFIa auto-inactivation mechanism

Similar to other human zinc-metalloprocarboxypeptidases, the TAFI structure consists of 2 domains: an N-terminal activation peptide and a catalytic domain. The activation peptide is connected to the catalytic domain by a linker region that is partially α-helical. Around the same time, crystal structure of bovine TAFI was published by Anand *et al.* (28). When compared to other human procarboxypeptidase, the catalytic site residues of bovine TAFI are in the "active" conformation with a rotation of the pro-domain away from its active site (28). The authors suggested that these observations may explain the reported TAFI zymogen activity for small peptide substrates (28). On the other hand, Marx *et al* (16) did not find such an open channel that allows for accessibility of macro-substrates, e.g. partially degraded fibrin, to the active site of the human TAFI zymogen.

The most significant discovery of Marx *et al.* on the structure of human TAFI is the identification of a highly mobile region of TAFI ranging from residues 296 to 350 (16). The dynamics of this region are reduced when carboxypeptidase inhibitor GEMSA was bound to

TAFI. The dynamics of the "flap" was further minimized when compared to TAFI mutant TAFI-IIYQ, where TAFI-IIYQ contains four mutations (T325I, T329I, H333Y, H335Q) and has 70-fold higher stability then that of the wild-type TAFI. Indeed, the existence of this dynamic region was presaged by studies of Boffa and coworkers that identified residues in this region that, when mutated, resulted in decreased stability (29). Schneider and coworkers observed that the naturally-occuring Thr/Ile polymorphism at position 325 influenced the stability of the respective TAFIa species (30). Marx and coworkers found that reversion of residues in this region to those found in the pancreatic CPB (stable) greatly increased the stability of TAFIa (31). Interestingly, mutations in this region that were shown to influence TAFIa stability, including the Thr/Ile 325 polymorphism, were also shown to influence the antifibrinolytic potential of TAFIa. Of note, the cryptic thrombin-cleavage site, Arg 302, which has been known to be cleaved by IIa, is also within this dynamic region.

As the researchers in the field race to work out the underlying cause behind the instability of TAFIa, the identification of this dynamic region represents a major breakthrough in solving the mystery (32). Based on the above mentioned data, Marx *et al.* (16) proposed a novel mechanism for TAFIa auto-inactivation (Fig. 2). In the zymogen form, the activation peptide interacts with the dynamic flap, consequently prevents it from unfolding. Such stabilization is lost when TAFI is activated and the activation peptide is dissociated from the protein, resulting in an increase in flap mobility. Ultimately, the dynamic region undergoes an irreversible conformational change, TAFIa activity is lost and the cryptic IIa cleavage site Arg302 is exposed.

1.2.4 The role of activation peptide

As mentioned above, TAFI is a glycosylated protein with four N-linked glycosylation sites (Asn22, Asn51, Asn63, and Asn86) on its activation peptide (23). Upon activation, TAFIa is less soluble than TAFI; TAFIa and TAFIai are prone to aggregate, consistent with the notion that N-linked glycosylation enhances the solubility of TAFI (33;34). A recent study using immunoprecipitation experiments reported that the activation peptide is noncovalently associated with TAFIa following cleavage. Furthermore, mutants lacking at least one glycoslation site, after IIa/TM activation, showed significant decreases in TAFIa activity (with the exception of TAFI-N86Q), suggesting that the glycans on the activation peptide can influence the properties of TAFIa (35). In contrast, Marx *et al.* (33) reported the following: 1. the activation peptide is not required for TAFIa activity; 2. no change in TAFIa activity is observed with or without activation peptide; 3. TAFIa inactivation is associated with decreased solubility, consequently, the activation peptide and TAFIai are in different fractions, soluble and pellets, respectively. Based on these findings, together with data from TAFI structure, the authors concluded that the activation peptide does not affect TAFIa activity or its stability; rather, the function of the activation peptide is to stabilize the structure of TAFI zymogen (16). More recently, Wu *et al.* (36) observed 1.7- to 8-fold decreases in catalytic efficiencies for TAFI activation by IIa/TM when selected arginine and lysine residues in the activation peptide were mutated. Therefore, the authors suggested that in addition to increasing TAFI solubility and stability, the activation peptide may also play a role in facilitating the binding of TAFI to IIa/TM.

1.3 Implication of TAFI as a risk factor for atherothrombotic diseases

Imbalance between coagulation and fibrinolysis can lead to disease. In keeping with the antifibrinolytic property of TAFI, elevated plasma TAFI levels (>90th percentile of the control) have been associated with a nearly two-fold increased risk for a first venous thrombosis event (37). Furthermore, high TAFI antigen levels (>75th percentile) also contribute to a nearly two-fold increased risk for recurrent venous thromboembolism (38).

High plasma TAFI levels have also been associated with increased risk for arterial thrombosis such as occurs in ischemic stroke (39;40) and coronary artery disease (CAD) (41). For example, a study by Leebeek *et al.* (39) measured functional plasma TAFI levels in 124 patients within one week after initial ischemic stroke, as well as 125 healthy age-and sex-matched controls. They reported that higher TAFI activity levels (highest quartile of the control) had a four-fold increased risk for ischemic stroke compared to that of the lowest quartile. High plasma TAFI levels following stroke seem to correlate with recurrent thrombotic events (40). A case-control study of 114 patients with at least one episode of ischemic stroke and 150 matched controls reported that high plasma TAFI levels (>120%) were associated with a six-fold increased risk for ischemic stroke (40). The same group also reported that high plasma TAFI activity (>126%) was associated with a four-fold increased risk of CAD (41). On the other hand, high plasma TAFI levels have been associated with decrease risks for myocardial infarction (MI) (42). These opposing views on the role of TAFI in arterial thrombosis may suggest that our understanding of the role of TAFI *in vivo*, under physiological or pathophysiological circumstances, is incomplete.

In contrast to thrombosis, excessive fibrinolysis can result in bleeding disorders such as haemophilia. The inability to sustain clots through TAFIa-mediated down-regulation of fibrinolysis has long been speculated as potential cause for premature clot lysis seen in haemophilia (10). However, at this point, this aspect of TAFI has not been studied extensively *in vivo*. Nonetheless, it has been reported that premature clot lysis in haemophilic plasma was observed using *in vitro* models of coagulation; and this defect could be rescued by the activation of TAFI (43;44). These results suggest that the inability to sustain the blood clot in haemophilia may be attributable to insufficient TAFI activation due to a defective intrinsic coagulation pathway. Hence, the possibility that differences in TAFI concentrations or TAFIa stability due to the Thr/Ile 325 polymorphism could influence the penetrance of hemophilia cannot be ruled out at this time. However, thus far, no clinical studies have been reported to address this question directly.

1.4 TAFI in inflammation

1.4.1 TAFIa as an anti-inflammatory molecule

In addition to partially-degraded fibrin, anaphylatoxins (C3a and C5a) and bradykinin have also been shown to be substrates for TAFIa both *in vitro* and *in vivo* (45-47). Most recently, thrombin-cleaved osteopontin (Opn) and plasmin-cleaved chemerin have also been documented to be substrates for TAFIa (48-50). TAFIa inactivates anaphylatoxins, bradykinin, and Opn by removing arginine residues from their carboxyl-termini, suggesting that in addition to regulating fibrin deposition, TAFIa may also play an anti-inflammatory role. Chemerin is a recently discovered chemoattractant that induces the migration of chemerin receptor chemokine-like

receptor 1 (ChemR23) expressing cells, including macrophages and platelets (50). In mouse model, the chemerin/ChemR23 system has been shown to possess anti-inflammatory properties, including mediating reduction in neutrophil infiltration and inflammatory cytokine release (51). Chemerin circulates in blood in an inactive form as prochemerin; a proteolytic cleavage of its carboxyl-terminal amino acids by plasmin releases its chemotactic activity. TAFIa removes the lysine residue from the carboxy-terminal end of the plasmin-cleaved chemerin, which dramatically enhances the chemotactic bioactivity of chemerin (50). Du *et al.* speculated that TAFIa participates in the anti-inflammatory response by activating chemerin, which then recruits immunosuppressive ChemR23-containing leukocytes to the site of injury (50).

1.4.2 TAFI is an acute phase protein in mice

It has been reported that TAFI is an acute phase protein in mice since both mouse *CPB2* mRNA expression and TAFIa activity were increased by at least 2-fold 24 hrs after intra-peritoneal lipopolysaccharide (LPS) injection (52). Furthermore, injection of a sub-lethal dose of LPS (to increase C5a receptor expression), followed by injection of cobra venom factor (to activate and deplete complement proteins) has a lethal effect on $TAFI^{-/-}$ mice, while wild-type and heterozygous TAFI mice showed limited dose tolerance. These results suggests that mouse TAFI may play a role in preventing hyper-inflammation *in vivo* by inactivating C3a and C5a (47).

1.4.3 Plasma TAFI level is associated with inflammatory disease states in humans

Unlike mouse TAFI, plasma TAFI levels seem to decrease in humans during the acute phase response. Both plasma TAFI antigen and activity levels have been reported to be significantly lower in patients with dengue hemorrhagic fever (human viral infection), disseminated intravascular coagulation (DIC) and sepsis when compared to healthy controls (53-55). In addition, a study reported a 20 % decrease in TAFI antigen levels 10 hrs after an injection of a low dose of LPS into 16 healthy subjects compared to the 2 hour time point (56). Indeed, a study using cultured human hepatoma (HepG2) cells have also shown that the expression of *CPB2* mRNA was decreased by ~60% following the treatment with IL-1β and IL-6 combined for 24 hours. This decrease was attributable to a decrease in *CPB2* mRNA stability in these cells (57).

In the same study, treatment with the synthetic glucocorticoid stress hormone dexamethasone increased both *CPB2* promoter activity as well as *CPB2* mRNA abundance in a dose-dependent manner, up to a maximum of 2-fold relative to the control (untreated HepG2) (57). This result led to the identification of a glucocorticoid response element (GRE) in the proximal region of the *CPB2* promoter (Fig. 3), suggesting that the TAFI pathway may play a role in the setting of chronic inflammation (57). Interestingly, elevated plasma TAFI levels compared to healthy controls have been reported in chronic inflammation-related diseases such as rheumatoid arthritis (58), type 2 diabetes (6), and obesity (6).

1.4.4 TAFI in wound healing

Coagulation, fibrinolysis and inflammation often occur at the site of tissue injury. Using the $TAFI^{-/-}$ mouse model, te Velde *et al.* (59) demonstrated that the TAFI pathway also plays a role in the wound healing response. In a cutaneous wound healing model, although all wounds were closed within 15 days for both wild-type and $TAFI^{-/-}$ mice, $TAFI^{-/-}$ mice had larger wound areas and aberrant keratinocyte and epithelial cell migration, resulting in a significant delay in complete re-epithelialization compared to the controls. In a more life-threatening wound healing model, in this case colonic anastomosis, the wound healing response in $TAFI^{-/-}$ mice was also impaired, as reflected by the decrease in tissue strength at the site of the suture. Moreover, these mice also showed increased weight loss, increased mortality, peritonitis, mesenterial thrombosis and ischemia. The mechanism underlying the impaired wound healing in $TAFI^{-/-}$ mice may arise from the ability of TAFIa to down-regulate plasmin formation. Indeed, a study using a plasminogen knock out mouse model reported a decrease in the level of inflammatory mediators, including tumor necrosis factor α (TNFα) and IL-5 in bronchoalveolar lavage fluid when challenged with ovalbumin-induced pulmonary inflammation (60). In this aspect, plasmin is important in processes related to wound repair including extracellular matrix remodelling, cell migration, and angiogenesis (61).

Taken all together, it is clear that TAFI has additional roles besides controlling the lysis of a blood clot.

1.5 Regulation of hepatic *CPB2* expression

Hepatic expression is the main source for the plasma pool of TAFI in both mice and humans (12;52). Even though the amino acid sequence identity between mouse and human TAFI is close to 84% (52), there exists little sequence identity between the two species in their respective 5'-flanking and 3'-flanking regions of the gene (Garand *et al*., unpublished data). These differences suggest that mouse and human TAFI have similar functions (i.e. carboxypeptidase-B-like activity), but the regulation of *CPB2* gene expression in these two species may be different. A study from our laboratory identified an NFκB binding site (between -43 and -32) in the proximal region of the mouse *CPB2* promoter; based on the sequence alignment and database searches, the presence of two key nucleotides substitutions A→T and C→T in the human promoter (thus altering the core consensus GGGAC to GGGTT) is expected to abolish the binding of human NFκB to the corresponding site in the human *CPB2* promoter (Fig. 3) (Garand *et al*., unpublished data). Furthermore, key nucleotides (ACA, nucleotides -105 to -103) that are important for the binding of the glucocorticoid receptor (GR) to the GRE in the proximal region of the human TAFI promoter (Fig. 3) are absent in the corresponding sequence in the mouse, indicating that the GRE site in the mouse may not be functional (Garand *et al*, unpublished data).

The 3'-untranslated region (3'-UTR) of mouse *CPB2* is very short with two polyadenylation sites (52), whereas the human *CPB2* 3'UTR is much longer and contains three confirmed polyadenylation sites that give rise to *CPB2* 3'-UTR sequences of 390, 423, and 549 nucleotides in length (12). The stability of these *CPB2* mRNA transcripts was found to decrease from the shortest to the longest (62). Treatment of HepG2 cells with IL-1β and IL-6 combined not only shifted the usage of the polyadenylation site in favour of the least stable transcript

(~1000 times more abundant than the two shorter ones), but also decreased the stability of this transcript by two-fold (62). Since the inflammatory response (i.e. LPS challenge) causes increased production of IL-1β, and IL-6, an increase in TAFI expression in the mouse during the acute phase may result in part from enhanced *CPB2* transcription initiation through the binding of NFκB (Garand *et al.*, unpublished data). In contrast, the decreased TAFI expression in humans during the acute phase can be attributed to the selection for the least stable TAFI transcript and the further modulation of its stability (62).

Molecular analysis of the human *CPB2* proximal promoter (up to nucleotide -425) using *in vitro* footprinting revealed ten potential liver transcription factor binding sites denoted Site A to J with transcription factor CCAAT/enhancer-binding protein (C/EBP), nuclear factor-Y (NF-Y) and glucocorticoid receptor (GR) binding to Site A, B, and C respectively (14;57;63). Moreover, hepatic nuclear factor-1 (HNF-1) binds in the region midway between Site C and Site B. Nucleotides -82 to -79 are required for that interaction, and the sequence between -80 and -73 of the human *CPB2* promoter has been shown to be essential for the liver-specific expression of TAFI (14;57) (Fig.3). Further matching of other transcription factors to the proposed transcription factor binding sites will enhance our understanding of hepatic TAFI expression in response to various stimuli, as well as the basic for restricted cell-type expression of *CPB2*.

Plasma TAFI antigen levels differ significantly in the human population ranging from 100 to 300 nM, and SNPs explain ~25% of the variation (3). A recent study reported that the SNPs in the 5'-flanking region of the human TAFI gene have no significant effect on TAFI promoter activity with two exceptions, both of which increase *CPB2* promoter activity by less than 20% (13). However, SNPs in the 3'-UTR appear to modulate TAFI mRNA stability significantly with half-life values ranging from 1.2 to 4.5 hours (the wild-type TAFI transcript exhibits a half-life of

3.2 hours), suggesting a direct effect of these SNPs on inter-individual TAFI antigen variation (13).

Recently, a study reported an expression of a novel alternatively spiced *CPB2* mRNA variant lacking exon 6 in human liver and HepG2 cells and found that the exon 6 skipping event is associated with the Ala147 of the common SNP Ala147Thr (64).

1.6. Non-hepatic TAFI pools

1.6.1 Brain TAFI, a potential role in Alzheimer's disease

The first non-hepatic TAFI was reported in 2000 by Matsumoto and coworkers (4). The authors identified a novel 40-kDa protein in human hippocampus that has ability to cleave amyloid precursor protein (APP) to become β-amyloid peptides. The β-amyloid peptides can aggregate to form amyloid plaques, which have been thought to trigger neuronal dysfunction and death in the brain, leading to Alzheimer's disease (4;65). Further protein purification and molecular analysis revealed that this novel protein has identical mRNA sequence as CPB2 with deleted exon 6 and a 52-base deletion in exon 10 (exon numbering as per Boffa and coworkers (12)). The resultant protein is a truncated TAFI protein that appeared to be brain specific (4). Unlike plasma TAFI, which is constitutively secreted from the liver, brain TAFI is uniformly expressed in the cytosol of normal hippocampal pyramidal neurons. In the neurons affected by Alzheimer's disease, brain TAFI appeared to be expressed in clusters rather than being ubiquitously expressed (4). The same group later reported the detection of brain TAFI in both human serum and cerebrospinal fluid (66). The western blot analysis of the human serum sample, what the authors claimed as plasma and brain TAFI species, showed apparent molecular mass of

43 and 40 kDa, respectively (66), a large deviation from the reported 60 kDa plasma TAFI (15). Further analyses are needed to confirm the identity and function of the brain TAFI. Of note, Matsumoto and coworkers are the first to report exon skipping events within *CPB2*. This discovery triggered interest in investigating the existence of alternative splice species in the cell types used throughout our studies and delineate what role, if any, they undertake in the regulation of *CPB2* expression.

1.6.2 Adipocytic and endothelial TAFI

As mentioned above, a significant increase in plasma TAFI antigen levels is observed for type 2 diabetic patients when compared to healthy controls (6;67;68). For example, Hori and coworkers,(6) reported a 2-fold increase in both plasma TAFI antigen and activity levels in patients with type 2 diabetes when compared to healthy controls (obese and non-obese combined). Moreover, both plasma TAFI antigen and activity levels were significantly higher in obese patients than in non-obese patients. These findings led the authors to hypothesize that obesity in combination with insulin resistance may stimulate TAFI expression in adipocytes. Indeed, *CPB2* mRNA was detected in the fatty tissue of type 2 diabetic patients, but none in healthy individuals (6;69). Furthermore, a study using cultured 3T3-L1 mouse adipocytes showed that mouse *CPB2* mRNA in the adipocyte is induced in a dose-dependent manner upon stimulation by insulin (70).

A weak correlation between plasma TAFI antigen levels and plasma soluble thrombomodulin concentration in type 2 diabetic patients has been reported, suggesting that increased plasma TAFI levels may be associated with vascular endothelial injury (67). However, contradicting reports concerning the detection of the *CPB2* transcript in HUVECs has appeared

(5;6;69). Collectively, these results may imply a role for the TAFI pathway in the development of atherothrombotic complications in type 2 diabetic patients and thrombotic complications observed in patients with chronic inflammation. Further studies in TAFI expression in adipocytes and endothelial cells will help advance our knowledge on this front.

1.6.3. Platelet TAFI

Following activation, platelets aggregate to form a platelet plug, a key process to prevent excessive blood loss at the site of vascular injury. A platelet pool of TAFI has been described by Mosnier and coworkers (5). Their results suggested that platelet TAFI is located in the α-granules of the platelet and can be released upon platelet activation; thrombin is the strongest agonist for the release of TAFI (~50% of the total amount) from platelets. Platelet TAFI has an apparent molecular mass of ~50 kDa. Following deglycosylation, both plasma and platelet TAFI migrated at the predicted molecular mass of 48 kDa on SDS-PAGE, suggesting that differences in glycosylation account for the differences in the apparent molecular mass. Like plasma TAFI, platelet TAFI is most efficiently activated by the IIa/TM complex *in vitro* (5). It is also intrinsically unstable at 37ºC, and can reduce the binding of plasminogen to minimally degraded fibrin (5). Most recently, a study from our laboratory showed that platelet TAFI is capable of attenuating platelet-rich thrombus lysis *in vitro* independently of plasma TAFI (71). Together, these results indicate that platelet TAFI and plasma TAFI have very similar enzymatic characteristics. *CPB2* mRNA was detected in megakaryocytic cell lines Dami and CHRF, but not in MEG-01 (5). Based on this evidence and the difference in glycosylation patterns, Mosnier *et al.* (5) hypothesized that the platelet pool of TAFI is synthesized in megakaryocytes rather than being

taken up from the plasma. Upon platelet activation, TAFI released from the platelet may significantly increase the local concentration of TAFI at the site of injury to ensure proper fibrin deposition and may play complementary roles in hemostasis. However, the specific role of each pool of TAFI remains obscure.

1.6.4 Keratinocytic TAFI

In a recent conference, Verkleij *et al.* (Abstract O12A-5, 20th ISFP Conference, 2010) identified a new source of TAFI: keratinocytes. TAFI was detected in skin tissues by way of immunohistochemical staining. TAFI was also detected in a keratinocytic cell line (HaCaT cells). Live-cell imaging revealed that TAFI can also be internalized into keratinocytes via receptor-mediated endocytosis. Taken together, the authors suggested that TAFI may play a role in keratinocyte proliferation and wound healing.

1.7 Physiological and pathological roles of macrophages and smooth muscle cells

Monocytes and macrophages play a central role in the host inflammatory response to bacterial infection and other insults. In to such insults, circulating monocytes migrate into extravascular tissues and differentiate to become macrophages. Macrophages are then activated by variety of stimuli such as cytokines or bacterial endotoxins to assist the immune system such as to destroy invading bacteria (72). Activated macrophages secrete other cytokines such as TNFα, IL-1β and interferon-γ (IFN-γ) to promote recruitment and activation of more macrophages. Accumulation of activated macrophages, if unregulated, can lead to chronic inflammation

resulting in tissue necrosis. Additionally, macrophages can accumulate in the vessel wall and sustain the inflammatory response as seen in atherosclerosis. In the context of atherosclerosis, accumulating macrophages not only promote lesion progression, but are also important sources of matrix metalloproteinases (MMPs). MMPs destabilize the atherosclerotic plaques, which consequently lead to plaque rupture and thrombus formation (73). In addition, the production of IFN-γ by the accumulating macrophages also induces the production of tissue factor from the macrophages. Upon plaque rupture, macrophages release TF in the milieu, consequently promoting coagulation. Thus, macrophages provide a potential link between inflammation and thrombus formation at the site of an atherosclerotic plaque (73).

Smooth muscle cells (SMCs) also play important roles in regulating vascular tone and pathologic processes such as hypertension and atherosclerosis. One major function of SMCs is to control vessel constriction and dilation in response to stimuli such as bradykinin, nitric oxide and Ca^{2+} (74). The ability of TAFIa to inactivate bradykinin suggests a possible role for the TAFI pathway in modulating vessel dilation and regulating blood pressure (10). Additionally, under inappropriate secretion of TNF and IFN-γ from the macrophages in developing atheromas, SMCs can migrate, proliferate, deposit extracellular matrix (ECM) components, and release various proteases at the site of atherosclerotic lesions (75). Moreover, SMCs can participate in the chronic inflammatory response observed in the development of an atherosclerotic lesion by producing pro-inflammatory cytokines and reducing contractility (75). To date, TAFI expression has not been assessed in macrophages or SMCs.

1.8 Rationale, hypothesis, and objectives

Evidence is emerging that TAFI may be expressed in cell types other than hepatocytes. Examination of TAFI expression in cell types that are crucially involved in physiological and pathological processes of vascular biology will enhance our understanding of how TAFI regulates the balance between coagulation and fibrinolysis in different settings. The expression of TAFI in non-hepatic cell types in turn suggests novel functions for the TAFI pathway in addition to the regulation of fibrin deposition.

The hypothesis of the present study is that TAFI is expressed in a variety of extra-hepatic cell types, and that expression of the *CPB2* gene in these cell types can be modulated in response to different external stimuli.

Three main objectives were formulated:

1. To assess TAFI expression in various non-hepatic cell types

2. To explore the regulation of TAFI expression in megakaryocytic cells and platelets, as well as monocytes (THP-1) and macrophages (differentiated from THP-1)

3. To investigate the expression of alternatively spliced *CPB2* mRNA in hepatic and non-hepatic cell types.

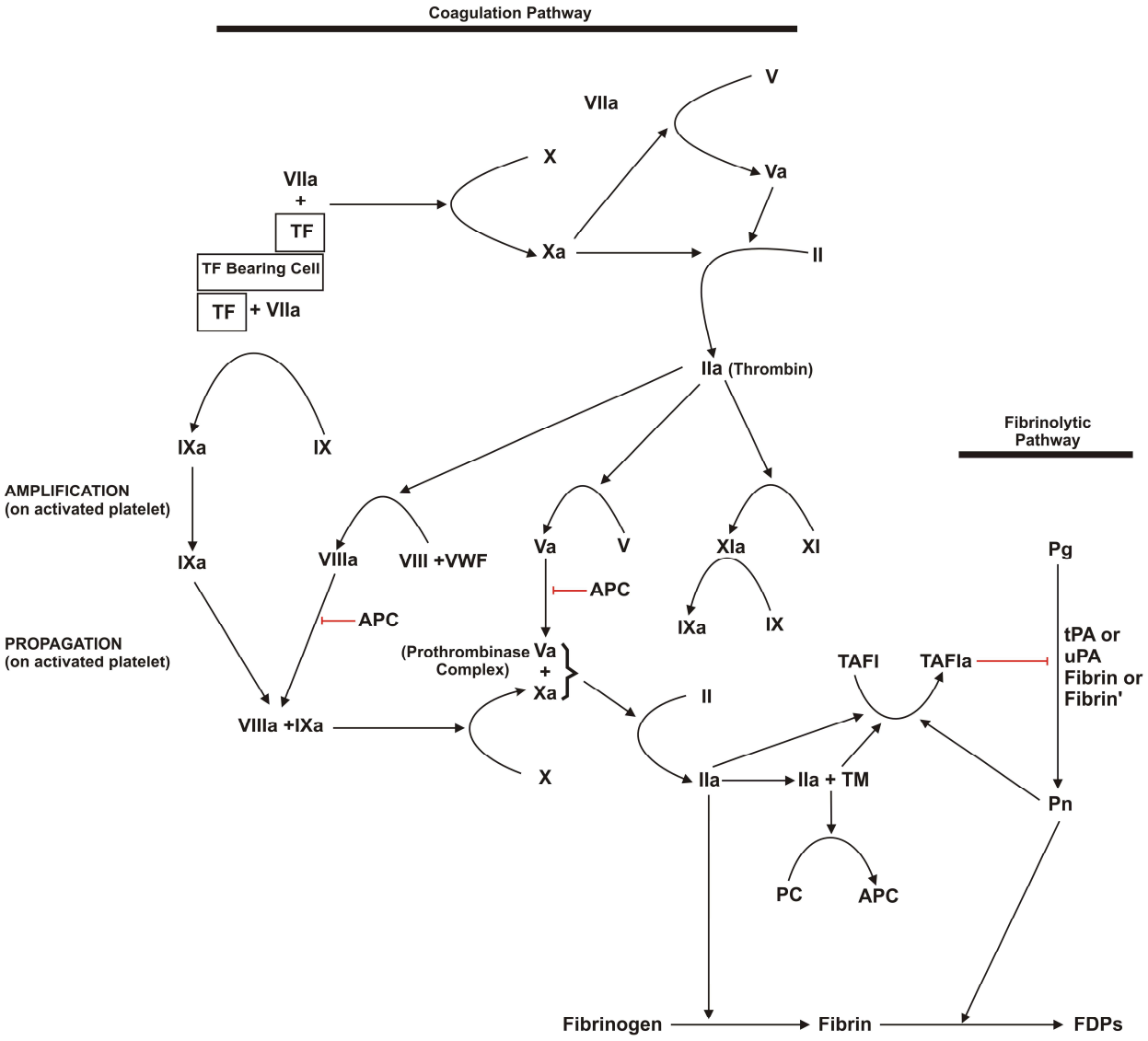

Figure 1. TAFI links the coagulation and fibrinolytic pathways. The cell-based model of hemostasis consists of three stages: initiation, amplification and propagation, resulting in a burst of thrombin (IIa) generation to form a clot by converting soluble fibrinogen to insoluble fibrin. In complex with thrombomodulin (TM), IIa activates protein C and TAFI to down regulate coagulation while preventing premature clot lysis, respectively. The lysis of blood clot is accomplished by the activation of plasminogen (Pg) to form plasmin (Pn), which cleaves insoluble fibrin clot to become soluble fibrin degradation products (FDPs). TAFIa attenuates the fibrinolysis by removing the carboxyl-terminal lysine residues from partially degraded fibrin, consequently TAFI interruptes several positive feedback loops within the fibrinolysis cascade (Figure adapted from (1)).

TAFI gene **(48 kb)**

TAFI mRNA **(~1.3 kb)**

TAFI

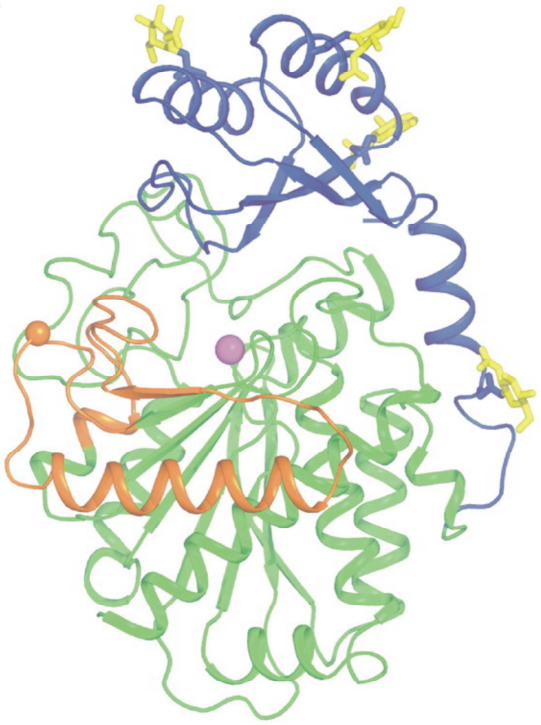

401 amino acids (48 kDa predicted molecular mass)

(60 kDa apparent molecular mass on SDS-PAGE)

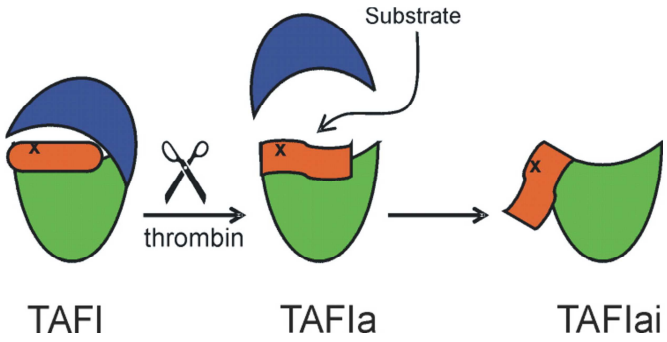

Figure 2. *CPB2* gene organization, TAFI protein and a model of its auto-inactivation. TAFI gene contains 11 exons and 10 introns spanning approximately 48 kb in length with a corresponding mRNA transcript of ~1.3 kb in size. The TAFI protein has an apparent molecular mass of 60 kDa and contains five potential N-linked glycosylation sites: 4 in the activation domain (yellow stick, Asn22, Asn51, Asn63, and Asn86) and 1 in the catalytic domain (Asn 219). TAFI structure consists of 2 domains: the activation peptide (shown in blue) and the catalytic domain (residues 93-401, shown in green) with a dynamic flap (residues 296-350, shown in orange). The catalytic zinc ion is shown as a magenta sphere. In the zymogen form, the dynamic flap is stabilized by the activation peptide, which also hinders substrate access to the active site. Cleavage by thrombin at Arg 92 releases the activation peptide, the substrate can enter and the mobility in the dynamic flap is increased. In time, an irreversible conformational change occurs in the dynamic flap, the catalytic site is disrupted, the TAFIa activity is lost and the cryptic thrombin cleavage site at Arg 302 is exposed (Figure adapted from (10;16)).

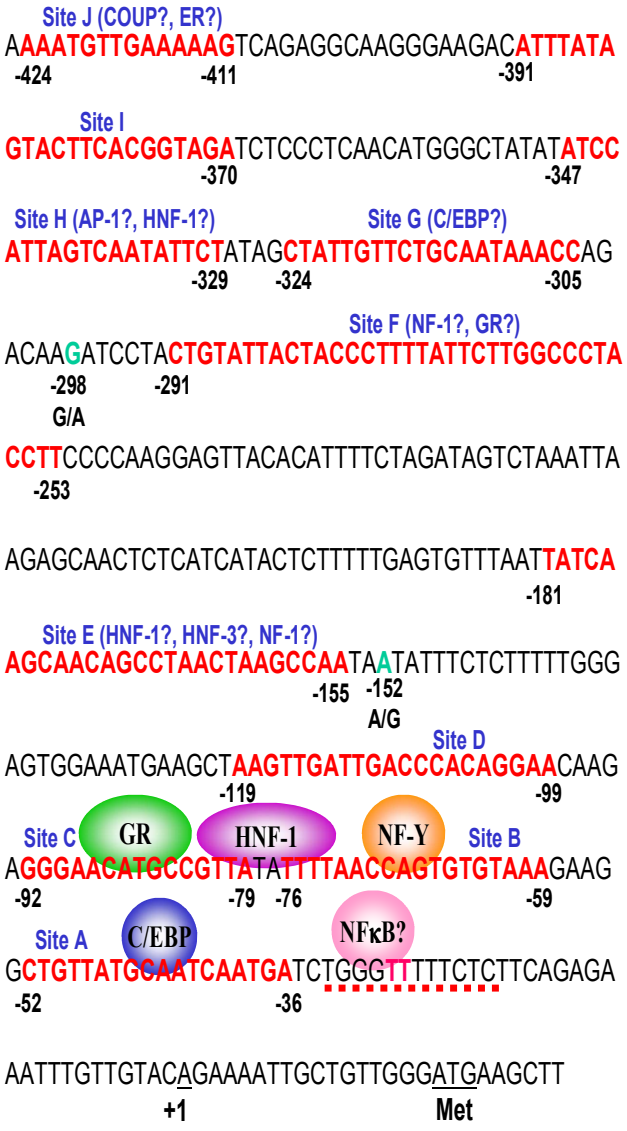

Figure 3. Respective transcription factors within the proximal region of the human *CPB2* promoter. The 5'-flanking region of the human *CPB2* gene depicted spans nucleotides from -424 to +16. Within this region, ten potential transcription factor binding sites have been mapped up to date, and are denoted Site A to Site J (nucleotide sequence in red). We have determined that Site A, Site B, and Site C correspond to C/EBP, NF-Y, and GR binding sites respectively. HNF-1 binds in the region between GR and NF-Y (nucleotides -82 to -72) with nucleotides, -82 to -79 being essential for its interaction with the promoter. The red underlined sequence represents the corresponding NFκB binding site in proximal region of the mouse *CPB2* promoter. Key nucleotide changes from AC to TT (coloured in pink) abolish the binding of NFκB to the human *CPB2* promoter. Potential transcription factors binding to the other mapped sites (Site E, F, G, H, and J) based on database searches are indicated in blue. Two SNPs identified within this region of the promoter are indicated with light green colour; the positions of +1 (transcriptional start site) as well as the first methionine codon are also included in this figure (Adapted from (14)).

Chapter 2: Identification of human thrombin-activatable fibrinolysis inhibitor in vascular and inflammatory cells

2.1 Statement of co-authorship

This chapter consists of a manuscript published in Thrombosis and Haemostasis (76). Dr. M. Garand participated in the data collection and analysis for results shown in Figure 5. He also participated in the collection and preparation of genomic DNA samples for data shown in Figure 6B, and captured and edited the immunocytochemistry images shown in Figure 8. B. Zagorac performed the Western Blot analysis shown in Figure 7A and participated in the collection and preparation of sample slides for data shown in Figure 8. S. Schadinger assisted in the optimization of TAFIa assay experiments corresponding to Figure 9A. C. Scipione assisted in the optimization of the immunocytochemistry, and participated in capturing the images shown in Figure 8. All of the remaining data were collected and analyzed by J. Lin. All sections of the manuscript were written by J. Lin with editorial assistance from Drs. M. Garand, M. Koschinsky and M. Boffa.

2.2 Abstract

TAFI (thrombin-activatable fibrinolysis inhibitor) is a carboxypeptidase zymogen originally identified in plasma. The TAFI pathway helps to regulate the balance between the coagulation and fibrinolytic pathways. Activated TAFI (TAFIa) can also inactivate certain pro-inflammatory mediators, suggesting that the TAFI pathway may also regulate communication between coagulation and inflammation. Expression in the liver is considered to be the source of plasma TAFI. TAFI has also been identified in platelets and *CPB2* (the gene encoding TAFI)

mRNA has been detected in megakaryocytic cell lines and in endothelial cells. We have undertaken a quantitative analysis of *CBP2* mRNA and TAFI protein in extrahepatic cell types relevant to vascular disease. Using RT-PCR and quantitative RT-PCR, we detected *CPB2* mRNA in the human megakaryoblastic cell lines MEG-01 and Dami, the human monocytoid cell line THP-1 as well as THP-1 cells differentiated into a macrophage-like phenotype, and in primary human umbilical vein and coronary artery endothelial cells. *CPB2* mRNA abundance in MEG-01, Dami, and THP-1 cells was modulated by the state of differentiation of these cells. Using a recently developed TAFIa assay, we detected TAFI protein in the lysates of the human hepatocellular carcinoma cell line HepG2 as well as in MEG-01 and Dami cells and in the conditioned medium of HepG2 cells, differentiated Dami cells, and THP-1 macrophages. We have obtained clear evidence for extrahepatic expression of TAFI, which has clear implications for the physiological and pathophysiological functions of the TAFI pathway.

2.3 Introduction

The balance between coagulation and fibrinolysis is critical for the hemostatic response upon injury, thereby preventing excessive blood loss while maintaining the fluidity of blood at sites away from the injury. Thrombin-activatable fibrinolysis inhibitor (TAFI, Human Genome Organization gene name carboxypeptidase B2, symbol *CPB2*) plays a key role in controlling this balance by attenuating fibrinolysis (2). TAFI is a basic carboxypeptidase zymogen that can be activated by thrombin (17), thrombin-thrombomodulin (25), or plasmin (77) to form TAFIa. Once activated, TAFIa removes carboxyl-terminal arginine and lysine residues from proteins and peptide substrates (78). TAFI was independently discovered by other groups; as such, TAFI is also known as plasma procarboxypeptidase B (15), procarboxypeptidase R (for arginine) (18) or procarboxypeptidase U (for unstable) (79). TAFIa retards fibrinolysis by removing carboxyl-

terminal lysine residues from partially degraded fibrin, resulting in attenuation of several positive feedback mechanisms in the fibrinolytic cascade (2;78;80;81).

Plasma TAFI antigen levels vary significantly in the human population ranging from approximately 100 to 300 nM (3). The K_m for TAFI activation by thrombin (1μM) is far above TAFI plasma concentrations, indicating that TAFIa generation is dependent on the initial TAFI concentraion (25). In keeping with the antifibrinolytic properties of TAFIa, elevated plasma TAFI levels (antigen or functional levels) have been associated with increased risk for thrombotic diseases such as venous thrombosis (37;82), recurrent venous thromboembolism (38), and ischemic stroke (39;40;83;84). Recent studies also showed that high plasma concentrations of activated TAFI (TAFIa)/inactivated TAFIa (TAFIai) level are associated with coronary heart disease (85) and increased risk of cardiovascular death (86).

The TAFI pathway may also play a role in the interplay between coagulation and inflammation. Several anti-inflammatory peptides including the anaphylatoxins (C3a and C5a) (45), bradykinin (46;87), thrombin-cleaved osteopontin (48), and plasmin-cleaved chemerin (50) have also been shown to be substrates for TAFIa. TAFIa activates chemerin and inactivates the rest by removing arginine residues from their carboxyl-termini.

Although hepatic expression is the main source for the plasma pool of TAFI (12;88), a platelet pool of TAFI has recently been described (5). Mosnier and coworkers demonstrated that platelet TAFI has an apparent molecular mass of approximately 50 kDa and is located in the α-granules of the platelet that can be released upon platelet activation (5). *CPB2* mRNA was detected in the Dami and CHRF (megakaryoblastic) cell lines, but not the MEG-01 cell line (5). *CPB2* mRNA has also been detected from the fatty tissue of patients with type 2 diabetes (6), but not from healthy individuals (69); *CPB2* mRNA expression in human umbilical vein endothelial cells has also been reported but is a point of controversy (5;6;69). No corresponding TAFI

protein expression in the above mentioned cultured cells has been reported to date. Nonetheless, evidence is emerging that TAFI may be expressed in cell types other than hepatocytes. Therefore, in the current work, we set out to examine TAFI expression in cell types that are crucially involved in physiological and pathological processes of vascular biology in order to enhance our understanding of the function of the TAFI pathway in hemostasis and beyond.

2.4 Materials and methods

2.4.1 Cell culture

All cells were maintained in a humidified incubator at 37 ºC and 95% air/5% CO_2 atmosphere. HepG2 cells (human hepatocellular carcinoma) (89) were purchased from the American Type Culture Collection (ATCC) and grown in 100 mm plates in minimal essential medium (MEM) (Invitrogen) supplemented with 10% fetal bovine serum (FBS) (ATCC) and 1% antibiotic-antimycotic (10 units/mL penicillin G sodium, 10 μg/mL streptomycin sulfate, and 25 ng/mL amphotericin B) (Invitrogen). MEG-01 cells (human megakaryoblastic leukemia) (90) were purchased from ATCC and cultured in 100 mm tissue culture plates with complete growth medium containing RPMI 1640 medium (Invitrogen) adjusted to contain 4.5 g/L glucose, 10 mM HEPES, 1.0 mM sodium pyruvate and supplemented with 10% FBS (ATCC) and 1% antibiotic-antimycotic. Dami cells (human megakaryoblastic leukemia) (91) were the generous gift of Dr. David Lillicrap (Queen's University, Kingston, Canada) and were cultured in 100 mm tissue culture plates with complete growth medium containing adjusted RPMI 1640 medium supplemented as described above for MEG-01 but without 1.0 mM sodium pyruvate. For differentiation of both MEG-01 and Dami cells, phorbol myristate acetate (PMA) (Sigma) was added to a final concentration of 0.1 μM to cells at a density of 1×10^7 cells/mL for up to 72 hours. THP-1 cells (human acute monocytic leukemia; ATCC) (92) were cultured in 100 mm

tissue culture plates with complete growth medium containing adjusted RPMI 1640 medium supplemented as described for MEG-01 cells with the addition of 0.05 mM 2-mercaptoethanol. In order to differentiate THP-1 into a macrophage-like phenotype, PMA was added to the final concentration of 0.1 μM to THP-1 cells at a density 1×10^7 cells/mL for 72 hours. Primary human umbilical vein endothelial cells (HUVEC) and primary human coronary artery endothelial cells (HCAEC) were purchased from Clonetics. HUVECs and HCAECs were cultured in 100 mm plates with complete endothelial growth medium (EGM-2 or EGM-2 MV, respectively; Clonetics). Primary human coronary artery smooth muscle cells (SMC) were purchased from Clonetics and were cultured in 100 mm plates with complete growth medium (SmGM-2; Clonetics). All primary cells were used between the fourth and fifth passage for experiments, except for HCAECs where the cells were used between the fifth and sixth passage. The preparation of human peripheral blood mononuclear cells (PBMNC) was performed as described (93) with the following changes: peripheral venous blood from healthy volunteers was drawn into BD Vacutainers containing acid citrate dextrose solution A (BD). The blood was then diluted in equal volumes of Hanks' Balanced Salt Solution (HBSS, Invitrogen). The diluted blood sample (27 mL) was layered on 20 mL of Ficoll-Paque Premium 1.073 (GE Healthcare). The harvested cells were washed twice with warm (37°C) HBSS before culturing in RPMI 1640 (Invitrogen).

2.4.2 RNA extraction

The RNeasy Mini kit (Qiagen) was used for total RNA extraction according to the manufacturer's protocol. For real-time RT-PCR analysis, on-column DNase digestion during RNA purification was performed using the RNase-Free DNase Set (Qiagen) as recommended by the manufacturer.

2.4.3 Reverse transcriptase-polymerase chain reaction (RT-PCR) analysis

Approximately 2.0 µg of RNA was used for RT-PCR experiments. RT-PCR was performed using OneStep RT-PCR Kit (Qiagen) following the manufacturer's instructions. The human TAFI fragment amplified and the primer sequences used are indicated in Table 1. Thermocycling conditions used for all amplification reactions were as follows: reverse transcription at 50 °C for 30 min; activation of the *Taq* polymerase at 95 °C for 15 min, 40 cycles of denaturation at 94 °C for 30 sec, annealing at 55 °C for 30 sec, and extension at 72 °C for 1 min; and a final extension at 72 °C for 10 min. The RT-PCR products (18 µL with the exception of HepG2 samples where 5 µL were used) were resolved on 1.5% or 2.0% agarose gels containing 0.5 µg/mL ethidium bromide; a reaction without RNA template (NTC) was used as negative control for reagent contamination and cross contamination of samples.

2.4.4 Real-time quantitative RT-PCR

Real-time RT-PCR analysis was carried out on an Applied Biosystems ABI Prism 7500 or BioRad CFX96 Real-Time System; procedures were as described (62) except that 1 µg of total RNA was used instead of 100 ng. Primers and probes for Taqman (Applied Biosystems) were designed using Primer Express 1.7 software (Applied Biosystems) to span one intron-exon junction thus minimizing the signal generated from contaminating genomic DNA in the template RNA. To control for the presence of genomic DNA contamination, control reactions with no reverse transcriptase were performed. The sequences for the primers and probes used are indicated in Table 2. The RNA standards for absolute quantification were generated as described (62).

2.4.5 Genotyping

QIAamp DNA Mini Kit (Qiagen) was used for genomic DNA extraction from cell lines and cultured primary cells following the manufacturer's protocol. Approximately 250 ng of the genomic DNA preparation was used for PCR experiments. PCR was performed using Go Taq Green Master Mix (Promega) following the manufacturer's instructions. The human TAFI exon 9 fragment (exon numbering based on Boffa (10;12)) was amplified using the primers indicated in Table 1; these primers hybridize in the introns flanking this exon. Thermocycling conditions used were as follows: activation of the *Taq* polymerase at 95°C for 2 min, 40 cycles of denaturation at 95°C for 1 min, annealing at 47°C for 1 min, extension at 72°C for 1 min and a final extension at 72°C for 5 min. A reaction without DNA template was used as negative control for reagent contamination and cross contamination of samples. In parallel, RT-PCR reactions were carried out using primers TAFI-5 and TAFI-6 (27) (see Table 1). PCR products derived from both the genomic and RNA templates were subjected to digestion with *Spe*I (10 units) (New England BioLabs) for 2 hours at 37 °C; the digestion products were then resolved on a 2% agarose gel containing 0.5 μg/mL ethidium bromide.

2.4.6 TAFI activation and western blot analysis

Purified plasma TAFI was purchased from Haematologic Technologies. For preparation of conditioned medium and cellular lysates, ~ 1×10^7 cells were cultured in 5 mL of Opti-MEM (Invitrogen) in the absence of any additives for 24 hours before harvesting. Three plates of the conditioned medium were pooled together and concentrated 60 to 80-fold using a 10-kDa cutoff centricon (Millipore). Cell lysates were prepared by washing the cells twice with 2 mL of cold phosphate-buffered saline (PBS) followed by lysis with 1 mL of lysis buffer (50 mM Tris-HCl, pH 8.0, 1% Nonidet P-40, 0.25% sodium deoxycholate, 150 nM NaCl, 1 mM EDTA) at room

temperature for 10 minutes. Three plates of lysates were then pooled together, filtered through a 0.8/0.2 μm syringe filter (Pall Life Science), and concentrated 3- to 4-fold using 10K centrifugal devices (Pall Life Science) For TAFI activation, conditioned media or cell lysates were supplemented with $CaCl_2$ (5 mM), human thrombin (25 nM) (Haematologic Technologies), and rabbit lung thrombomodulin (100 nM) (Haematologic Technologies) and were incubated at room temperature. Twenty microliters of the mixtures were removed at 30, 60, and 120 min after the addition of thrombin and each reaction was stopped by the addition of irreversible thrombin inhibitor D-phenylalanylprolylarginyl chloromethyl ketone (PPAck, 100 nM). Samples were then subjected to western blot analysis. Following SDS-PAGE on 10% polyacrylamide gels, proteins were transferred to a PVDF membrane (Millipore) and blocked with blocking buffer consisting of 6% (w/v) non-fat milk in 1× NET (150 mM NaCl, 5 mM EDTA, 50 mM Tris pH 7.4, and 0.05% Triton X-100) for at least 1 hour at room temperature. Next, blots were incubated with affinity-purified polyclonal sheep anti-human TAFI antibody (Affinity Biologicals; 1 in 10,000 dilution in blocking buffer containing 3% (w/v) non-fat milk) at room temperature for 1 hour. After washing with 1× NET, (four times for 10 minutes each), the blots were incubated with horseradish peroxidase-conjugated rabbit anti-sheep IgG secondary antibody (Pierce) (1 in 3,000 dilution in blocking buffer containing 3% non-fat milk) at room temperature for 1 hour. The membranes were then washed with 1× NET as described above. Immunoreactive bands were visualized using chemiluminescence (ECL System; Amersham Biosciences) and exposure to X-OMAT AR film (Kodak) or using SuperSignal West Femto Maximum Sensitivity Substrate (Thermo Scientific) and a FluorChem Q Gel Imaging System (Alpha Innotech).

2.4.7 Immunocytochemistry

Cells were seeded on poly-L-lysine-precoated (1 hr at 37°C, Sigma) glass coverslips at a density of 1×10^6/mL in 6-well tissue culture dishes. Cells were washed three times with PBS before fixing with 3.7 % paraformaldehyde solution in PBS for 5 min, washed once with PBS, and permeabilized with 1.4 % formaldehyde containing 0.1 % Nonidet P-40 in PBS for 1.5 min. After washing three times with PBS, the cells were incubated in blocking buffer (0.05% Tween 20, 5% normal goat serum in PBS) at room temperature for 1 hour. For TAFI staining, cells were incubated with mouse anti-human TAFI monoclonal antibody T4E3 (94) at a concentration of 10 µg/mL in saponin buffer at 4°C overnight. Following three washes with PBS, cells were incubated for 1 hour with Alexa Fluor 488 goat anti-mouse antibody (Invitrogen) at concentration of 0.5 µg/mL. Following three washes with PBS, the coverslips were mounted to slides using an anti-fade mounting solution (Dako) containing DAPI (0.75 µg/mL, Sigma) and examined using a Leica DMI600B inverted fluorescence microscope (40× Leica HC× PL S-APO objective with NA = 0.75) equipped with a Leica DFC 360 FX camera. Images were captured using Leica Advanced Application Suite Advanced Fluorescence software.

2.4.8 TAFIa assay

The TAFIa assay and preparation of TAFIa standards were performed as described by Kim and coworkers (22) with the following modifications. Fluo-plasminogen (100 nM) was mixed with 1.0 µM fibrin degradation products labeled with QSY9 C_5 maleimide (QSY-FDPs) in a buffer containing 20 mM HEPES, 0.2 M NaCl and 10 mg/mL bovine serum albumin (BSA). A separate set of TAFIa standards for quantification of TAFIa in cell lysates was made by diluting known amounts of TAFIa in PBS. Prior to measurement, concentrated conditioned media (60- to 80-fold) and cell lysates were diluted in TAFI-deficient plasma or PBS, respectively, in order to

obtain measurements within the range of the standard curve (10-200 pM TAFIa). Concentrated conditioned media were prepared as described above; however, a freeze-thaw method was used to obtain the cell lysates. First, 3×10^7 cells were washed three times with 2 mL of PBS. Subsequently, cells were suspended in 50 µL of PBS and subjected to six freeze-thaw cycles: a 10 minute snap-freeze stage in a dry ice/ethanol bath followed by a thawing stage at 37 °C for approximately 1 minute. Supernatants were collected by centrifugation for 1 min at 21,000 × *g* and stored at -70 °C until use. The conditioned medium and cell lysates were treated with thrombin and thrombomodulin as described above for 30 minutes in order to activate any TAFI present in the sample. In some samples, potato tuber carboxypeptidase inhibitor (PTCI, 50 µg/mL final) was added to the reaction to inhibit TAFIa activity.

2.5 Results

2.5.1 Detection of human *CPB2* mRNA in vascular cell types

Several lines of evidence suggest that TAFI is expressed in cell types other than hepatocytes (5;6). Thus, we set out to investigate, in a quantitative manner, TAFI expression in vascular cell types that are important in the pathology of cardiovascular diseases. As *in vitro* model cell types, we selected the megakaryoblastic cell lines MEG-01 and Dami, the monocytoid cell line THP-1 as well as peripheral blood mononuclear cells (PBMNC), primary human umbilical vein and coronary artery endothelial cells (HUVEC and HCAEC), and primary human coronary artery smooth muscle cells (SMC). Treatment of MEG-01 and Dami cells with the phorbol ester PMA was used to differentiate these cells further along the megakaryocytic lineage (91;95). Similarly, THP-1 cells were treated with PMA to differentiate them into macrophage-like cells (96).

Expression of human *CPB2* mRNA in various cell types was first studied using RT-PCR. Two primer sets were employed (27): TAFI 1-4 that amplifies the 5' portion of the *CPB2* open reading frame (ORF) and TAFI 5-6 that amplifies the 3' end of the *CPB2* ORF with expected fragments of 951 and 426 bp, respectively. Since liver is the main source of plasma TAFI production (12), the human hepatocellular carcinoma cell line HepG2 was used as the positive control.

Total RNA isolated from the above listed cell types plus differentiated MEG-01 and Dami (dMEG-01 and dDami, respectively) was subjected to RT-PCR experiments using the indicated primer sets. The results showed that *CPB2* transcripts are present in all the cell types investigated except SMC (Fig. 4). A band of the expected size was detected in the HCAEC total RNA sample when the TAFI 5-6 primer set was used, but not when the TAFI 1-4 primer set was used.

To determine the level of expression of *CPB2* mRNA in these cell types, quantitative real time RT-PCR (qRT-PCR) experiments were performed. Consistent with the RT-PCR results (Fig. 4), the qRT-PCR results showed that TAFI transcripts were detected in all the cell types investigated except SMC. HepG2 cells showed the highest expression of *CPB2* transcripts: approximately 100- to 1000-fold higher compared to the rest of the cell types (Fig. 5). *CPB2* mRNA abundance in Dami cells was approximately 4-fold higher than that in MEG-01 cells; moreover, an almost 5-fold increase in *CPB2* mRNA abundance was observed when MEG-01 and Dami cells were differentiated along the megakaryocyte lineage by PMA treatment (Fig. 5). A 74% decrease in *CPB2* mRNA abundance was observed when THP-1 cells were differentiated into macrophage-like cells with PMA treatment (Fig. 5). In addition, *CPB2* mRNA expression in PBMNC is similar in magnitude to that in THP-1 and THP-1ma (Fig. 5), indicating that THP-1 cells are a good model for studying TAFI *in vitro*.

2.5.2 Genotyping for a common SNP (+1040C/T) in the *CPB2* gene

We desired to rule out the possibility that the *CPB2* mRNA amplification observed arose from contamination of the mRNA samples, such as from the strong positive control HepG2 cell line, during experimental procedures. Therefore, we performed genotyping experiments that took advantage of the common single nucleotide polymorphism (SNP) +1040C/T located in exon 9 of *CPB2* where the single nucleotide change from C to T abolishes the restriction enzyme site for *Spe*I (Fig. 6A). Genomic DNA from HepG2, MEG-01, Dami, and THP-1 cells as well as from HUVEC, HCAEC and SMC was subjected to PCR using an intronic primer set that amplifies *CPB2* exon 9 with an expected fragment size of 180 bp; the PCR products were then digested with *Spe*I (Fig. 6B). In parallel, RT-PCR products encompassing this exon were amplified from RNA harvested from the respective cell lines/types and also digested with *Spe*I (Fig. 6C). The results indicate that the genomic DNA and the mRNA bear the same genotype in all cases: HepG2, MEG-01, and THP-1 cells as well as HCAEC were homozygous for the more common +1040C allele, while Dami cells, HUVEC and SMC were heterozygous (Fig. 6). These data are strong evidence that the TAFI mRNA amplified from the non-hepatic cell types represents *bona fide* expression of *CPB2*.

2.5.3 Detection of human TAFI protein in vascular cell types

Expression of human TAFI in the vascular cell types was studied using western blot analyses using polyclonal anti-TAFI antibodies. First, TAFI was detected in concentrated condition medium of HepG2 cells and showed the same apparent molecular mass (60 kDa) as purified plasma TAFI (Fig. 7A). In keeping with the results of the quantitative mRNA analysis, TAFI was readily detectable in the conditioned medium of HepG2 cells but was barely detectable, if at all, in the medium of the other cell types, even after 60- to 80-fold concentration

(Fig. 7B). Almost all of the medium samples had an immunoreactive band of similar, albeit significantly lower, electrophoretic mobility compared to TAFI. The exception was differentiated Dami cells, where a faint band of approximately 60 kDa was observed. In order to substantiate the identity of this protein as TAFI, we attempted to detect activation by addition of thrombin-thrombomodulin to the conditioned medium followed by western blot analysis. As observed for the positive control HepG2 conditioned medium sample (Fig. 7C), thrombin-thrombomodulin resulted in the disappearance of the 60 kDa TAFI band from the differentiated Dami conditioned medium and appearance of a 35 kDa TAFIa band (Fig. 7D). Neither the 60 kDa nor 35 kDa bands were observable in undifferentiated Dami cells (Fig. 7D).

We considered the possibility that, in non-hepatic cells, TAFI is not constitutively secreted from the cells but instead is packaged inside secretory granules. Precedent for this concept comes from the apparent localization of platelet TAFI within α-granules (5). Accordingly, we subjected lysates from all of the cell types, including HepG2, to western blot analysis. In some cases, we also treated the lysates with thrombin-thrombomodulin prior to western blot analysis. In no case could we detect TAFI or TAFIa in the lysate samples (data not shown). Of note, we even failed to detect TAFI in the lysates of HepG2 cells.

An alternative method to investigate the storage of TAFI inside the cells is by way of immunocytochemistry. We performed this analysis on HepG2 cells, differentiated Dami cells, and THP-1 macrophages (because the latter two cells types are adherent, unlike their undifferentiated counterparts), as well as SMC, which served as a negative control. Cells were seeded onto poly-L-lysine pre-coated slides and co-stained with monoclonal mouse anti-human TAFI antibody and DAPI to visualize the nuclei. HepG2 cells, differentiated Dami cells and THP-1 macrophages stained positive with the antibody, indicating the presence of TAFI in these cells (Fig. 8A-C). The staining pattern was generally diffuse throughout the cytoplasm. In

differentiated Dami cells, a perinuclear structure that may be the Golgi apparatus was also strongly stained with the anti-TAFI antibodies. The fluorescence signal for TAFI was absent in SMC, consistent with our RT-PCR and western blot findings that TAFI is not expressed in SMC (Fig. 8D).

A more sensitive method for TAFI detection and quantification is the TAFIa assay developed by Kim and coworkers (22), which is sensitive for TAFIa at a concentration as low as 12 pM. In this functional assay, FDPs labeled with the quenching moiety QSY (QSY-FDPs) are mixed with fluorescein-labeled plasminogen (Fluo-Pg). The QSY moiety quenches the fluorescence of Fluo-Pg bound to FDPs. Once TAFIa is introduced to the reaction, it removes lysine residues from the FDPs and consequently decreases the binding sites available for Fluo-Pg, resulting in increase in fluorescent signals that are TAFIa concentration dependent. A set of TAFIa standards diluted in either TAFI deficient plasma or PBS was used to quantify the amount of TAFIa in the concentrated conditioned medium and lysate samples, respectively, prepared from the cell types of interest.

To quantify the amount of TAFI present in each cell type studied, samples were first subjected to thrombin-thrombomodulin treatment for 15 min to activate any TAFI present, then applied to the TAFIa assay; a set of samples not incubated with thrombin-thrombomodulin were also included to control for background signal in the assay. As shown in Fig. 9A, TAFIa is detected in the conditioned medium of HepG2 cells, differentiated Dami cells, and THP-1 macrophages at levels averaging 16.4, 2.5 and 2.4 ng per 10^7 cells, respectively. TAFIa is also detected in the lysates of HepG2, MEG-01, differentiated MEG-01, Dami, and differentiated Dami cells averaging in the range between 1 to 2 ng per 10^7 cells. In all of these cases, no TAFIa activity was observed in the absence of thrombin-thrombomodulin treatment. No TAFIa signal was detected in the media or lysates of HUVEC, HCAEC, or SMC.

In the lysates of THP-1 cells, and in the medium and lysates of THP-1 macrophages, a significant apparent TAFIa activity was observed (Fig. 9A). However, at least some of this apparent activity was observed even in the absence of prior treatment of the lysate or medium with thrombin-thrombomodulin. The apparent activity is decreased by the addition of potato tuber carboxypeptidase inhibitor (PTCI) only in the thrombin-thrombomodulin treated THP-1 macrophages and HepG2 medium (Fig. 9B); the apparent TAFIa activity in the thrombin-thrombomodulin-treated THP-1 macrophage medium was reduced by PTCI to a level similar to that detected in the absence of thrombin-thrombomodulin. Our criteria for *bona fide* TAFIa activity is that it must (a) be generated only after treatment with thrombin-thrombomodulin; and (b) be sensitive to PTCI. Therefore, the apparent TAFIa activity present in THP-1/THP-1 macrophage lysates is artefactual. On the other hand, the medium of THP-1 macrophages does contain *bona fide* TAFIa activity, indicating that these cells express and secrete TAFI.

2.6 Discussion

Evidence for extra-hepatic expression of TAFI has arisen from several studies over the past decade. A pool of TAFI present in platelets has been reported, and RT-PCR was used to demonstrate expression of *CPB2* mRNA in megakaryocytic cell lines (5). Other studies have identified *CPB2* mRNA in adipose tissue and HUVEC (6), again utilizing RT-PCR, although these findings could not be repeated by other groups (5;69). The common feature of the existing investigations is that they are not quantitative with respect to *CPB2* mRNA transcript abundance and they fail to account for the possible presence of TAFI protein. In the current study we have attempted to address these issues by utilizing a quantitative real-time RT-PCR approach, and by using western blot analysis, immunocytochemistry, and a functional assay for TAFIa. We have also accounted for the possibility of intracellular storage of TAFI protein. Our data substantiate

the notion that TAFI is expressed in the megakaryocyte lineage but cast further doubt on expression of this protein in endothelial cells. Finally, our data reveal a new potential site of extrahepatic expression of TAFI: monocyte-derived macrophages.

In a previous study, *CPB2* mRNA was detected in megakaryocytic cell lines Dami and CHRF, but not in MEG-01 (5), where MEG-01, Dami and CHRF were proposed to represent the early, intermediate and late stages of megakaryocyte development, respectively (90;91;97). These results suggested that platelet TAFI is synthesized in megakaryocytes rather than acquired by uptake from the plasma (5). Our results confirm the expression of *CPB2* mRNA in Dami cells, and also indicate that this gene is expressed, albeit at a lower level, in MEG-01 cells. More interestingly, we found that when either of these cell lines were treated with PMA to further their differentiation along the megakaryocyte lineage, their expression of *CPB2* mRNA increased by a factor of approximately 4.8 and 4.5-fold in MEG-01 and Dami, respectively. In fact, a trend towards increasing *CPB2* mRNA expression as a function of the "stage" of megakaryocyte differentiation is clearly observed, with MEG-01 cells having the lowest expression and PMA-treated Dami cells having the highest. In preliminary double immunofluorescence microcopy studies of human bone marrow (Lin *et al.,* unpublished data, Fig 10), we found evidence of cells in which TAFI was co-expressed with CD41, a marker of megakaryocytes and the megakaryocyte lineage. Together, these results strongly support the idea that the platelet pool of TAFI arises from expression of *CPB2* in megakaryocytes.

Our quantitative analysis of *CPB2* mRNA expression indicates that the abundance of the transcript is very much lower in megakaryocytic cells than in hepatic cells. Indeed, both western blot analysis as well as a quantitative assay for TAFIa showed substantially lower TAFI protein expression in megakaryocytic cells, and we were only able to detect TAFI protein in the medium of differentiated Dami cells (which have the highest level of *CPB2* mRNA) using either

technique. The concentration of TAFI in the differentiated Dami cell medium is approximately one-seventh that in the medium of HepG2 cells. Consistent with the results of immuncytochemistry where both HepG2 and differentiated Dami stained positive for TAFI (Fig. 8A,B), we also detected TAFI in the lysates of all megakaryocytic cells examined using the TAFIa assay, and the levels of TAFI in the lysates were comparable to those in HepG2 lysates.

The observation of secretion of TAFI from differentiated Dami cells is noteworthy. MEG-01 and Dami cells only exhibit immature granules (90;91;95;98), and as such secretion of granular proteins is observed. For example, while the platelet α-granule protein von Willebrand Factor (vWF) can be detected in the lysate samples of PMA treated and non-treated Dami cells, PMA treatment also increases the vWF secretion from Dami cells (91).

The western blots show clearly that the apparent size of the Dami-expressed TAFI (60 kDa) is similar to that of the HepG2-expressed TAFI as well as plasma-derived TAFI. These findings are in agreement with our own studies of platelet TAFI using western blot analysis of proteins secreted from washed human platelets after activation by thrombin, we found that platelet TAFI was very similar to plasma-derived TAFI in size (71).

In the present study, we report for the first time that *CPB2* is expressed in monocytes and monocyte-derived macrophages. THP-1 cells are a human cell line that is a well-accepted model of macrophage differentiation (99), and we further supported this notion by demonstrating the detection of *CPB2* mRNA in PBMNC (Fig. 4C-D); furthermore, qRT-PCR showed that PBMNC expression of *CPB2* mRNA is in the same magnitude as THP-1 and THP-1 macrophages (Fig. 5). Immunocytochemistry results showed THP-1 macrophages staining positive for TAFI (Fig. 8), and we also detected a small amount of TAFI in the medium of THP-1 macrophages using a TAFIa assay (Fig. 9). Moreover, preliminary studies of human bone marrow revealed cells co-expressing TAFI and CD163, a marker of monocytes/macrophages (Lin *et al.,* unpublished data,

Fig. 10). We were not able to detect TAFI protein by western blot analysis of THP-1 cell lysates, likely because the low level of TAFI is below our limits of detection; moreover, an artefact in the TAFIa assay observed specifically with THP-1 and THP-1 macrophage cell lysates renders the detection of TAFI in these samples inconclusive. We do not know the nature of this artefact, which may involve either removal of carboxyl-terminal lysines from the quencher-labeled FDPs or displacement of fluorescently-labeled plasminogen from these sites. However, studies with both thrombin-thrombomodulin and PTCI, a specific inhibitor of TAFIa, definitively rule out this artefactual activity as being TAFI/TAFIa.

The significance of detection of TAFI in the lysates of Dami and THP-1 cells is not clear at this time. We cannot assess if the detected TAFI represents that in the constitutive secretion pathway (as would presumably be the case for hepatocytes) or a pool of TAFI that is stored intracellularly. Although immunocytochemistry does not reveal an obviously granular intracellular staining pattern that might be consistent with regulated secretion of TAFI from Dami or THP-1 cells, further studies using markers of secretory granules will be required to definitely address this issue. It will also be interesting to identify a secretagogue for intracellular TAFI, since it appears that differentiation of Dami or THP-1 cells triggers TAFI secretion (Fig. 9A).

Monocytes and macrophages play a central role in the host immune response to bacterial infection; macrophages also accumulate in the vessel wall and sustain the inflammatory response as seen in atherosclerosis. The ability of monocytes/macrophages to express TAFI suggests that these cells may be a source of TAFI within atherosclerotic plaques as well as other extra-vascular sites during inflammation. TAFI may play a number of roles in inflammation. TAFIa is capable of inactivating a variety of pro-inflammatory substrates (45;46;48;50;87). In addition, modulation of pericellular plasminogen activation and/or extravascular fibrin deposition have been postulated as mechanisms by which TAFI can influence cell migration (59;100). Plasma TAFI levels are

decreased in mild experimental endotoxemia in humans (56), while the TAFI pathway has been associated with the outcome of meningococcal infection in children (101) and activation of TAFI on the surface of *Streptococcus pyrogenes* helps the pathogen to modulate the host inflammatory response through cleavage of bradykinin (102). The roles and significance of expression of TAFI in monocytes and macrophages are not clear at this time, but will serve as an exciting new avenue for TAFI research in the future.

In addition to in megakaryocytes and monocyte/macrophages, TAFI gene expression in endothelial and smooth muscle cells was also investigated in the current study. The vascular endothelium not only forms a permeability barrier between the circulating blood and the extra-vascular tissues, but also mediates local responses to physiological and pathological stimuli such as an increase in permeability during inflammation and exposure of tissue factor to trigger the coagulation cascade upon vessel injury. SMC also play important roles in regulating vascular tone and the pathological process of atherosclerosis (75). To date, TAFI expression has not been assessed in HCAEC nor SMC, but one group has reported expression of *CPB2* mRNA in HUVEC (6). In the current study, using RT-PCR and qRT-PCR, we find that *CPB2* mRNA can be readily detected in endothelial cells HUVECs. However, this message is in much lower abundance in HCAEC, as evidenced by its only occasional observation in RT-PCR and its approximately 57% lower abundance than in HUVEC as assessed by real-time quantitative PCR (Fig. 5). More importantly, we were not able to detect TAFI protein in the medium or lysates of endothelial cells. We were also not able to detect *CPB2* mRNA or TAFI protein in SMC (Figs. 4,5). Therefore, we conclude that neither vascular endothelial cells nor smooth muscle cells are likely to be significant sources of TAFI *in vivo*.

In conclusion, we have identified *CPB2* mRNA in non-hepatic cell types including megakaryocytes (represented by the MEG-01 and Dami cell lines), monocytes, macrophages

(represented by the THP-1 cell line), PBMNC and both venous and arterial endothelial cells (represented by primary HUVEC and HCAEC, respectively). TAFI protein was also detected in the lysates of MEG-01 cells, differentiated MEG-01 cells, Dami cells, differentiated Dami cells, and the conditioned medium of differentiated Dami cells and THP-1 macrophages. The detection of *CPB2* mRNA and protein in megakaryocytes provides further evidence supporting the notion that platelet TAFI is originated from megakaryocyte expression of the *CPB2* gene; the detection of TAFI expression in monocytes/macrophages may reflect novel roles for extra-hepatic TAFI expression in the many emerging roles of the TAFI pathway beyond regulation of fibrin clot breakdown.

2.7. Acknowledgements

We thank Dr. David Lillicrap (Dept. of Pathology & Molecular Medicine, Queen's University) for providing Dami cells. We thank Nicole Feric at Queen's University for preparing Fluo-plasminogen, Tanya Marar at University of Windsor for purified recombinant TAFI protein. We would also like to thank Dr. Michael Nesheim and Jonathan Foley at Queen's University for their assistance with the TAFIa assay.

2.8. Financial support

This work was supported by a grant (NA-6439) from the Heart and Stroke Foundation of Ontario to M. L. Koschinksy, who is also a Career Investigator of the Heart and Stroke Foundation of Ontario.

2.9. Conflict of interest

None declared.

Table 1. Primer sequences for RT-PCR and PCR analyses

Primer Name	Sequence (5' → 3')	Size of Amplicon
TAFI-1	CTGTTGGGATGAAGCTTTGC	951 bp
TAFI-4	GCTGGGAGTATGAATGCATG	
TAFI-5	GCATACATCAGCATGCATTC	426 bp
TAFI-6	CAATGATTTGGTCTTGCTGG	
Exon9-5'	TTCAAAGCTGCACATTAACTG	180 bp
Exon9-3'	CTTTAGTAGCTCAAAGTTCTC	

Table 2. Primer and probe sequence for quantitative RT-PCR analysis

Name	Sequence (5' → 3')
hTAFI-5'	[a](+)TGCATCGGAACAGACCTGAA
hTAFI-3'	[b](−)CTGGATGCACCTTCCTCACA
hTAFI probe	[c]6FAM−TTGCTTCCAAACACTG−MGBNFQ

[a](+), forward primer; [b](-), reverse primer; [c]6FAM-MGBNFQ probes: 6FAM(6-carboxyfluorescein), the 5'-end reporter dye; MGBNFQ (minor groove binder nonfluorescent quencher), the 3'-end nonfluorescent quencher.

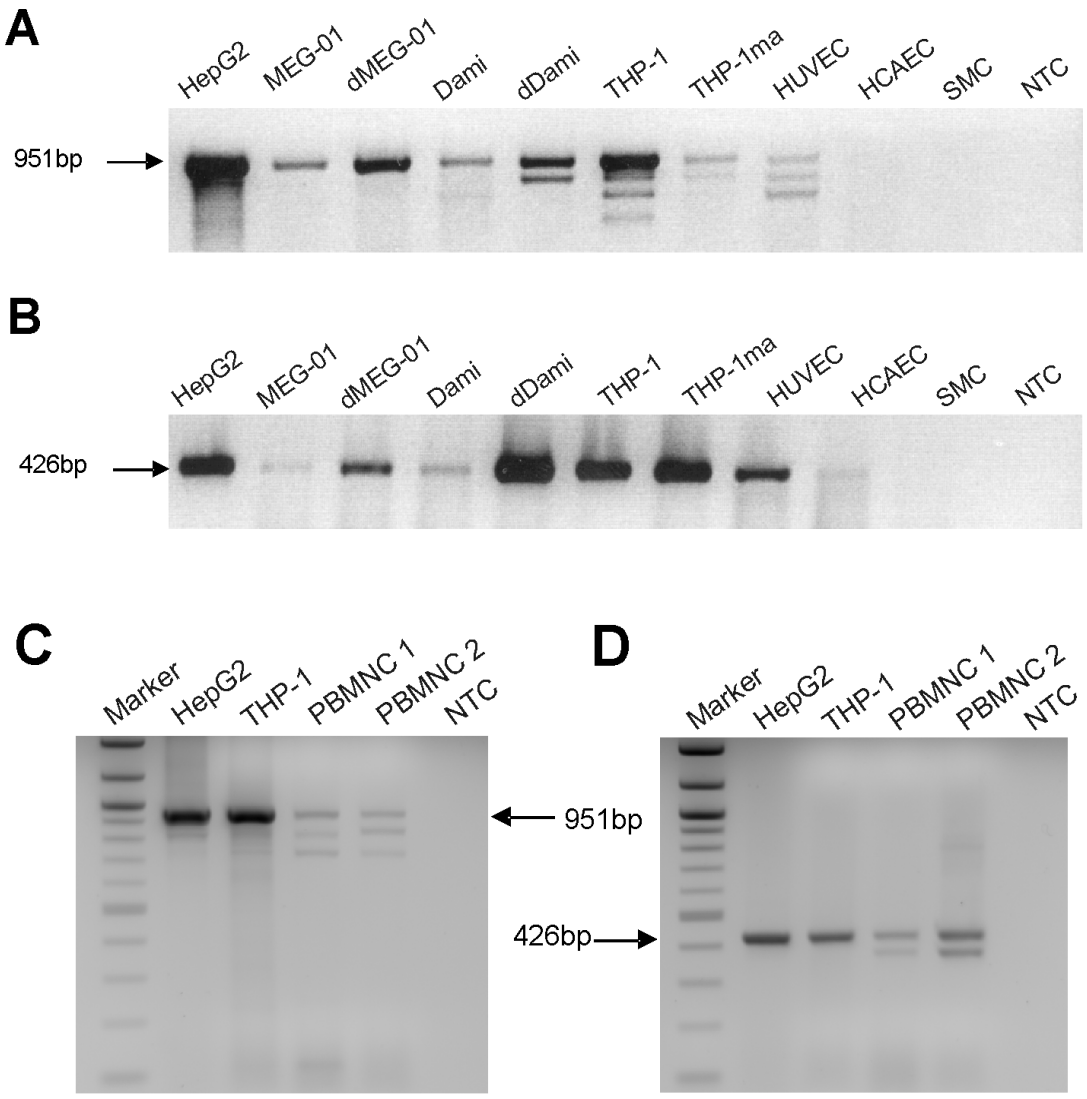

Figure 4. Detection of *CPB2* mRNA in various cell types using RT-PCR. RT-PCR was performed from 2.0 µg of total RNA isolated from the following cell types: HepG2, MEG-01, differentiated MEG-01 (dMEG-01), Dami, differentiated Dami (dDami), THP-1, THP-1 macrophage (THP-1ma), HUVEC, HCAEC, SMC and PBMNC. A reaction without any RNA template (NTC) was also included as a negative control. Primer sets TAFI 1-4 (**A, C**) and TAFI 5-6 (**B, D**) amplify 951 bp and 426 bp amplicons, respectively, from the *CBP2* open reading frame (ORF). The RT-PCR products were resolved on agarose gels; arrows indicate the expected amplification products.

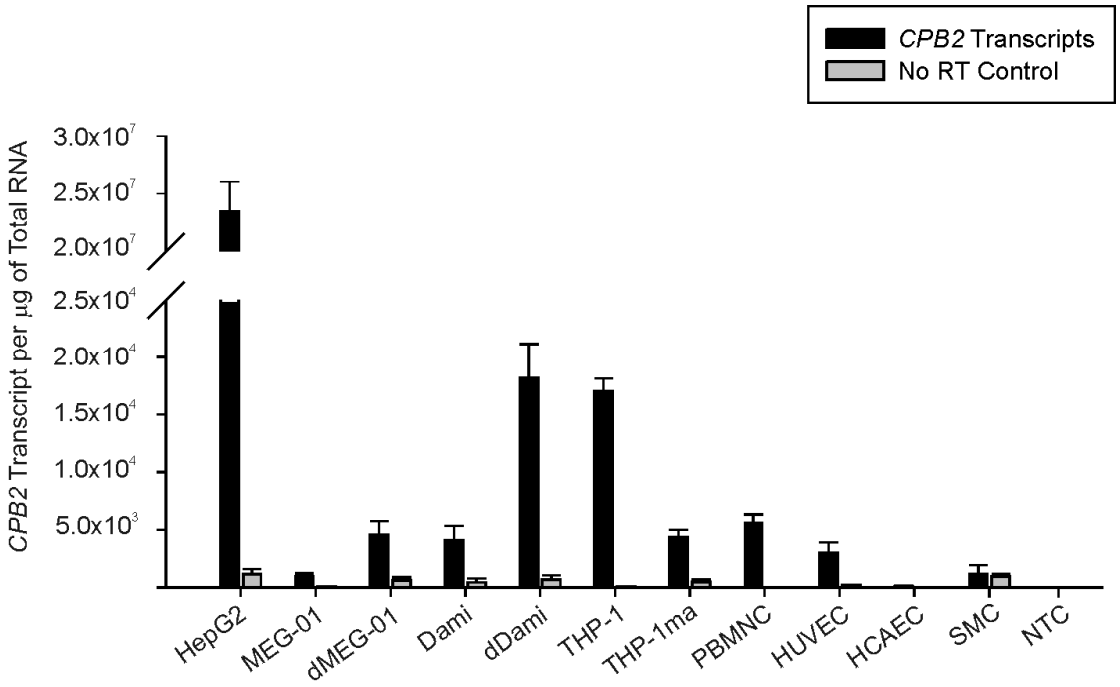

Figure 5. Quantitative analysis of human *CPB2* mRNA in various cell types. The abundance of *CPB2* mRNA from HepG2, MEG-01, differentiated MEG-01 (dMEG-01), Dami, differentiated Dami (dDami), THP-1, THP-1 macrophage (THP-1ma), HUVEC, HCAEC, SMC, and PBMNC was analyzed by quantitative real-time RT-PCR experiments using 1 µg of total RNA, with primers and probe specific for human *CPB2* mRNA. The absolute quantification was based on an *in vitro* transcribed human TAFI mRNA standard; quantities of unknown were interpolated from the standard curve. The data shown are the means of two to four independent experiments performed in triplicate. The error bars represent the standard error of the mean. NTC, no template control; No RT Control, no reverse transcriptase control.

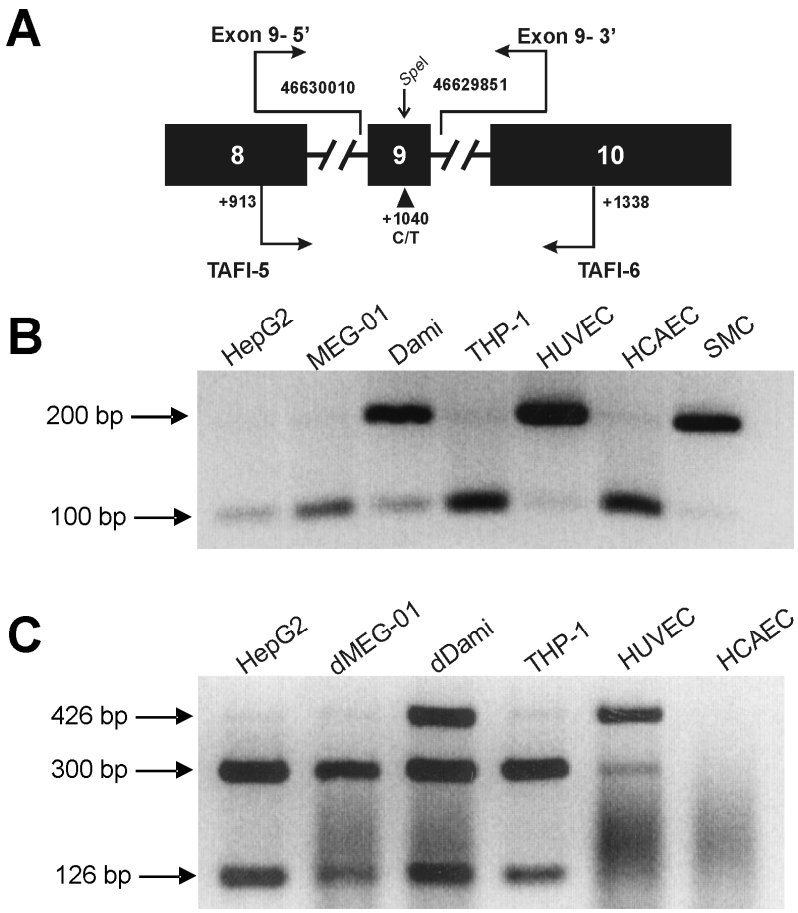

Figure 6. Genotyping for a common SNP (+1040C/T) in the *CPB2* gene. A. Scheme for amplification of a region spanning the +1040C/T SNP in *CPB2* from genomic DNA or total RNA isolated from different cell types. Primers Exon 9-5' and Exon 9-3' span the indicated nucleotides (chromosome 13 numbering), hybridize within the introns flanking exon 9 and amplify a 180 bp product. Primers TAFI-5 and TAFI-6 amplify a 426 bp fragment from the *CPB2* ORF that contains exon 9. **B.** PCR with primers Exon 9-5' and Exon 9-3' was performed using 250 ng of genomic DNA isolated from the indicated cell lines/types. Subsequently, 10 μL of the PCR product from each cell type was subjected to digestion of restriction enzyme *Spe*I; the digested products were then resolved on a 2% agarose gel. **C.** RT-PCR with primers TAFI-5 and TAFI-6 was performed using total RNA from the indicated cell lines/types; the RT-PCR products were subjected to *Spe*I digestion; the digested products were then resolved on a 2% agarose gel.

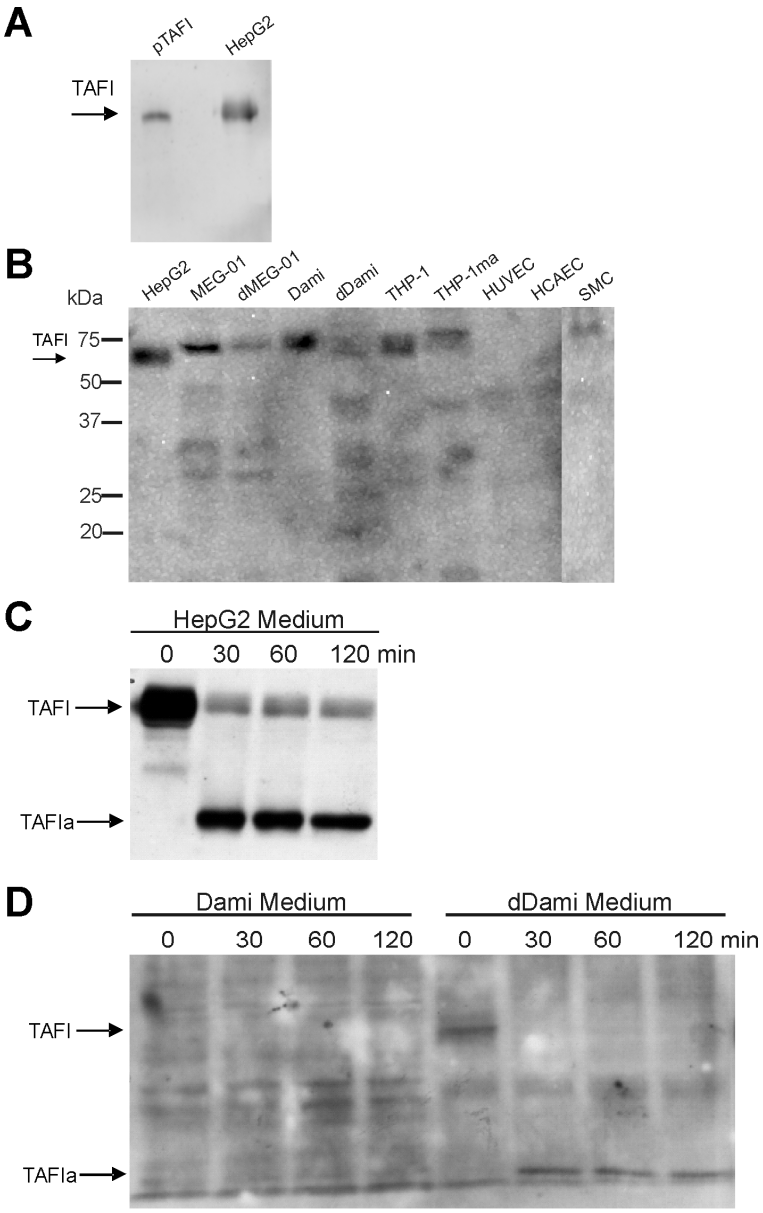

Figure 7. Detection of human TAFI protein in various cell types using western blotting. Samples included: (**A**) purified plasma TAFI (pTAFI, 250 ng/lane) and a concentrated (60-fold) HepG2 conditioned medium sample; (**B**) conditioned medium harvested from the indicated cell lines/types and concentrated 60-80-fold using centrifugal concentrators; concentrated (60-80-fold) media samples from HepG2 cells (**C**) and Dami and differentiated Dami (dDami) cells (**D**) treated with thrombin (25 nM final) and thrombomodulin (100 nM final) (IIa/TM) to activate TAFI; aliquots were taken at 0, 30, 60, and 120 min after initiation of the reaction and the thrombin was quenched by the addition of PPAck (100 nM final). Samples were resolved on 10% or 12% SDS-PAGE gels followed by western blotting using polyclonal sheep anti-human TAFI antibody. Arrows show the positions of TAFI (60 kDa) and TAFIa (35 kDa) on the blots.

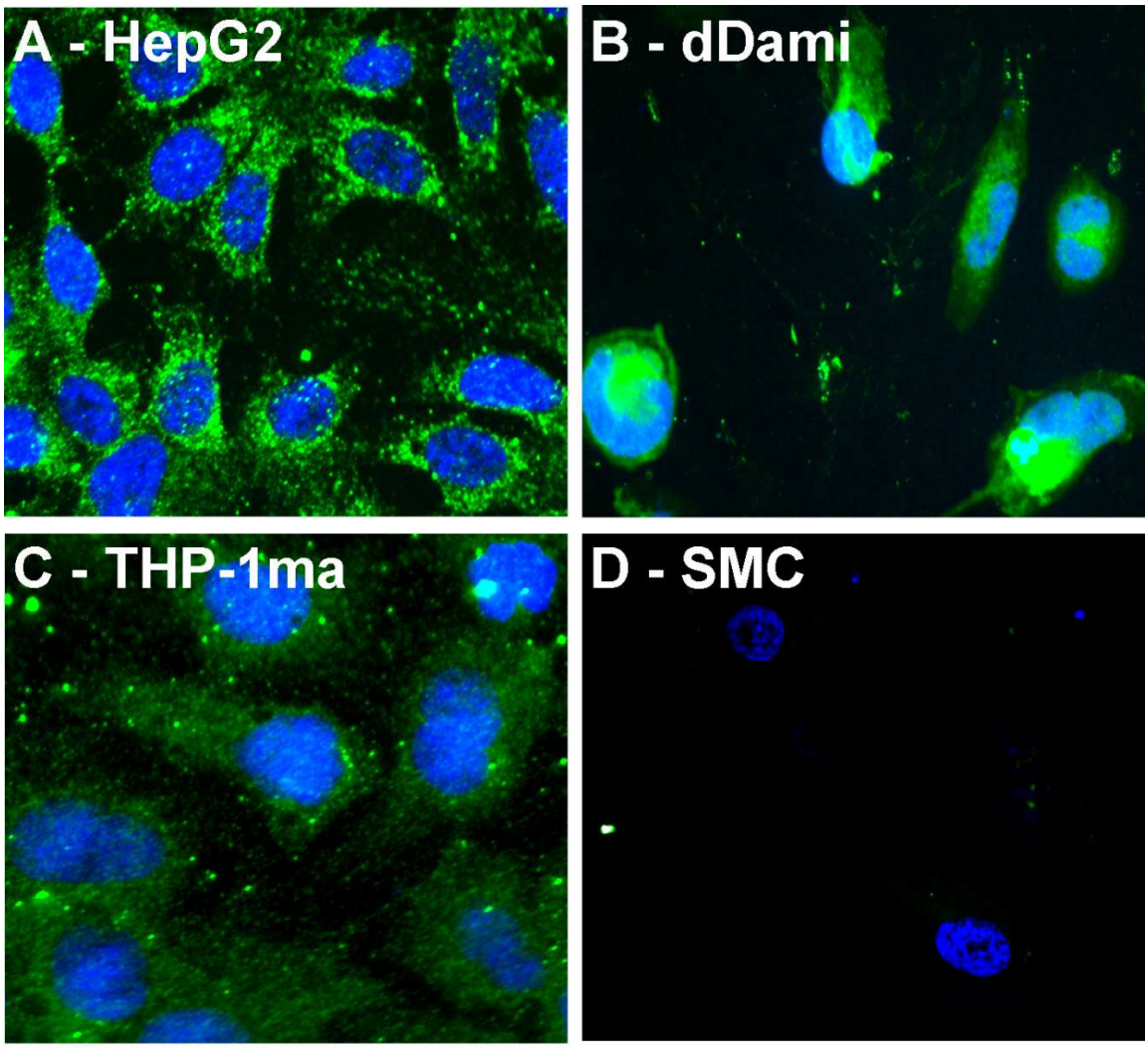

Figure 8. Identification of human TAFI protein using immunocytochemistry. HepG2 cells (**A**), differentiated Dami cells (**B**), THP-1 macrophages (**C**), and SMC (**D**) were seeded on poly-L-lysine pre-coated coverslips, fixed with paraformaldehyde, permeabilized with formaldehyde containing Nonidet P-40, and stained for TAFI (green) with a monoclonal anti-TAFI antibody followed by an Alexa-488-linked secondary antibody. Nuclei (blue) were visualized with DAPI.

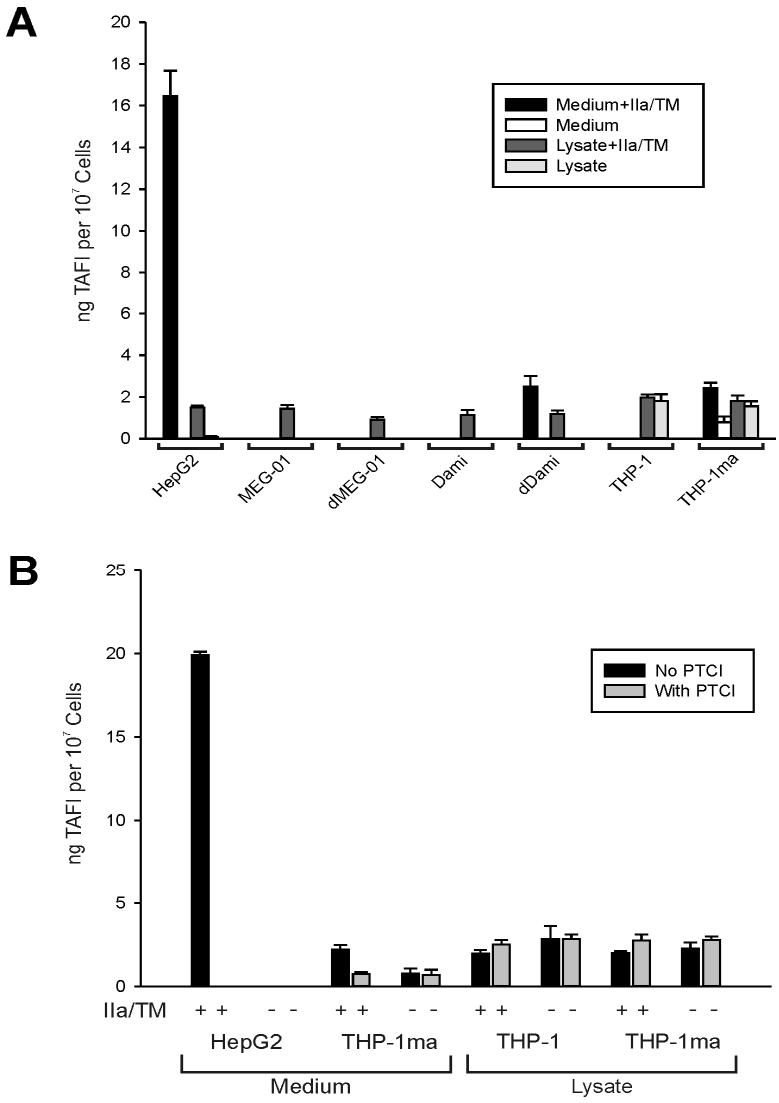

Figure 9. Quantification of human TAFI protein in various cell types using TAFIa assay. A. Medium and lysate samples were prepared from the indicated cell lines/types. Conditioned media samples were concentrated approximately 60- to 80-fold using centricons whereas lysates samples were harvested by applying 6 free/thaw cycles in phosphate-buffered saline (PBS) buffer. Where indicated, thrombin (25 nM final) and thrombomodulin (100 nM final) (IIa/TM) were added to activate potential TAFI in the sample. Then, samples were subjected to a quantitative TAFIa assay in which the concentration of TAFIa is determined from a standard curve. The data shown are the means of at least two independent experiments performed in duplicate; the error bars represent the standard errors of the mean. **B.** HepG2 medium, THP-1 lysate, THP-1ma medium and THP-1ma lysate samples with or without IIa/TM treatments were subjected to the TAFIa assay in the presence or absence of potato tuber carboxypeptidase inhibitor (PTCI, 50 µg/mL final). The data shown are the means of at least three independent experiments performed in duplicate; the error bars represent the standard errors of the mean.

Chapter 3: Regulation of *CPB2* gene expression in megakaryocytes, platelets, and monocyte/macrophage cells

3.1 Statement of co-authorship

This chapter consists, in part, of data published in *Journal of Thrombosis and Haemostasis* (Figures 11-12, Table 3) (71). Dr. M. Garand participated in the data collection and presentation of Figure 10. He also performed the western blot analysis for the data shown in Figure 11. All of the remaining data were collected and analyzed by J. Lin. Sections of the manuscript related to platelet data were adapted from reference (71). The rest of the manuscript was written by J. Lin with editorial assistance from Drs. M. Garand, M. Koschinsky and M. Boffa.

3.2 Abstract

Thrombin-activable fibrinolysis inhibitor (TAFI) is a carboxypeptidase zymogen that, once activated to form TAFIa, down regulates fibrinolysis by cleaving lysine residues from partially degraded fibrin. TAFIa can also inactivate pro-inflammatory peptides such as anaphylatoxins and bradykinin, suggesting that TAFI may possess an anti-inflammatory property. Although the liver is the main source of plasma TAFI, TAFI has also been identified in platelets and PMA-treated Dami and THP-1 cells. It has been hypothesized that platelet TAFI arises from *CPB2* gene expression in megakaryocytes. Using immunocytochemistry, we now report the identification of TAFI in CD163-expressing mononuclear cells and CD41-expressing megakaryocytes from human bone marrow. In addition, we confirm the presence of TAFI in the supernatent of washed thrombin-stimulated platelets and found that platelet TAFI is very similar

in electrophoretic mobility to plasma-derived TAFI. We also show that platelet-derived TAFI is capable of cleaving lysine-residues from fibrin degradation products. Using real-time RT-PCR, we found that *CPB2* mRNA abundance was increased up to 8-fold 48 hours after PMA treatment in Dami cells. Using transfection experiments with luciferase reporter plasmids containing progressive deletions of the human *CPB2* 5'-flanking region, we identified the sequences between -620 and -417 (relative to the transcription start site) to be responsible for the enhanced *CPB2* gene transcription. Together, these data provide further evidence supporting the idea that platelet TAFI is generated from *CPB2* gene expression in megakaryocytes. To study *CPB2* gene regulation in monocytes and macrophages with external stimuli, real-time RT-PCR and the luciferase reporter assay were used to quantify *CPB2* mRNA expression and to study promoter activities, respectively. An 85% decrease in *CPB2* mRNA level was observed 24 hours after PMA treatment in THP-1 cells. Transfection experiments using luciferase reporter plasmids showed an approximately 50% decrease in promoter activity in THP-1 cells 24 hours after PMA treatment (for each construct between -2699 -140). An initial increase (1.5- and 1.3-fold for THP-1 and differentiated THP-1 cells, respectively) followed by a decrease (of approximately 60%) in *CPB2* mRNA level was observed for THP-1 and differentiated THP-1 cells within 48 hours of treatment with lipolysaccharide. Together, our findings suggest novel modes of regulation of *CPB2* gene expression as well as roles for TAFI pathway beyond regulation of fibrin clot breakdown.

3.3 Introduction

Platelets constitute a critical component of the hemostatic response (8). In addition to their roles as the initial hemostatic structure and in amplifying the coagulation pathway, platelets influence fibrinolysis through a variety of mechanisms (103). Platelet-rich thrombi are more resistant to fibrinolysis than clots composed of fibrin alone (104). This differential lysis rate is probably the result of structural differences between thrombi dictated by the number and distribution of platelets, and platelet secretion of antifibrinolytic factors, including α_2-antiplasmin and plasminogen activator inhibitor (PAI-1) (104;105). An additional component that has been reported to be released from platelets that may regulate fibrinolysis is thrombin-activatable fibrinolysis inhibitor (TAFI) (5).

Monocytes and macrophages are widely recognized for their roles in the host inflammatory response to bacterial infection. Macrophages also accumulate in the vessel wall and sustain the inflammatory response as seen in atherosclerosis. Studies have demonstrated an increasingly important role for monocytes in thrombosis (1;8;103;106). Monocytes constitute a major source of blood tissue factor. Moreover, an increase in tissue factor expression is observed when monocytes are stimulated with lipopolysaccharides (LPS) as well as when they transmigrate through the arterial wall and differentiate into macrophages (106). Monocytes also form aggregates with platelets at the site of vascular injury, thus have been implicated in influencing the structure of thrombi (103;106).

TAFI is a single-chain glycoprotein zymogen that circulates in human plasma at a concentration of approximately 100-300 nM (3). Human plasma TAFI is expressed in the liver, and mature, circulating TAFI consists of 401 amino acids with an apparent molecular mass of 60

kDa on sodium dodecyl-sulfate polyacrylamide gel electrophoresis (SDS-PAGE) (15). This differs from the predicted peptide mass of 48 kDa because of *N*-linked glycosylation at four sites on the amino-terminal activation peptide (Asn22, Asn51, Asn63, and Asn86) (23). Proteolytic cleavage of this 92 amino acid amino-terminal fragment gives rise to activated TAFI (TAFIa), a 35-kDa zinc ion-dependent carboxypeptidase B-like enzyme (23). Once exposed, the active site of the enzyme moiety catalyzes the removal of carboxyl-terminal lysines and arginines from protein and peptide substrates. TAFIa attenuates fibrinolysis by removing the carboxyl-terminal lysines from partially degraded fibrin that mediate positive feedback in the fibrinolytic cascade (2).

Mosnier and coworkers (5), reported the existence of a distinct pool of TAFI located in platelets. The platelet-derived TAFI could be activated by thrombin-thrombomodulin, and was capable of cleaving both small (hippuryl-arginine) and macromolecular (Desafib X) substrates. Immunofluorescence microscopy indicated that TAFI was present in granules within the platelet. Two lines of evidence suggested that platelet TAFI originates from endogenous synthesis in megakaryocytes, rather than uptake from plasma. First, expression of *CPB2* mRNA in megakaryocytic cell lines was detected by reverse transcription polymerase chain reaction (RT-PCR). Second, platelet TAFI migrated much faster on SDS-PAGE (apparent molecular mass of 50 kDa) than plasma-derived TAFI (60 kDa). This was ascribed to differences in *N*-linked glycosylation, as both zymogens exhibited the same electrophoretic mobility after deglycosylation with PNGase F.

Most recently, our laboratory demonstrated the expression of *CPB2* mRNA in monocytic cell line THP-1 as well as in human peripheral blood mononuclear cells (76). We also detected TAFI protein in THP-1 differentiated macrophage-like cells (THP-1ma) using

immunocytochemistry and functional TAFIa assay (22). In addition, our laboratory showed that platelet-derived TAFI can attenuate the lysis of platelet-rich thrombus *in vitro* (71). In the present study, we document the presence of TAFI in bone marrow and verify its presence in platelets. Platelet TAFI is secreted following platelet activation in a manner consistent with its localization in α-granules. We found little, if any, difference in electrophoretic mobility between plasma and platelet TAFI, in contrast to the previous finding. In addition, we set out to study the effect of external stimuli such as phorbol myristate acetate (PMA) on *CPB2* gene expression in megakaryocytic cell line, Dami, and monocytic cell line, THP-1, as well as the effect of LPS in *CPB2* gene expression in THP-1 and differentiated-THP-1 cells.

3.4 Material and methods

3.4.1 Immunocytochemistry

For double immunofluorescence studies of bone marrow and bone marrow mononuclear cells (BMMNCs), unprocessed fresh human bone marrow was purchased from Lonza (Walkersville, MD, USA). Upon arrival, isolation of BMMNCs was performed immediately following the procedures described for PBMNCs (76). Meanwhile, unprocessed bone marrow was cultured in complete growth medium for Dami cells (described below) before fixing on the slides. For both unprocessed bone marrow and BMMNCs, cells were attached on clean microscope slides pre-coated with poly-L-Lysine using a smear technique and fixed with 1% (w/v) paraformaldehyde in PBS for 5 min. The slides were washed with PBS and incubated in blocking solution (5% (v/v) normal goat serum in PBS) at 37 °C for 30 min. followed by incubation with the indicated primary antibodies diluted in saponin buffer (0.025% saponin, 5

mM KPO_4, 2.5 mM PIPES pH 6.8, 1.25 mM EGTA, 0.5 mM $MgCl_2$, 5% normal goat serum) at 4°C overnight. Following two washes with PBS, cells were incubated with goat anti-mouse Alexa488-conjugated antibody (0.5 µg/mL final concentration; Invitrogen) and goat anti-rabbit IgG-Cy5 conjugated antibody (1:1,200 dilution, Abcam) in saponin buffer at room temperature for 1 hour. After two washes with PBS, cells were mounted to slides using an anti-fade mounting solution (Dako) containing DAPI (0.75 µg/mL, Sigma) and examined using a Leica DM IRB inverted fluorescence microscope powered by an X-Cite Series 120 Mercury light source, utilizing a 40× Leica HC× PL S-APO objective with NA = 0.75 and a Retiga 1300i black and white camera. Dilutions of primary antibodies were as follows: mouse anti-human TAFI monoclonal antibody T4E3 (84) (10 µg/mL final concentration), rabbit anti-CD 41/integrin alpha 2b (1: 100, Abcam), and rabbit anti-CD 163 (1: 100, Abcam).

3.4.2 Cell culture

All cells were maintained in a humidified incubator at 37 ºC under a 95% air/5% CO_2 atmosphere. Dami cells (human megakaryoblastic leukemia) (91) were the generous gift of Dr. David Lillicrap (Queen's University, Kingston, Canada) and were cultured in 100 mm tissue culture plates with complete growth medium containing RPMI 1640 medium (Invitrogen) adjusted to contain 4.5 g/L glucose, 10 mM HEPES, and supplemented with 10% FBS (ATCC) and 1% antibiotic-antimycotic. THP-1 cells (human acute monocytic leukemia; ATCC) (92) were cultured in 100 mm tissue culture plates with complete growth medium containing adjusted RPMI 1640 medium supplemented as described for Dami cells with the addition of 1.0 mM sodium pyruvate and 0.05 mM 2-mercaptoethanol. For differentiation of both Dami and THP-1 cells, phorbol myristate acetate (PMA) (Sigma) was added to a final concentration of 0.1 µM to cells at a density of 1×10^7 cells/mL for up to 72 hours. Where indicated, lipopolysaccharide

(LPS; *E. coli* 0111:B4; Sigma) was added to a final concentration of 100 ng/mL to the cells at a density of 1-2 × 10^6 cells/mL for up to 48 hours.

3.4.3 Reporter gene assay

Dami and THP-1 cells at density of 4 × 10^7 cells were washed twice with 1× Tris-buffered saline solution (TBSS, 25 mM Tris-HCl, 137 mM NaCl, 5 mM KCl, 0.6 mM Na_2HPO_4, 0.7 mM $CaCl_2$, 0.5 mM $MgCl_2$, pH 7.4) by centrifugation at 12 × g for 10 min. DEAE-dextran (160 µg/mL, Sigma) was mixed with 5 µL of firefly luciferase reporter plasmid (0.2 µM stock) (12) as well as 5 µg of Renilla luciferase (pRL-CMV) construct, as an internal control for differences in transfection and harvesting efficiency, in 500 µL of 1 × TBSS, and the mixture was added to the cells and incubated at 37 °C for 10 min. The reaction was stopped by adding 15 mL of 1× TBSS and washed two times with centrifugation. Cells were then resuspended in 30 mL of the respective complete growth media and incubated at 37 °C over-night. Where applicable, PMA (0.1 µM final) was added to the media for 24 hours. Cells were then washed 2 times with PBS and the cytoplasmic extracts were prepared using Passive Lysis Buffer (Promega) following the manufacturer's instructions. The firefly luciferase and Renilla luciferase activity assays were performed on the cytoplasmic extracts using Dual-Luciferase Reporter Assay System (Promega) following the manufacturer's instructions. The normalized luciferase activities were calculated by dividing the firefly luciferase activities by the renilla luciferase activities for each sample. The relative luciferase activities were calculated by dividing the normalized luciferase activities by the luciferase activity detected in cells transfected with a promoterless luciferase reporter plasmid (pGL3 Basic).

3.4.4 RNA extraction and quantitative real-time quantitative RT-PCR

The RNeasy Mini kit (Qiagen) was used for total RNA extraction according to the manufacturer's protocol. For quantitative real-time RT-PCR analysis, on-column DNase digestion during RNA purification was performed using the RNase-Free DNase Set (Qiagen) as recommended by the manufacturer. Real-time RT-PCR analysis was carried out on an Applied Biosystems ABI Prism 7500; procedures were as described (76). Primers and probes for Taqman (Applied Biosystems) were as described (76). The RNA standards for absolute quantification were generated as described (62). The absolute quantities of human *CPB2* mRNA detected were then normalized by dividing the quantity observed for each time point with the respective quantity observed for the 0 hr.

3.4.5 Preparation and activation of washed human platelet suspensions

Human platelets were obtained from pooled four-unit buffy coat donor packs obtained from the Kingston General Hospital. Pooled platelets were centrifuged at 1200 × *g* for 25 min at room temperature. The plasma supernatant was decanted, and platelets were resuspended in a total of 1 L of calcium-free Tyrode's buffer (CFTB; 137 mM NaCl, 2.7 mM KCl, 11.9 mM $NaHCO_3$, 0.42 mM NaH_2PO_4, 1 mM $MgCl_2$, 0.26 mM EGTA, 5 mM PIPES, pH 6.5) containing 0.35% (w/v) bovine serum albumin (BSA) (wash 1). Red blood cells and platelets not readily resuspended were discarded. Suspended platelets in CFTB were centrifuged at 1200 × *g* for 25 minutes at room temperature. Platelets were washed a second time in fresh CFTB (wash 2), centrifuged again at 1200 × *g* and then resuspended in a final volume of 100 mL in HEPES-Tyrode's buffer (HTB; 137 mM NaCl, 2.7 mM KCl, 11.9 mM $NaHCO_3$, 0.42 mM NaH_2PO_4, 1 mM $MgCl_2$, 2 mM $CaCl_2$, 5 mM HEPES, pH 7.4). Platelet counts were determined in a haemacytometer (Reichert Analytical Instruments). For activation, the final suspension of

isolated platelets was adjusted to a concentration of 2.5×10^9 platelets/mL in HTB and activated by the addition of 5 nM thrombin (Haematologic Technologies) for 30 minutes at room temperature with occasional mixing; this was followed by pelleting of the activated platelets by centrifugation for 5 min at 3000 × *g* at room temperature. As a control, a portion of the suspension was removed prior to addition of thrombin, and the platelets were pelleted and discard (platelet suspension). Hence, the TAFI content in the supernatant prior to and following thrombin activation of the platelets can be directly compared.

3.4.6 TAFI activation and western blot analysis

For TAFI activation, samples were supplemented with $CaCl_2$ (5 mM), human thrombin (25 nM) (Haematologic Technologies), and rabbit lung thrombomodulin (100 nM) (Haematologic Technologies) and incubated at room temperature for 15 min. The reaction was then stopped by the addition of PPAck (100 nM).

For western blot analyses using sheep anti-human TAFI antibodies (Affinity Biologicals), SDS-PAGE was performed as described (76) on 12% polyacrylamide gels under reducing conditions. For western blot analyses using sheep anti-vWF antibodies (Haematologic Technologic), SDS-PAGE was performed on 8% polyacrylamide gels under reducing conditions. Proteins were electrophoretically transferred to a PVDF membrane (Millipore) and blocked with blocking buffer consisting of 5% (w/v) non-fat milk in 1× TBST (15 mM Tris-HCl pH 7.6, 140 mM NaCl, 0.05% (v/v) Tween 20) at 4°C over night. Next, blots were incubated with polyclonal sheep anti-human vWF antibody (1:3,000 dilution in 1× TBST) at room temperature for 1.5 hours. The blots were then washed 10 times with H_2O and incubated with horseradish

peroxidase-conjugated rabbit anti-sheep IgG secondary antibody (Pierce) (1:7,500 dilution in 1× TBST) at room temperature for 1 hour. The membrane was then washed 20 times with H_2O followed by a 10-min wash in 1× TBST and another 20 times with H_2O. Immunoreactive bands were visualized as described below.

For western blot analysis using sheep-anti PF4, the procedures are as described (76) with the following changes: samples were electrophoresed on a 20% polyacrylamide SDS-PAGE gel under reduced condition. Sheep-anti human PF4 antibody (Affinity Biologicals) as well as the horseradish peroxidase-conjugated rabbit anti-sheep IgG secondary antibody were diluted 1: 7,500 in 1× NET containing 3% milk.

In all cases, immunoreactive bands were visualized using SuperSignal West Femto Maximum Sensitivity Substrate (Thermo Scientific) and a FluorChem Q Gel Imaging System (Alpha Innotech).

3.4.7 TAFIa assay

The assay was implemented as described by Kim and coworkers (22). Eighty microliters of a solution in HEPES-buffered saline (HBS) of 1.0 μM QSY9 C5-maleimide-conjugated high molecular mass fibrin degradation products and 75 nM Fluo-plasminogen was added to wells of a white opaque microtiter plate, and fluorescence intensity was monitored with excitation and emission wavelengths of 480 and 520 nm, respectively, with a 495-nm emission cutoff filter, using a Spectra Max M5e fluorescence plate reader (Molecular Devices).

3.5 Results

3.5.1 Detection of human TAFI protein in human bone marrow

Previously, we reported the detection of human TAFI protein in the lysates of a megakaryocytic cell line (Dami) as well as conditioned medium and lysates of differentiated Dami cells using a TAFIa assay (76). We also detected *CPB2* mRNA in peripheral blood mononuclear cells (PBMNC) using RT-PCR and qRT-PCR, as well, we detected TAFI protein in the conditioned medium of differentiated THP-1 (THP-1ma) cells using TAFIa assay. Moreover, we reported the detection of TAFI protein in dDami and THP-1ma cells using immunocytochemistry (76). To provide further physiological evidence for TAFI expression in megakaryocytes and monocytes, we performed immunocytochemistry using human bone marrow (BM) and bone marrow mononuclear cells (BMMNC) to co-localize TAFI with cell-type specific markers: CD163 for monocytes (107) and CD41 for megakaryocytes (108;109).

Smears of bone marrow or bone marrow mononuclear cells (BMMNC) were prepared on poly-L-lysine pre-coated slides and co-stained with monoclonal mouse anti-human TAFI antibody, CD163 or CD 41, and DAPI to visualise the nuclei. The preliminary result is shown in Figure 10. Monocyte marker CD163 is present in both BMMNC and unprocessed bone marrow, and TAFI was found to be co-localized with CD163-expressing cells in both sample types (Fig. 10A), providing further evidence for TAFI expression in monocytes. In addition, TAFI was found to be detected in CD41-expressing magakaryocytes in bone marrow sample (Fig. 10B), consistent with the reported TAFI expression in Dami and dDami cells (76). These results also provide physiological evidence for TAFI expression in megakaryocytes and support the notion that Dami is a suitable model to study TAFI gene expression in megakaryocytes. Moreover, it

also supports the hypothesis that platelet TAFI originates from *CPB2* gene expression in megakaryocytes.

3.5.2 TAFI detection in human platelet releasates

It has been shown on only one occasion that TAFI is released from human platelet following activation by thrombin (5). We decided to recapitulate the result of that report and confirm the existence of a platelet-derived TAFI. First, we performed western blot analyses at each step of platelet releasate preparation (Fig. 11). The amount of plasma-derived TAFI decreases with successive washing, and eventually became undetectable in the final platelet suspension. To the final platelet suspension, thrombin was added to activate platelets, resulting in a strong detection of TAFI in the platelet releasate. The releasable nature of platelet TAFI is consistent with the notion that TAFI resides within secretory granules inside the platelets.

The identity of the immunoreactive bands detected by western blotting for each step of the platelet releasate preparation was confirmed by adding thrombin and thrombomodulin (IIa/TM) into a small aliquot representing each washing step. The cleavage of TAFI, which causes the release of the activation peptide, yield a 35 kDa TAFIa band (Fig. 11). The apparent molecular mass of platelet TAFI was found to be approximately 60 kDa, similar to that of plasma-derived TAFI as well as TAFI secreted from differentiated Dami cells (Fig. 4A and D, (76)). These findings are considerably different to the previously reported size difference (50 vs. 60 kDa) between the platelet-derived and plasma-derived TAFI (5).

For additional validation of our experimental design, we performed western blot analysis with antibodies against von Willebrand factor (vWF) and platelet factor 4 (PF4) in parallel with

the TAFI western blot. VWF can be found in both plasma and the α-granules of human platelets. Consistent with the detection of TAFI protein, the amount of vWF (270 kDa) is gradually decreased to a nearly undetectable level during the washing of platelets. Although a small amount of vWF is present in the washed platelet suspension, activation of platelets with thrombin resulted in a strong release of vWF in the platelet releasate (Fig. 12). These results suggest that we achieved the clearing of contaminating plasma protein from our platelet preparation and that we can successfully trigger the release of TAFI upon platelet activation. Furthermore, PF4 (7.8 kDa) was only observed in the platelet releasate (Fig. 12). Altogether, these results suggest that platelet-derived TAFI is secreted similarly to other protein known to be stored within the α-granules and can be secreted upon platelet activation.

Next, we used a highly sensitive method of detection of TAFI, based on the capability of TAFIa to cleave the lysin residue from fibrin degradation products (TAFIa assay described in the Materials and Methods section). The results confirmed our western blot analyses that there was negligible amount of TAFI detected in the second wash fraction and in the final platelet suspension (in most trials, no TAFIa activity was detected in these samples). We calculated the concentration of TAFIa in the platelet releasate (originating from 2.5×10^9 platelet per mL) to be 0.55 ± 0.17 nM. This concentration of TAFIa corresponds to the secretion of 12 ± 4 ng of activatable TAFI per 10^9 thrombin-stimulated platelets, while Mosnier and coworkers reported 25 ± 5 ng per 10^9 thrombin-stimulated platelets. Notably, the intraplatelet TAFI concentration is similar in magnitude to the concentration of TAFI in plasma (5).

3.5.3 Transcriptional activity of human *CPB2* promoter in Dami and THP-1 cells

Previous studies from our laboratory (76) had established that *CPB2* mRNA is expressed in cell types including Dami, THP-1, and PBMNC. In the current study, we also demonstrated the detection of TAFI protein in megakaryocytes and monocytes from human bone marrow (Fig. 10). Our next goal was to study the mechanisms that direct the cell-type specific *CPB2* gene expression in megakaryocytes and monocytes using the Dami and THP-1 cell lines, respectively.

First, we assessed whether the 5'-flanking region of *CPB2* can support transcription in Dami and THP-1 cells. Luciferase reporter plasmids containing progressive deletions of the TAFI 5'-flanking region of human *CPB2* promoter, as described in Boffa and coworkers (12), were transfected into both cell types using DEAE-dextran. Each reaction contained an equimolar amount of the respective reporter plasmids, as well as a fixed amount of a renilla luciferase (pRL-CMV) internal control plasmid in order to correct for differences in transfection and harvesting efficiencies. Luciferase activity was expressed relative to the promoterless luciferase reporter plasmid construct (pGL3 Basic).

As shown in Figure 13, transfection of human *CPB2* promoter constructs representing progressive deletions from -2699 to -140 resulted in a gradual increase in relative luciferase activities in Dami cells. The -417, -236, -140, and -110 constructs showed higher luciferase activities than pGL3 Basic, indicating that the proximal region of the 5'-flanking region of the *CPB2* gene contains sequences capable of directing transcription in Dami cells. The constructs from -2699 to -620 generated relative luciferase activities lower than pGL3 Basic, suggesting that the region upstream of -620 contain repressor elements. Transfection of a reporter plasmid containing the longest *CPB2* promoter (-2699 construct) available into THP-1 cells resulted in a

5-fold higher luciferase activity than pGL3 Basic, indicating that the 5'-flanking region of the *CPB2* gene contains sequences capable of directing transcription in THP-1 (Fig. 13). Similar to HepG2 cells (12), transfection of the -73 construct abolished the relative Luciferase activities to the level of the promoterless plasmid in both Dami and THP-1 cells, suggesting that the sequence between -110 and -73 harbours promoter elements crucial for the *CPB2* gene expression in these cell types.

3.5.4 Effect of PMA on *CPB2* gene expression in Dami and THP-1 Cells

As reported previously (76), *CPB2* mRNA is detected in both Dami and PMA-treated Dami (dDami) cells using RT-PCR and qRT-PCR analyses (Fig. 4-5). To investigate *CPB2* gene expression throughout Dami differentiation, Dami cells were treated with PMA for up to 60 hours, and total RNA isolated at various time points throughout the differentiation was subjected to qRT-PCR analysis using the primers and probe specific for human *CPB2* mRNA (Fig. 14A). A progressive increase in *CPB2* mRNA abundance up to nearly 8-fold higher than the control was observed within 48 hours of PMA treatment with significant increases after 24 hours.

To assess if the increase in *CPB2* mRNA abundance observed with PMA treatment in the Dami cells (Fig. 14A) corresponds to a change in transcriptional activity, we measured the effect of PMA on Dami cells that had been transiently transfected with a luciferase *CPB2* promoter-reporter plasmid. The constructs used contained progressive deletions of the human *CPB2* 5'-flanking region, with -2699 constructs corresponding to the longest length of 5'-flanking region (12). Dami cells were transfected with equimolar amounts of the respective constructs; cells were then allowed to grow overnight followed by PMA treatment for 24 hours. Luciferase activity was

expressed relative to that of the promoterless luciferase reporter plasmid pGL3 Basic. As shown in Figure 14B, PMA treatment resulted in increases in relative luciferase activities from -2699 to -620 constructs. Deletion of the sequence between -620 and -417 resulted in almost complete elimination of the increase, suggesting that this region harbours promoter elements responsible for enhanced *CPB2* gene transcription as Dami cells differentiate further along the megakaryocytic lineage.

We have also demonstrated that *CPB2* mRNA is expressed in both THP-1 monocytic cells and PMA-treated THP-1 macrophage-like cells (THP-1ma) using RT-PCR and qRT-PCR (76) (Fig. 4-5). To investigate TAFI gene expression throughout THP-1 differentiation, THP-1 cells were treated with PMA for up to 72 hours, and total RNA isolated at various time points throughout the differentiation was subjected to qRT-PCR analysis using the primers and probe specific for human *CPB2* mRNA. The *CPB2* mRNA quantification was normalized to that of the 0 hr time point (Fig. 15A). A progressive decrease in the *CPB2* mRNA abundance to a maximum of approximately 20% of undifferentiated cells was observed within 24 hours of PMA treatment, with significant decreases observed after 5 hours of treatment.

To assess if the decrease in *CPB2* mRNA abundance observed with PMA treatment in THP-1 cells (Fig. 15A) corresponds to a change in transcriptional activity, we measured the effect of PMA on THP-1 cells that had been transiently transfected with *CPB2* promoter-luciferase reporter plasmids. The experimental procedure and plasmids utilized were the same as described for Dami cells above. As shown in Figure 15B, PMA treatment resulted in approximately a 50% decrease in relative luciferase activities from -2699 to -140 constructs. These data suggest that the decrease in *CPB2* mRNA level observed in THP-1 cells with PMA treatment is caused, at least in part, by a decrease in *CPB2* promoter activity.

3.5.5 Effect of LPS on *CPB2* mRNA abundance in THP-1/THP-1ma cells

LPS is the main structural component of the cell membrane of Gram-negative bacteria. LPS can induce an inflammatory response by stimulating the production of pro-inflammatory proteins such as complement proteins, tissue necrosis factor α (TNFα), NFκB, IL-1 and IL-6 (47;72). To investigate the effect of LPS on human *CPB2* mRNA expression, THP-1 or THP-1ma were treated with LPS for up to 48 hours; total RNA isolated at each time point was subjected to qRT-PCR analysis, and the data shown are normalized to the 0 hr time point. The results for THP-1 and THP-1ma are shown in Figure 16A and 16B, respectively. A biphasic response of *CPB2* mRNA abundance was observed for both cell types. A statistically significant increase in *CPB2* mRNA abundance was observed, peaking at 0.5 hr for THP-1 and 1.5 hr for THP-1ma, followed by significant decreases after the 12 and 10 hr time points for THP-1 and THP-1ma, respectively. An approximate 60% decrease in *CPB2* mRNA abundance was observed for both cell types after LPS treatment for 24 hours.

3.6 Discussion

Liver is the main source for plasma TAFI (12). Over the past decade, sources for extra-hepatic expression of TAFI have been reported including human hippocampus, adipocytes of patients with type II diabetes, HUVECS, platelets, megakaryocytic cell lines (MEG-01, Dami, and CHRF-288), and most recently the monocytic cell line THP-1 as well as peripheral blood mononuclear cells (4-6;76). However, the actual presence of TAFI protein in human megakaryocytes and monocytes is still unproven. In the current study, we report for the first time the detection of TAFI in CD41-expressing megakaryocytes and CD163-expressing monocytes

from human bone marrow samples using immunocytochemistry (Fig. 10). These results prove the expression of TAFI protein in these cell types by using a physiologically-relevant source of cells, versus immortalized cell lines, thereby solidifying the *in vitro* data regarding the existence of extra-hepatic TAFI in megakaryocytic and monocytic cell lines reported thus far.

Mosnier and coworkers (5) reported an apparent difference in molecular mass between platelet-derived (~ 50 kDa) and plasma-derived (~ 60 kDa) TAFI, which subsequently attributed to variation in glycosylation patterns. However, in the current study, we detected only subtle, if any, difference in the apparent molecular mass between platelet-derived and plasma-derived TAFI (Fig. 11). Moreover, this observation is consistent with our previous report that megakaryocytic-derived TAFI was observed to be a ~60 kDa protein on SDS-PAGE (Fig. 7D) (76). It is possible that subtle differences in the composition of *N*-linked glycans exist between plasma-derived and platelet-derived TAFI. These differences, in turn, may give rise to functional differences between these forms of TAFI. Although plasma-derived TAFI and recombinant TAFI (rTAFI) have clear differences in glycosylation, their functional properties are almost identical (27).

It is tempting to speculate that plasma-derived and platelet-derived TAFI have similar functionality due to the striking size and concentration similarities between them. Indeed, we demonstrated, via the TAFIa assay, that platelet-derived TAFI possesses the ability to cleave lysine residues from fibrin degradation products, suggesting that platelet-derived TAFI may play a significant role in affecting fibrinolysis *in vivo*. In typical human plasma, platelet-derived TAFI would constitute about 0.1% of the total plasma TAFI pool (5). However, when platelets aggregate and form a platelet-rich thrombus, platelet-derived TAFI may be a significant factor capable of influencing clot lysis time. Mutch and coworkers (110) have detected TAFI within

thrombi obtained from human platelets. They observed TAFI along fibrin strands as well as within platelet-rich area. It is tempting to speculate that the TAFI detected by the authors were platelet-derived TAFI.

Evidence for megakaryocytic-derived TAFI as the source of platelet TAFI was first proposed by Mosnier and coworkers (5) where authors observed *CPB2* mRNA in intermediate- and late-stage megakaryocytic cell lines. Indeed, data from our laboratory (76) further indicated that megakaryocytic cell lines both express *CPB2* mRNA (Fig. 4-5) and secrete TAFI protein (Fig. 7D and 9A). These data in turn suggest that TAFI might be actively sequestered in platelet granules following endogenous mRNA translation. This assertion is further strengthened by the detection of TAFI protein in CD41-expressing megakaryocytes from human bone marrow (Fig. 10).

After demonstrating that Dami and THP-1 are suitable models for studying TAFI gene regulation in megakaryocytes and monocytes, respectively (76), we next set out to investigate TAFI gene regulation in these cell types. Specifically, we are interested in the changes in TAFI gene expression when treated with external stimuli such as PMA and LPS. First, we tested whether the 5'-flanking region of the *CPB2* gene can support transcription in Dami and THP-1 cells. As shown in Figure 13, the *CPB2* promoter is active in both cell types. Similar to what was observed for HepG2 cells (12), the transfection of the -73 construct abolished the relative luciferase activities to the level of pGL3-basic in both cell types, suggesting that the sequence between -110 and -73 contains minimal promoter elements crucial for *CPB2* gene expression in a variety of cell types including HepG2, Dami and THP-1. Within this region, we have reported the binding of nuclear-factor Y (NF-Y) and hepatic nuclear-factor 1 (HNF-1) in HepG2 (14). The expression of HNF-1 has not been reported for megakaryocytes and monocytes. However, NF-Y

is expressed in both megakaryocytic cell line and monocytes (111;112); therefore, it is likely that the binding of NF-Y plays a role in enhancing *CPB2* promoter activities in these two cell types *in vivo*.

The explanation for the lower promoter activities from the longest *CPB2* promoter constructs available in our laboratory, -2699 to -620, compared to that of the empty vector in Dami cells (Fig. 13) is not clear. One possibility is that the region between -2699 and -620 contains element(s) that can either enhance or repress *CPB2* promoter activity, depending on the specific cellular environment. One example of such DNA element that acts as either an enhancer or a silencer depending on what binds to it is thyroid hormone response element (TRE) (113). In the absence of its ligand, thyroid hormone receptor (TR) can repress the transcription of many genes such as β-amyloid precursor protein (APP) (114). On the other hand, when TR is bound to its ligand such as triiodothyronine (T3), there is a conformational change of TR such that it is then able to recruit other activator proteins to form a multi-protein complex that enhance the promoter activity when binds to TRE (113). It will be interesting to see if *CPB2* promoter also possesses analogous dual-function response elements between sequence -2699 and -620.

Consistent with the hypothesis that platelet-derived TAFI originates from megakaryocytes, we observed a significant increase in *CPB2* mRNA expression 24 hours after PMA treatment (Fig.14A). Such an increase is attributable, at least in part, to an increase in *CPB2* promoter activity. Transfection experiments with progressive deletion of *CPB2* promoter constructs into Dami cell showed an increase in *CPB2* promoter activity upon PMA treatment for 24 hours (Fig 14B). Deletion of the sequence between -620 and -417 resulted in complete elimination of the increase in promoter activity after PMA treatment, suggesting that this region harbours promoter elements responsible for enhanced *CPB2* gene transcription as Dami cell

differentiate into more mature megakaryocytes. The observation that after PMA treatment, a significant increase in promoter activity can be achieved even when the promoter activity is lower than the empty vector, suggested that the "PMA-responsive element" is located between sequence -620 and -417, and it does not interfere with the action of enhancer/repressor element present between -2699 and -620, as discussed above, in Dami cells.

In contrast to what we observed in Dami cells, a significant decrease in *CPB2* mRNA abundance was observed 5 hours after PMA treatment in THP-1 cells, with an approximately 85% decrease in *CPB2* mRNA abundance after 24 hours of PMA treatment (Fig. 15A). To assess if such decrease in TAFI mRNA abundance corresponds to a change in transcriptional activity, we measured the effect of PMA on THP-1 cells transfected with *CPB2* promoter-luciferase reporter plasmid as described for Dami cells above. A significant decrease (~50 % for most constructs) in *CPB2* promoter activity after 24 hours of PMA treatment was observed with all the *CPB2* promoter constructs used except for -73 and pGL3 Basic (Fig. 15B), suggested that a decrease in promoter activity is, at least partially, responsible for the observed decrease in *CPB2* mRNA abundance after PMA treatment. The fact that the PMA treatment of Dami and THP-1 did not increase or decrease the *CPB2* promoter activity, respectively, as much as the changes in *CPB2* mRNA levels observed, suggests the possibility that in addition to the transcriptional regulation through the *CPB2* promoter, alterations in the stability of *CPB2* mRNA may also play a role in the changes in *CPB2* mRNA abundance in these cell types upon PMA treatment.

When THP-1 and THP-1ma cells were treated with LPS for up to 48 hours, the levels of *CPB2* mRNA showed a biphasic pattern with an initial increase in *CPB2* mRNA abundance up to 0.5 and 1.5 hours, respectively, followed by a progressive decrease (Fig. 16). The mechanism that is responsible for the biphasic response observed is unknown. However, it might be postulated

that the increase in *CPB2* mRNA reflects the potential need for enhanced TAFI expression in the beginning of the acute phase to prevent hyper-inflammation at the site of tissue injury through inactivation of pro-inflammatory cytokines such as Opn and C5a (48). In addition, the increase in *CPB2* mRNA level after LPS treatment may also reflect the need for TAFI to down-regulate fibrinolysis at the site of injury as a recent study showed that LPS-stimulated monocytes prolonged clot lysis time compared to unstimulated ones (115). With respect to the ultimate decrease in *CPB2* mRNA abundance, it is reasonable to hypothesize that LPS induces the expression of inflammatory cytokines in these cells, which then modulate *CPB2* mRNA processing and stability in a manner analogous to liver cells (57;62).

In conclusion, this current study evaluated the expression of TAFI in megakaryocytes and monocytes isolated from human bone marrow and also evaluated the changes of *CPB2* mRNA abundance as well as promoter activity in different cell types with external stimuli. TAFI was detected in CD41-expressing megakaryocytes. In addition, an increase in *CPB2* mRNA abundance as well as an increase in promoter activity when Dami cells were differentiated to more mature megakaryocytes was observed, indicating that platelet TAFI, at least in part, originates from megakaryocytic expression of *CPB2* gene. TAFI is also detected in CD163-expressing monocytes from human bone marrow. An overall decrease in *CPB2* mRNA abundance was observed in THP-1 cells after PMA and/or LPS treatments for 24 hours. A decrease in promoter activity was observed in THP-1 after PMA treatment, consistent with the notion that TAFI is a negative acute phase protein (57). However, more studies are required to elucidate the role of monocytic TAFI in inflammation and hemostasis.

3.7. Acknowledgements

The authors wish to thank B. Zagorac at University of Windsor for processing and culturing the human bone marrow, J. Foley and N. Feric at Queen's University for the experimental protocols and Fluo-plasminogen, respectively, and Tanya Marar at University of Windsor for purified recombinant TAFI protein used in the TAFIa assay.

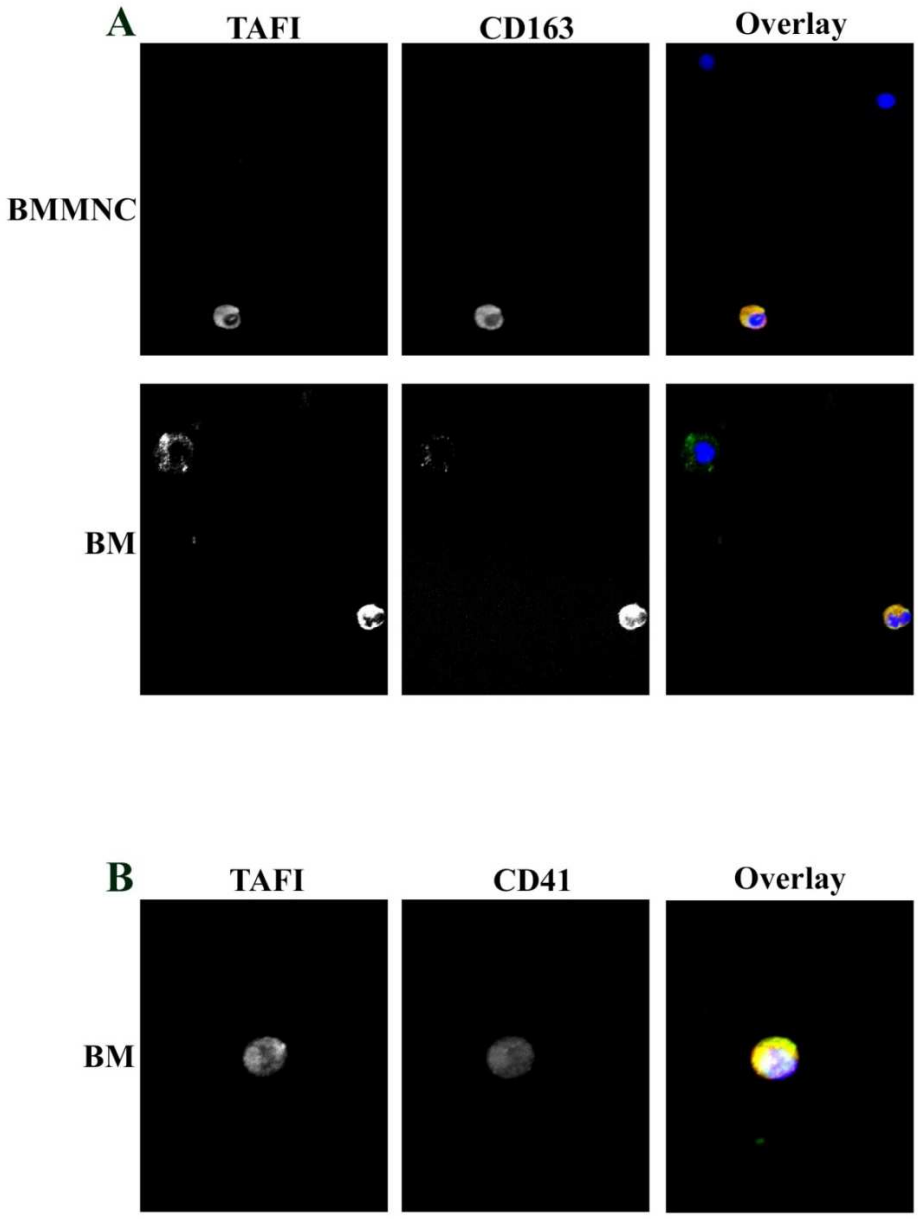

Figure 10. Detection of human TAFI protein in bone marrow samples using immunocytochemistry. Bone marrow mononuclear cells (BMMNC) or bone marrow (BM) were smeared on poly-L-lysine pre-coated coverslips, fixed with paraformadehyde, and co-stained for **A.** TAFI and CD163, or **B.** TAFI and CD41. Colocalization of red and green signals (yellow) is shown in the overlays. Nuclei (blue) were visualised with DAPI.

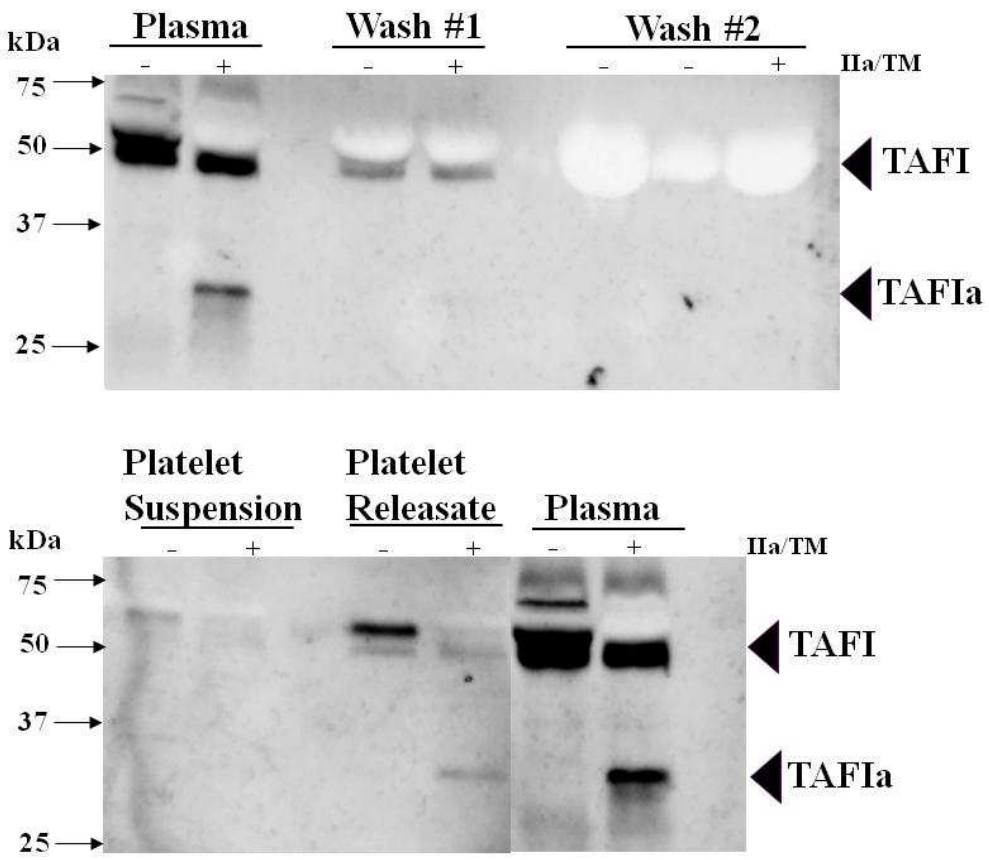

Figure 11. Washing of human platelets and secretion of TAFI. The presence of TAFI in the medium of human platelets throughout the isolation procedure was analyzed by western blot. Human platelets were centrifuged and washed twice with calcium-free Tyrode's buffer; the final platelet suspension was activated by thrombin (IIa) in HEPES-Tyrode's buffer. Where indicated, IIa and thrombomodulin (TM) were used to activate TAFI. Samples were subjected to SDS-PAGE on 12% polyacrylamide gels under reducing conditions, followed by western blot analysis with polyclonal sheep-anti human TAFI antibody. TAFIa, activated TAFI.

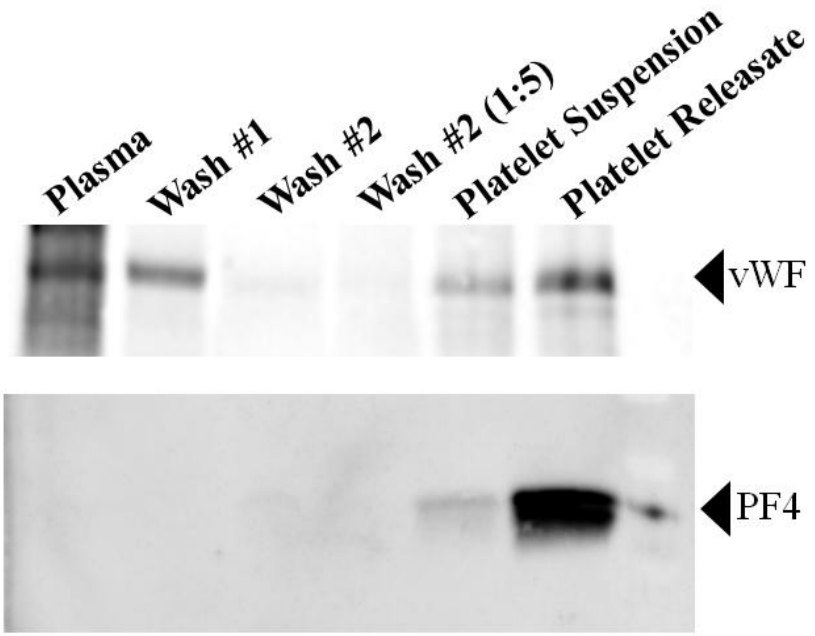

Figure 12. Washing of human platelets and secretion of von Willebrand factor (vWF) and platelet factor 4 (PF4). The presence of vWF and PF4 throughout the platelet washing and activation process were analyzed by western blot. Human platelets were washed and then activated by thrombin. Samples were subjected to SDS-PAGE on 8% or 20% polyacrylamide gels under reducing conditions for vWF-specific and PF4-specific western blot analysis, respectively.

Table 3. Washing of human platelets and secretion of TAFI

Fraction	[TAFIa](nM)	[TAFI](µg/mL)
Plasma	$1.5 \times 10^2 \pm 0.5 \times 10^{2*}$	(6-12µg/mL)
Wash 1	$0.20 \pm 0.04^{*}$	
Wash 2	$0.017 \pm 0.017^{*}$	
Platelet suspension	$0.014 \pm 0.014^{*}$	
Platelet releasate	$0.55 \pm 0.17^{**}$	(1.9µg/mL/ platelet)

[Means of 3(*) or 4(**) independent platelet washing experiments]

Platelet-rich plasma was obtained from a hospital blood bank and were washed as described in Material and methods. The TAFI concentration in each fraction was calculated from the amount of TAFIa detected with the TAFIa assay. The data shown are the means ± standard errors of the mean (71).

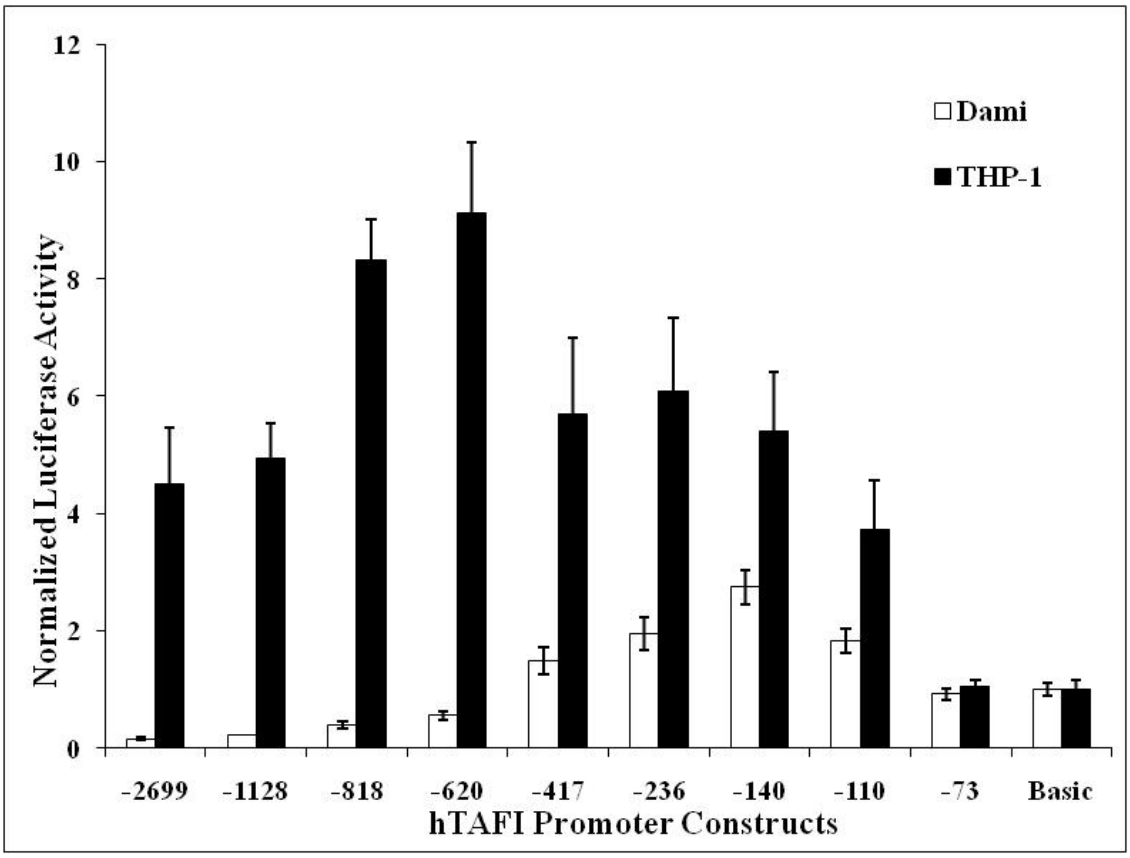

Figure 13. *CPB2* promoter is active in both Dami and THP-1 cells. Progressive deletion of promoter constructs containing human *CPB2* 5'-flanking region were transiently transfected (at equimolar concentrations) into Dami and THP-1 cells using DEAE-dextran for 3 hours and the cells were allowed to grow for a further 24 hours. Included in each transfection was an equal amount of renilla luciferase (pRL-CMV) construct as an internal control for differences in transfection and harvesting efficiency. Firefly and renilla luciferase activity assays were performed on cytoplasmic extracts prepared from the transfected cells. Firefly luciferase activities were normalized by dividing by the renilla luciferase activities. The relative luciferase activities (mean ± standard deviation of three independent transfection experiments) are calculated by dividing the luciferase activity observed with the luciferse activity detected in the cells transfected with a promoterless luciferase reporter plasmid (pGL3 Basic).

A.

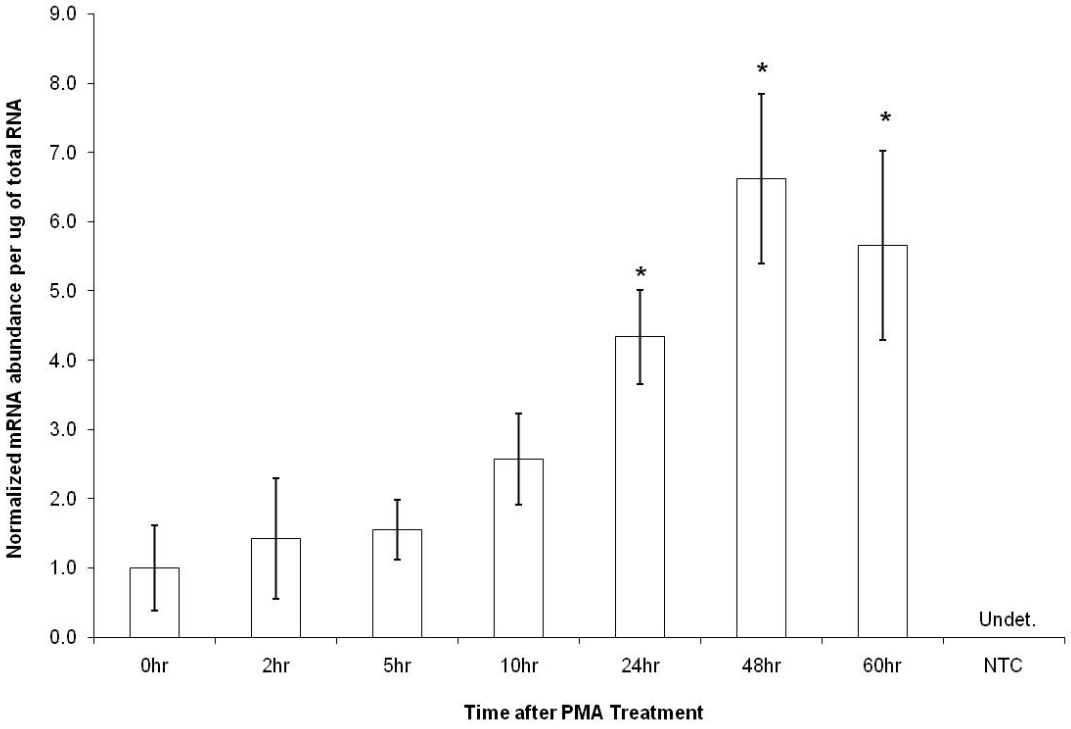
Normalized mRNA abundance per ug of total RNA
9.0
8.0
7.0
6.0
5.0
4.0
3.0
2.0
1.0
0.0
*
*
*
Undet.
0hr
2hr
5hr
10hr
24hr
48hr
60hr
NTC
Time after PMA Treatment

B.

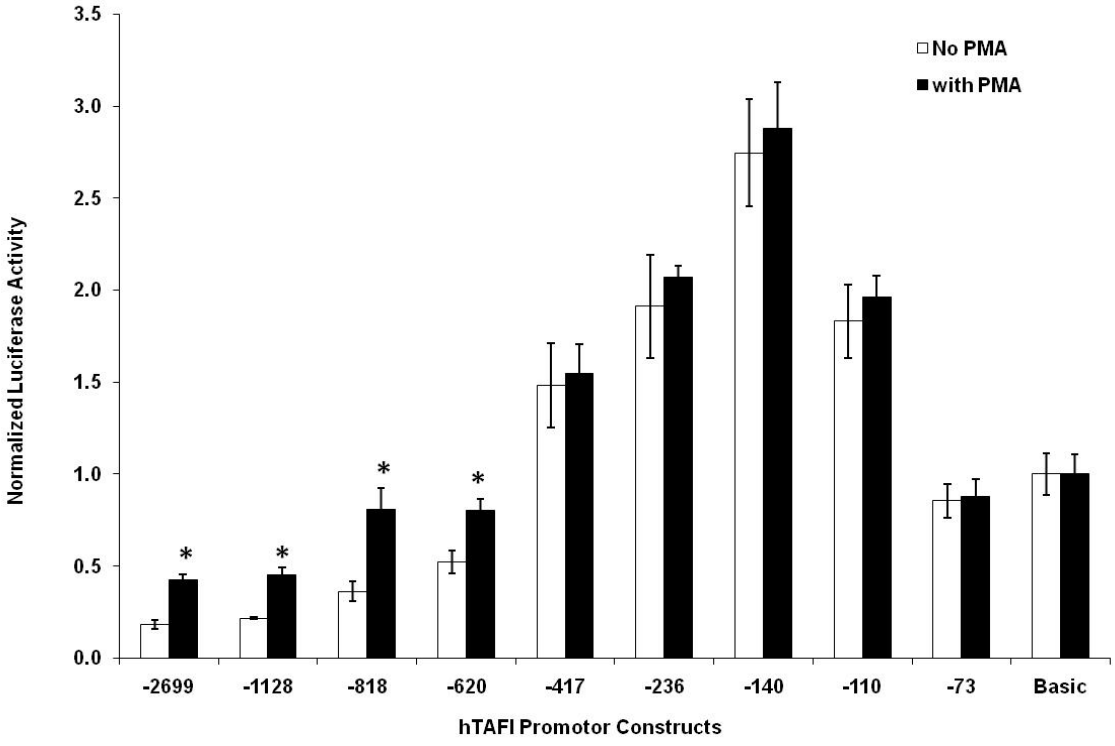
Normalized Luciferase Activity
3.5
3.0
2.5
2.0
1.5
1.0
0.5
0.0
No PMA
with PMA
*
*
*
*
-2699
-1128
-818
-620
-417
-236
-140
-110
-73
Basic
hTAFI Promotor Constructs

Figure 14. PMA modulation of human *CPB2* gene expression in Dami differentiation. A. Expression of human *CPB2* mRNA throughout Dami differentiation. Dami cells were treated with PMA (0.1 μM final) for up to 60 hours. Total RNA was harvested at various time points after the addition of PMA. *CPB2* mRNA abundance was analyzed by quantitative real-time RT-PCR experiments using 1 μg of total RNA harvested at indicated time points. The absolute quantification was based on *in vitro* transcribed human *CPB2* mRNA standards. The *CPB2* mRNA abundance was then normalized to that of the 0 hr time point. The data shown are the mean of three independent experiments; the error bars represent the standard error of the mean. * indicates a significant increase of *CPB2* mRNA expression compared to that of the 0 hr time point ($p<0.05$); NTC, no template control. **B.** Effect of PMA on *CPB2* promoter activity in Dami cells. Reporter constructs representing progressive deletions of the *CPB2* 5'-flanking region were transiently transfected (at equimolar concentrations) into Dami cells using DEAE-dextran for 3 hours and the cells were allowed to grow overnight followed by, where indicated, a treatment of PMA for 24 hours. Including in each transfection was an equal amount of renilla luciferase (pRL-CMV) construct as an internal control for differences in transfection and harvesting efficiency. Relative luciferase activities were calculated as described in the legend of Fig. 13. * indicates a significant increase of *CPB2* promoter activity compared to that of *CPB2* promoter activity without PMA treatment ($p<0.05$).

A.

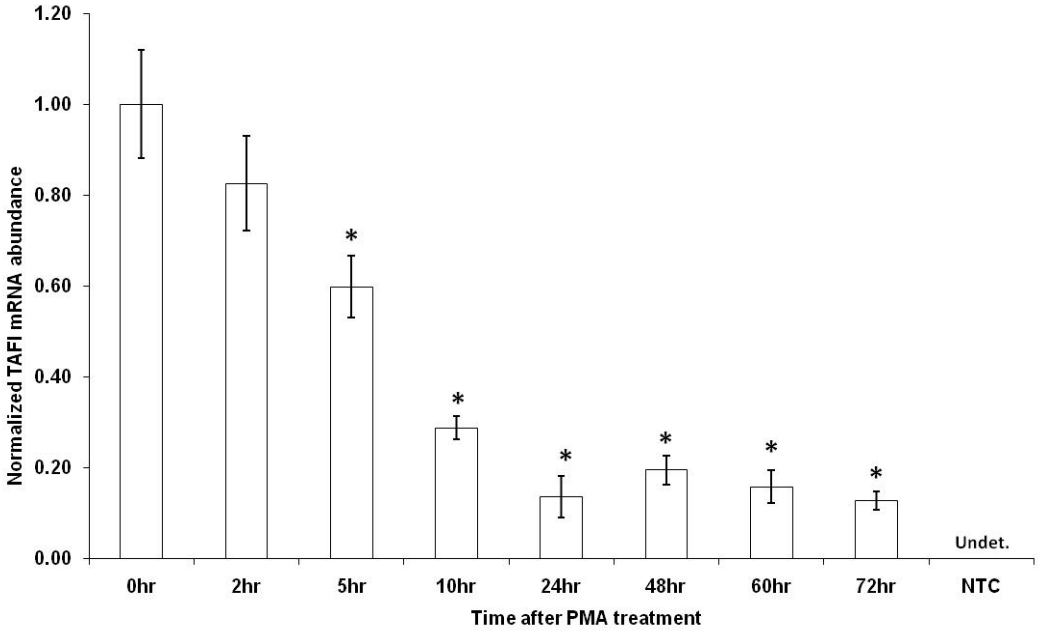
1.20
1.00
0.80
0.60
0.40
0.20
0.00
Normalized TAFI mRNA abundance
*
*
*
*
*
*
Undet.
0hr
2hr
5hr
10hr
24hr
48hr
60hr
72hr
NTC
Time after PMA treatment

B.

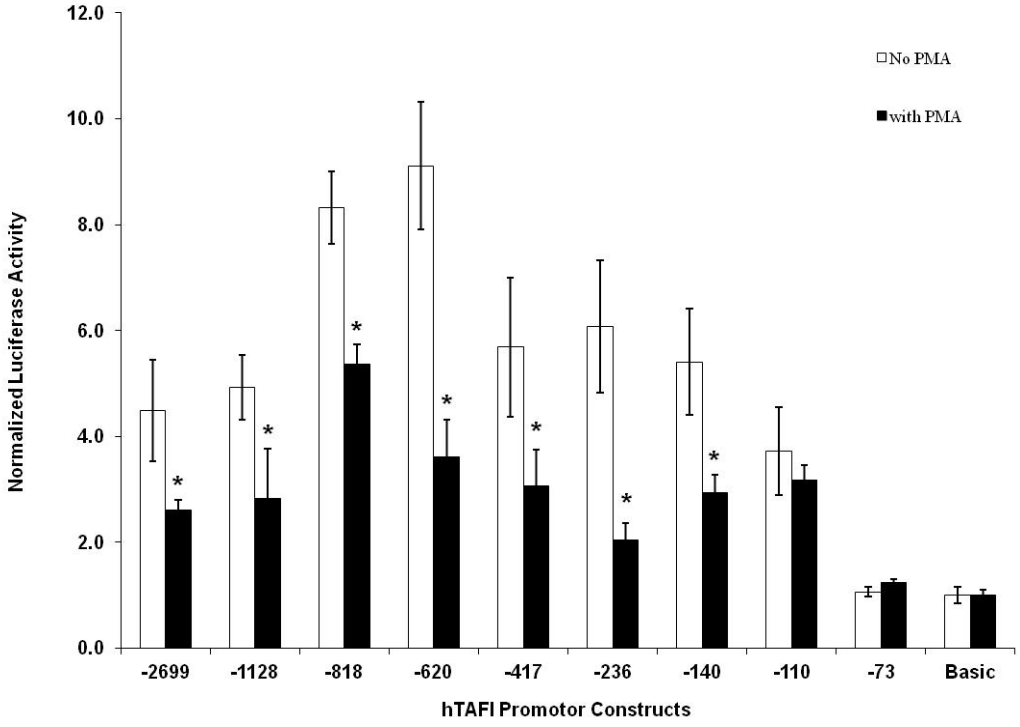
12.0
10.0
8.0
6.0
4.0
2.0
0.0
Normalized Luciferase Activity
No PMA
with PMA
-2699
-1128
-818
-620
-417
-236
-140
-110
-73
Basic
hTAFI Promotor Constructs

Figure 15. PMA modulation of human *CPB2* gene expression in THP-1 differentiation. A. THP-1 cells were treated with PMA (0.1 μM final) for up to 72 hours. *CPB2* mRNA abundance was analyzed by quantitative real-time RT-PCR experiments using 1 μg of total RNA harvested at indicated time point. The absolute quantification was based on *in vitro* transcribed human *CPB2* mRNA standards. The *CPB2* mRNA abundance was then normalized to that of the 0 hr time point. The data shown are the mean of three independent experiments; the error bars represent the standard error of the mean. * indicates a significant decrease of *CPB2* mRNA expression compared to that of the 0 hr time point ($p<0.05$); NTC, no template control. **B.** Analysis of the human *CPB2* promoter activity in THP-1. Progressive deletion of promoter constructs containing human *CPB2* 5'-flanking region were transiently transfected with equimolar concentrations into THP-1 cells using DEAE-dextran for 3 hours and allowed the cells to grow overnight. Where applicable, cells were treated with PMA (0.1 μM final) for 24 hours. Including in each transfection was an equal amount of renilla luciferase (pRL-CMV) construct as an internal control for differences in transfection and harvesting efficiency. Relative luciferase activities were calculated as described in the legend of Fig. 13. * indicates a significant decrease of *CPB2* promoter activity compared to that of the *CPB2* promoter activity without PMA treatment ($p<0.05$).

A.

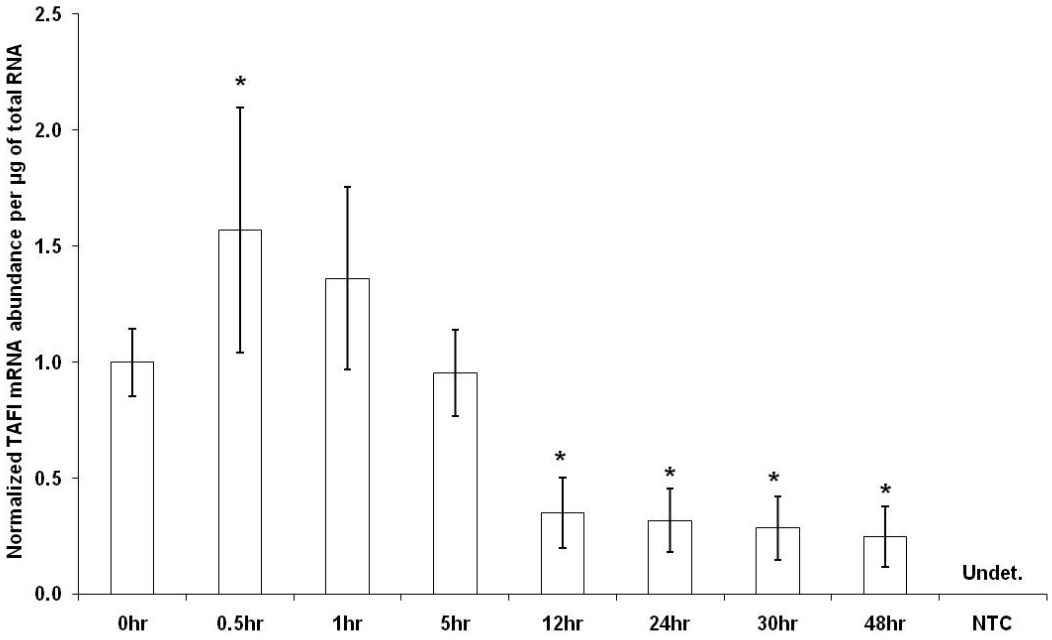
Normalized TAFI mRNA abundance per µg of total RNA
2.5
2.0
1.5
1.0
0.5
0.0
*
*
*
*
*
Undet.
0hr
0.5hr
1hr
5hr
12hr
24hr
30hr
48hr
NTC

B.

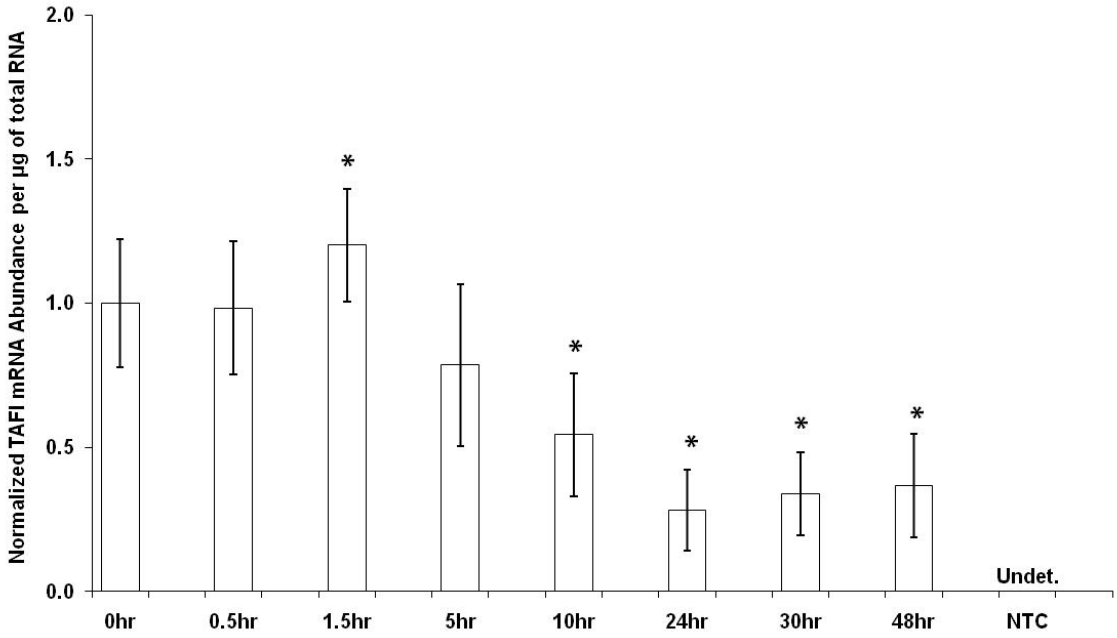
Normalized TAFI mRNA Abundance per µg of total RNA
2.0
1.5
1.0
0.5
0.0
*
*
*
*
*
Undet.
0hr
0.5hr
1.5hr
5hr
10hr
24hr
30hr
48hr
NTC

Figure 16. LPS modulation of human *CPB2* mRNA in THP-1 and THP-1ma. A. THP-1 cells, and **B.** THP-1 cells at density of 10^6 cells/mL differentiated into macrophage-like cells (THP-1ma) by treating the cells with PMA (0.1 μM final) for 72 hours, were treated with lipopolysaccharide (LPS, 100 ng/mL) for up to 48 hours. Total RNA was harvested at indicated time points after the addition of LPS. The expression of *CPB2* mRNA was analyzed by quantitative real-time RT-PCR using 1μg of total RNA. The quantification was based on *in vitro* transcribed human *CPB2* mRNA standards, and the *CPB2* mRNA abundance was then normalized to that of the 0 hr time point. The data shown were the mean of three independent experiments; the error bars represent the standard error of the mean. * indicates a significant change of *CPB2* mRNA expression compared to that of the 0 hr time point ($p<0.05$). NTC, no template control.

Chapter 4: *CPB2* mRNA undergoes alternative splicing event in a variety of cell types

4.1 Statement of co-authorship

Dr. M. Garand participated in the data collection and analysis of Figure 17 and 21. Dr. M. Garand also performed the transfection experiments and established the alternatively spliced TAFI-pNUT stable lines. B. Zagorac participated in the data collection of Table 6. B. Zagorac also participated in the sub-cloning of alternatively spliced *CPB2* cDNA into pNUT vector, made the alternatively spliced *CPB2* mRNA standards for qRT-PCR experiments, performed tissue culture for all the alternatively spliced TAFI-pNUT stable lines, and harvested conditioned medium and lysate samples from the alternatively spliced TAFI pNUT stable lines for downstream experiments. All of the remaining data were collected and analyzed by J. Lin. All sections of the manuscript were written by J. Lin with editorial assistance from Drs. M. Garand, M. Koschinsky and M. Boffa.

4.2 Abstract

Alternative splicing has evolved to produce protein diversity and maintain the ability to create novel proteins under evolutionary pressure with a limited set number of genes. TAFI (thrombin-activatable fibrinolysis inhibitor) is a carboxypeptidase that once activated (TAFIa), down-regulates fibrinolysis by cleaving lysine residues from partially degraded fibrins. TAFIa can also down-regulate inflammation by inactivating pro-inflammatory mediators. Liver is the main source for plasma TAFI. TAFI has also been identified in platelets and megakaryocytic cell line Dami cells; *CPB2* mRNA has been detected in monocytoid cell line THP-1 as well as peripheral blood mononuclear cells (PBMNC). A recent study reported an alternatively spliced

CPB2 mRNA variant lacking exon 6 (Δ6) in HepG2 cells and liver tissue. Another study identified a *CPB2* mRNA variant lacking exon 6 with a 52 bp deletion in exon 10 (Δ6+10) in human hippocampus. Using RT-PCR and quantitative RT-PCR, we report for the first time the expression of *CPB2* mRNA in platelets. We also detected Δ6 mRNA containing variants in Dami, platelets, THP-1 and PBMNC with quantities less than 1% of the total *CPB2* transcripts. Furthermore, cloning experiments revealed the expression of a new *CPB2* mRNA variant Δ6+7 in HepG2 and human liver. We also identify the expression of Δ6+10 mRNA variant in platelets. Experiments using Baby Hamster Kidney (BHK) cells transfected with wild-type *CPB2*-, Δ6-, Δ6+10-, and Δ10-cDNA revealed that alternatively spliced TAFI is stored inside the cells, cannot be activated by thrombin-thrombomodulin, and does not have the ability to cleave lysine residues from fibrin degradation products. The alternative splicing events may be a mechanism to down-regulate *CPB2* gene expression by producing truncated TAFI proteins that are misfolded, rendering them non-functional and subject to degradation.

4.3 Introduction

Thrombin-activatable fibrinolysis inhibitor (TAFI) is a carboxypeptidase B-like pro-enzyme that, upon activation by plasmin, thrombin or the thrombin/thrombomodulin complex, attenuates fibrinolysis (26). Full-length TAFI has apparent molecular mass of approximately 60 kDa on SDS-PAGE and consists of 401 amino acids that can be further divided into an activation peptide and a catalytic domain. TAFI is activated to become a 35 kDa enzyme, TAFIa, through a proteolytic cleavage at Arg92, which releases the activation peptide (10).

TAFIa retards fibrinolysis by removing carboxyl-terminal lysine residues from partially degraded fibrin, resulting in attenuation of several positive feedback mechanisms in the fibrinolytic cascade (2). In addition to hemostasis, TAFI has been implicated as a modulator of inflammation. Several pro-inflammatory peptides including anaphylatoxins (C3a and C5a) (45), bradykinin (46), and thrombin-cleaved osteopontin (48), as well as the anti-inflammatory plasmin-cleaved chemerin (50), have been shown to be substrates for TAFIa. TAFIa inactivates the pro-inflammatory molecules and activates the anti-inflammatory molecule by removing arginine/lysine residues from their carboxyl termini. Because TAFI was independently discovered by three other groups, TAFI is also known as CPU ('unstable' carboxypeptidase) (79), CPR ('R' for arginine) (18), and plasma procarboxypeptidase B (based on its homology to the pancreatic carboxypeptidase B) (15).

The human gene encoding TAFI (designated *CPB2* by the Human Genome Organization) is located on chromosome 13 (13q14.11) and contains 11 exons and 10 introns spanning 48 kb in length (11;12). TAFI is primarily expressed by the liver, accounting for the plasma pool of TAFI. Over the past decade, several non-hepatic pools of TAFI have also been identified. TAFI has been reported to be present in the α-granules of the platelets, and can be released upon platelet activation (5); platelet-derived TAFI is capable of attenuating platelet-rich thrombus lysis *in vitro* independently of plasma TAFI (71). Furthermore, *CPB2* mRNA was detected in megakaryocytic cell lines MEG-01, Dami, and CHRF (5;76), supporting the hypothesis that platelet-derived TAFI is synthesized in the megakaryocytes. *CPB2* mRNA has also been detected in the fatty tissue of patients with type 2 diabetes (6), human umbilical vein endothelial cells (6;76), human peripheral blood mononuclear cells (PBMNC) (76), and monocytic cell line THP-1 (76).

In a study by Matsumoto and coworkers (4), a novel alternatively spliced TAFI variant was identified from human brain hippocampal homogenate that appeared to be brain-specific, thus was given the name human brain carboxypeptidase B (HBCPB). They identified HBCPB as a 40 kDa protein that can cleave amyloid precursor protein (APP) to become β-amyloid peptides. The β-amyloid peptides aggregate to form amyloid plaques, which have been thought to trigger neuronal dysfunction and death in the brain, leading to Alzheimer's disease (4;65). Further molecular analysis revealed that HBCPB has an identical mRNA sequence as liver-expressed *CPB2* except for a deleted exon 6 and a 52-base deletion in exon 10 (exon numbering is as described in Boffa and coworkers (12)); the latter variation results in a frameshift resulting in a carboxyl-terminal peptide with 14 unique amino acid residues (4). Immunohistochemical analysis of the brain showed that brain TAFI is uniformly expressed in the cytosol of normal hippocampal pyramidal neurons, but is much more clustered in neurons affected by Alzheimer's disease. The same group later reported the detection of brain TAFI in both human serum and cerebrospinal fluid (66). Recently, an alternatively spliced *CPB2* mRNA lacking exon 6 was identified in HepG2 (human hepatoma) cells and human liver (64). Although the functionality of this *CPB2* mRNA lacking exon 6 is not known, the region between exon 5 and exon 6 showed high nucleotide diversity among several different ethnic groups. Furthermore, the exon 6 skipping event is preferentially associated with a previously known single nucleotide polymorphism (+505A→G, resulting a Thr to Ala substitution at position 147), while the exon 6 containing segment showed no significant preference for either +505A of G. The authors suggested that such nucleotide diversity was shaped by balancing selection in order to maintain heterozygote advantage.

In a previous study from our laboratory surveying *CPB2* gene expression in vascular and inflammatory cells, we also noticed potential exon skipping events from our RT-PCR results (Fig. 4, (76)). In this current work, we set out to characterize the pattern of alternatively spliced *CPB2* mRNA variants in cell types that are crucially involved in physiological and pathological processes of vascular biology. We also attempted to study the expression of TAFI protein variants arising from these alternatively spliced *CPB2* mRNA species.

4.4 Materials and methods

4.4.1 Cell culture and transfection of mammalian cells

All cells were maintained in a humidified incubator at 37 ºC and 95% air/5% CO_2 atmosphere. HepG2 cells (human hepatocellular carcinoma) (89) were purchased from the American Type Culture Collection (ATCC) and grown in 100 mm plates in minimal essential medium (MEM) (Invitrogen) supplemented with 10% fetal bovine serum (FBS) (ATCC) and 1% antibiotic-antimycotic (10 units/mL penicillin G sodium, 10 μg/mL streptomycin sulfate, and 25 ng/mL amphotericin B) (Invitrogen). Dami cells (human megakaryoblastic leukemia) (91) were the generous gift of Dr. David Lillicrap (Queen's University, Kingston, Canada) and were cultured in 100 mm tissue culture plates with complete growth medium containing RPMI 1640 medium (Invitrogen) adjusted to contain 4.5 g/L glucose, 10 mM HEPES, and supplemented with 10% FBS (ATCC) and 1% antibiotic-antimycotic. THP-1 cells (human acute monocytic leukemia; ATCC) (92) were cultured in 100 mm tissue culture plates with complete growth medium consisting of adjusted RPMI 1640 medium supplemented as described for Dami cells with the addition of 1.0 mM sodium pyruvate and 0.05 mM 2-mercaptoethanol. For

differentiation of both Dami and THP-1 cells, phorbol myristate acetate (PMA) (Sigma) was added to a final concentration of 0.1 μM to cells at a density of 1×10^7 cells/mL for 72 hours. The preparation of human peripheral blood mononuclear cells (PBMNC) was performed as described (76).

General procedures for the cloning of Δ6-pNUT, Δ6+10-pNUT, Δ10-pNUT constructs were as described by Boffa and coworkers (27), except that an extra *Xma* I site (CCCGGG) was added to the end of primer 6 for sticky end sub-cloning from the pBluescript SK+ vector into the pNUT vector. Baby Hamster Kidney (BHK) cells were cultured in 100 mm tissue culture plates in DMEM/F12 (Invitrogen) containing 5% newborn calf serum (Sigma) and 1% antibiotic-antimycotic. Cells were transfected using Effectene reagent (Qiagen) following the manufacturer's protocol. Approximately 2.5×10^6 cells per plate were transfected with 2 μg of TAFI-pNUT (27), Δ6-pNUT, Δ6+10-pNUT, Δ10-pNUT construct, or the empty pNUT vector. After an overnight incubation with the transfection mixture, cells were then transferred to a 15 cm plate (Corning) and allowed to grow overnight; after which the medium was replaced with DMEM/F12 complete growth medium supplemented with 400 μM methotrexate. After a 2-week selection period, the surviving cells were pooled and seeded in a 100 mm plate. Upon growth to confluence, a portion of the cells were harvested and analyzed for expression of *CPB2* mRNA and TAFI protein.

4.4.2 RNA isolation

For human tissue samples including liver, cortex, cerebellum, testis, and platelet, total RNA was isolated using Trizol (Invitrogen) as per the manufacturer's protocol.

For cultured cell lines, the RNeasy Mini kit (Qiagen) was used for total RNA isolation according to the manufacturer's protocol. For real-time RT-PCR analysis, on-column DNase digestion during RNA purification was performed using the RNase-Free DNase Set (Qiagen) as recommended by the manufacturer.

4.4.3 Reverse transcriptase-polymerase chain reaction (RT-PCR)

Approximately 1 µg of total RNA was used for RT-PCR experiments. RT-PCR was performed using OneStep RT-PCR Kit (Qiagen) following the manufacturer's instructions. The size of the *CPB2* cDNA fragment amplified and the primer sequences used are indicated in Table 4. Thermocycling conditions used for all amplification reactions were performed as previously reported (76), except for the TAFI 1-6 RT-PCR reaction where denaturation and annealing times were extended from 30 sec to 1 min.

4.4.4 Real-time quantitative RT-PCR (qRT-PCR)

Real-time quantitative RT-PCR analysis was carried out on a BioRad CFX96 Real-Time System (BioRad); procedures were as described (76). Primers and probes for Taqman (Applied Biosystems) were designed using Primer Express 1.7 software (Applied Biosystems) to span one intron-exon junction thus minimizing the signal generated from contaminating genomic DNA in the template RNA. To control for the presence of genomic DNA contamination, control reactions with no reverse transcriptase were performed. The sequences for the primers and probes used are indicated in Table 5. The RNA standards for absolute quantification were generated as described (62).

4.4.5 TAFI activation and western blot analysis

For TAFI activation, samples were supplemented with $CaCl_2$ (5 mM), human thrombin (25 nM) (Haematologic Technologies), and rabbit lung thrombomodulin (100 nM) (Haematologic Technologies) and incubated at room temperature for 15 min. The reaction was then stopped by the addition of PPAck (100 nM).

For western blot analyses using sheep-anti human antibody (Affinity Biologicals), experiments were performed as described (76) using SDS-PAGE on 12% polyacrylamde gels, except that the blots were incubated with affinity-purified polyclonal sheep anti-human TAFI antibody (Affinity Biologicals; 1 in 15,000 dilution in blocking buffer containing 3% (w/v) non-fat milk) and incubated at 4°C overnight. Before visualizing, the blots were washed 20× with distilled H_2O. Immunoractive bands were visualised using SuperSignal West Femto Maximum Sensitivity Substrate (Thermo Scientific) and a FluorChem Q Gel Imaging System (Alpha Innotech).

4.4.6 TAFIa assay

The TAFIa assay was implemented as described by Kim and coworkers (22). Eighty microliters of a solution in HEPES-buffered saline (HBS) of 1.0 μM QSY9 C5-maleimide-conjugated high molecular mass fibrin degradation products and 100 nM Fluo-plasminogen was added to wells of a white opaque microtiter plate, and fluorescence intensity was monitored with excitation and emission wavelengths of 480 and 520 nm, respectively, and a 495-nm emission cutoff filter, using a Spectra Max M5e fluorescence plate reader (Molecular Devices). After the fluorescence signal stabilized, TAFIa standards or samples (20 μL) were added to the 96-well plate between readings. TAFIa level measured from each sample was divided by its respective

total cellular protein obtained using BCA assay (Pierce Chemical) to account for differences in cell numbers. Results were then normalized to the wild-type conditioned medium or lysate sample expressed in percentage per mg of total cellular protein.

4.5 Results

4.5.1 Characterization of alternatively spliced *CPB2* mRNA in various human tissue samples and cultured cell lines

A previous study by Matsumoto and coworkers (4) described a novel *CPB2* mRNA variant that lacked exon 6 (hereafter referred to as Δ6) combined with a 52-base deletion in exon 10. Although the latter is not a full exon 10 deletion, for the sake of simplicity, this 52 base deletion is hereafter referred to as Δ10; exon numbering is as described by Boffa and coworkers (12). Based on northern blot analysis of 7 different tissue samples, the authors concluded that this alternatively spliced variant, TAFI-Δ6+10, was brain specific. Furthermore, a recent study by Cagliani and coworkers (64) detected a *CPB2* mRNA species that lacks only exon 6 from human liver and HepG2 cells. The authors reported that they did not detect any Δ10 species in these samples. Because these were the first and only reports of the existence of alternatively spliced *CPB2* mRNA species in brain and liver tissues, we set out to verify the existence of these variants from the collection of tissue total RNA samples available in our laboratory.

The expression of human *CPB2* mRNA variants in our human tissue samples was first assessed using RT-PCR. Two primer sets were employed (Fig. 17A) (27): TAFI 1-4 that amplifies the 5' portion of the *CPB2* open reading frame (ORF) and TAFI 5-6 that amplifies the 3' end of the *CPB2* ORF with expected amplicons of 951 and 426 bp, respectively (Fig. 17B,C). To confirm the identity of the amplified fragments, restriction enzymes *Eco*RI and *Hin*dIII were

used to digest the PCR products from TAFI1-4 and TAFI 5-6 reactions, respectively (Fig. 17D). To our surprise, the results from TAFI 1-4 primer set showed 2 distinct bands from one of the cerebellum samples corresponding to both full-length as well as exon 6-skipped *CPB2* cDNA (Fig. 17B). Furthermore, 3 distinct bands were observed in liver and testis (Fig. 17B). Similarly, the 2 larger bands were compatible in size with the predicted wild-type and Δ6 *CPB2* mRNA species. Only a wild-type TAFI band was observed in the cortex sample using TAFI1-4 primer set (Fig. 17B). Little to no alternatively spliced *CPB2* mRNA species were detected using the TAFI 5-6 primer set (Fig. 17C). Consistent with the literature, our data demonstrated the existence of TAFI-Δ6 mRNA species in human liver. However, we could not firmly report the existence of TAFI-Δ6+10 mRNA specie in the brain.

Similar RT-PCR experiments were performed using RNA harvested from HepG2 cells as well as from platelets. Again, we utilized the TAFI1-4 and TAFI 5-6 primer sets (Fig. 18). Similar to what was observed in the liver sample, TAFI 1-4 amplification in HepG2 cells showed an extra fragment in addition to the expected wild-type and Δ6 *CPB2* mRNA variants (Fig. 18A). In platelet samples, two distinctive bands were observed form RT-PCR reaction with both TAFI1-4 and TAFI5-6 primer sets (Fig 18B).

In order to confirm the identity of the apparent exon skipping events and to determine the nature of the third band observed using the TAFI 1-4 primer set in HepG2 cells, amplified products from HepG2 and platelets using primer sets TAFI 1-4 and TAFI 5-6 as well as TAFI 1-6 encompassing the entire ORF (27) were cloned and sequenced. The sequencing results are summarized in Table 6. The results confirmed the expression of the in-frame deletion TAFI-Δ6 mRNA in HepG2 cells. In addition, we also identified a new *CPB2* mRNA variant in HepG2 that lacks both exon 6 and exon 7, an out-of-frame splicing event leading to the formation of a unique

carboxyl-terminal peptide sequence of 23 amino acid in length and a premature stop codon 70 bases into exon 8. Platelets appear to express the full-length *CPB2* transcript as well as a variant, similar to that described in brain (4), that has both the exon 6 deletion and the exon 10 frameshift. A schematic representation of the *CPB2* mRNA splicing events identified in this study is depicted in Figure 19.

In a previous study, our group had used RT-PCR to detect *CPB2* mRNA in a variety of vascular and inflammatory cell types (76). In the course of these investigations, we likewise detected RT-PCR products that were smaller than the expected size, along with products of the expected size (Fig. 4). Accordingly, we became interested in determining if these smaller products corresponded to the alternatively spliced variants described above. Therefore, RT-PCR experiments with primer sets designed specifically to detect the alternatively spliced variants Δ6 and Δ6+7 were performed using total RNA isolated from Dami cells (megakaryoblastic leukemia) cells, Dami cells differentiated further along the megakaryocytic lineage by PMA treatment (dDami), THP-1 (monocytic leukemia) cells, and THP-1 cells differentiated into macrophage-like cells by PMA treatment (THP-1ma). We also performed these RT-PCR reactions with RNA from human liver, HepG2, and cerebellum cells as well as platelets. The results show that the exon 6 skipping event is detectable in liver and HepG2 cells and in platelets (Fig. 20A), in accordance with the results described above, as well as in dDami cells, THP-1ma, and platelets. The exon 6+7 skipping event is readily detectable in liver and HepG2 cells with very faint RT-PCR products observable in dDami cells and cerebellum (Fig. 20B).

4.5.2 Quantification of the Δ6 transcript

As the Δ6 variant is the only alternative splicing event common to all cell types examined that exhibit alternative splicing, we set out to measure the absolute levels of this variant using quantitative real-time RT-PCR. Absolute expression levels of both total and Δ6 mRNA were obtained based on their respective *in vitro* transcribed mRNA standards. Liver and HepG2 showed the highest expression of the Δ6 mRNA (Fig. 21). A low expression level of *CPB2* mRNA variants lacking exon 6 is detected in all non-hepatic cell types examined (Fig. 20). Relative to the total amount of CPB2 mRNA present, however, the Δ6 variant represented between a high of 5% (HepG2) and a low of 0.004% (platelets) (Fig. 21).

4.5.3 *In vitro* expression of alternatively spliced TAFI variant

Matsumoto and coworkers (4) suggested that the 40 kDa brain carboxypeptidase B has the ability to cleave β-amyloid precursor protein to β-amyloid and is the translational result of TAFI-Δ6+10 mRNA expressed in human brain hippocampus tissue. To examine the ability of the various alternatively spliced forms of *CPB2* mRNA to encode functional proteins with carboxypeptidase activity, we generated Baby Hamster Kidney (BHK) cells lines stably transfected with expression plasmids encoding the Δ6-, Δ6+10, and Δ10 variants. Stable line transfected with the wild-type TAFI-pNUT (27) plasmid and the empty pNUT vector as well as non-transfected BHK cells were included as controls.

We first confirmed the expression of the *CPB2* mRNA variants in these stable lines using RT-PCR with primer set TAFI 1-6, which amplifies the entire *CPB2* open reading frame. As shown in Figure 22A, the expected fragments of 1235 bp, 1183 bp, 1294 bp, and 1346 bp were

observed from Δ6-, Δ6+10-, Δ10-, and wild-type TAFI-pNUT line, respectively, indicating that the transfections were successful and the alternatively spiced *CPB2* mRNA variants were transcribed properly in BHK cells. No amplification of TAFI mRNA was observed from the cell line transfected with empty pNUT vector nor from the non-transfected BHK line.

Next, we set out to examine the expression of these truncated TAFI proteins using western blot analyses with polyclonal anti-TAFI antibodies. As expected, the 60 kDa wild-type TAFI, activatable by thrombin-thrombomodulin, was detected in the conditioned media of the wild-type TAFI-expressing cell line as well as the conditioned media of HepG2 cells (Fig. 22B). On the other hand, no immunoreactive bands of the appropriate size were observed in the media of cell lines expressing any of the three alternatively-spliced variants. Conversely, immunoreactive bands of approximately 45-48 kDa appeared in the lysate of cell lines expressing wild-type TAFI as well as the three alternatively-spliced variants, but not in the cells transfected with the empty vector or the untransfected cells (Fig. 22C). The lysates of cells expressing wild-type TAFI also contained a band of approximately 60 kDa, the same size as the secreted form of wild-type TAFI observed in the conditioned medium. The wild-type TAFI present in the lysates could be cleaved by thrombin-thrombomodulin to yield a 35 kDa TAFIa species, but, interestingly, the alternatively spliced variants could not (Fig. 22C).

In order to assess if the alternatively-spliced TAFI variants could develop carboxypeptidase activity, the conditioned medium and lysates from all of the stable-transfected cells were subjected to a highly sensitive assay that uses a TAFIa substrate soluble fibrin-degradation products that contain carboxyl-terminal lysine residues. The medium and lysate samples were either pre-treated with thrombin-thrombomodulin or were left untreated prior to the TAFIa assay. In accordance with the western blotting data, neither the medium nor the lysates

from cells transfected with the alternatively-spliced TAFI variants showed significant TAFIa activity (Fig. 23). By contrast, both the medium and lysate of cells expressing wild-type TAFI resulted in significant TAFIa activity, specifically after treatment with thrombin-thrombomodulin.

4.6 Discussion

Alternative splicing is a mechanism that has evolved to increase proteome diversity using a limited number of genes. A recent study using high-throughput sequencing technologies estimated that approximately 92-97% of multiexon genes in human are alternatively spliced (116). While it has been argued that most of the alternatively spliced variants are aberrant splicing (117) or nonfunctional stochastic noise (118), alternative transcripts from the same gene have the possibility of encoding (i) a protein with similar function as the native protein, as seen in the case for tissue factor , or, (ii) encoding a premature stop codon leading to degradation via nonsense mediated mRNA decay, as seen in the case for coagulation factor XI (119); or, as reported by Matumoto and coworkers (4) and Cagliani and coworkers (64) for the case of TAFI, (iii) encoding a protein with an entirely different function, or, (iv) with the purpose to maintain heterozygote advantage, respectively.

Using northern blot analysis and molecular cloning, Matsumoto and coworkers (4) reported the detection of a novel alternatively spliced *CPB2* mRNA variant TAFI-Δ6+10 from the poly(A)-rich RNAs of the human hippocampus. They reported that this was the only *CPB2* mRNA species detected in hippocampus, while the full-length transcript was the only *CPB2*mRNA present in human liver. In a recent genetic study, Cagliano and coworkers reported

the detection of the Δ6 transcript in human liver and HepG2 cells (64). Our own experiments using RT-PCR, molecular cloning, and quantitative real-time RT-PCR, have revealed the presence of a variety of alternatively spliced forms in virtually all cell types examined including liver, brain, immune/inflammatory and hematopoietic cells. In all cases, however, including cortex and cerebellum, the full-length transcript (i.e., containing the entire ORF) was detected. However, as a hippocampus sample was not readily available to us, we cannot rule out the possibility that TAFI-Δ6+10 is the dominant species, if not the only species, in this particular region of the brain.

In addition, our RT-PCR experiments showed, for the first time, that full-length *CPB2* mRNA is expressed in platelets, adding to the accumulating evidence supporting the hypothesis that platelet TAFI originates from *CPB2* gene expression in megakaryocytes. The RT-PCR results also demonstrated that platelets have potential to express the alternatively spliced TAFI variants TAFI-Δ6, TAFI-Δ6+10, and TAFI-Δ10 (Fig.18B, Table 6). Platelets contain a complement of megakaryocyte-derived pre-mRNA species as well as functional splicing machinery that can respond to stimuli such as platelet adherence and thrombin (120). It remains to be determined if the alternatively-spliced *CPB2* forms detected in platelets are generated in megakaryocytes or later in platelets subject to regulatory control. These effects may serve to control the pool of functional TAFI present in the platelet.

Our RT-PCR and molecular cloning experiments also led to the discovery of a novel alternatively spliced variant lacking exons 6 and 7, expressed in human liver and HepG2 cells. This variant encodes a drastically truncated TAFI species lacking amino acids 176 to 244 followed by a unique carboxyl-terminal peptide sequence of 23 amino acids in length. No TAFI-Δ6+7 transcripts were detected in platelets (Fig. 20). However, sequencing results of cDNA

clones amplified from platelets using the TAFI1-6 primer set revealed a preference for the combination of Δ6 and Δ10 in platelets.

We suspected potential alternatively spliced *CPB2* mRNA variants from our previous report on the expression of *CPB2* mRNA in megakaryoblastic cell line Dami, differentiated Dami (dDami), and monocytoid cell line THP-1, macrophage-like THP-1 (THP-1ma), as well as PBMNC (76). Further RT-PCR and qRT-PCR analyses using primer sets specifically designed to amplify Δ6 and Δ6+7 mRNA variants showed the expression of Δ6 variants in megakaryocytic and monocytic cell lines (Fig. 20, 21).

As depicted in Figure 19, Δ6+7 mRNA contains a frame-shift that introduces a premature stop codon. Nonsense-mediated mRNA decay (NMD) is a pathway that prevents the production of truncated proteins by depleting premature stop codon-containing transcripts. For example, three out-of-frame alternatively spliced transcripts of coagulation factor XI observed in HepG2 cells were regulated by NMD (119). However, we failed to observe the accumulation of Δ6+7 transcripts in HepG2 cells when treated with cycloheximide or puromycin, two known inhibitors of NMD pathway (121) (data not shown). These results suggested that the Δ6+7 transcript variant is not regulated by NMD. Indeed, a study using quantitative microarray profiling estimated that ~80% of premature stop codon-containing splicing events are not affected by NMD; moreover, the authors hypothesized that these alternatively spliced transcripts do not encompass functional roles (122).

Platelets have been known to contain mRNA of factors involved in hemostasis (119;123). Because TAFI-Δ6 mRNA is the only variant detected so far that possess the physiological stop codon, and is expressed in all the cell types of interest, we set out to quantify its expression level.

The quantification of *CPB2* mRNA variants lacking exon 6 in non-hepatic cells were averaged around the magnitude of 1×10^2 transcripts per μg of total RNA, which translates into approximately 0.8% of the total TAFI mRNA expressions in these cell types. Interestingly, the high absolute numbers of Δ6 mRNA detected in liver and platelets can be translated into less than 0.05% of the total TAFI mRNA abundance. This observation is consistent with a recent model showing that the number of "noise transcripts" produced is inversely proportional to the total number of transcripts generated (118). Overall, our observations agree with the notion that total number of "noise transcripts" is limited by a selection pressure to minimize the production of nonfolding protein products that could aggregate, consequently increase cellular toxicity or potentially overwhelm cellular metabolism (118;124).

In order to assess the functional properties of the TAFI proteins encoded by the alternatively spliced transcripts, we assembled a series of expression plasmids and stably transfected BHK cells with the plasmids. The most striking result is that none of the variants were able to be secreted by the cells (Fig. 22), although each contained an intact signal peptide. As we expressed recombinant proteins that only lacked exon 6 residues or the truncated carboxyl-terminus, it appears that either of these variations are sufficient to inhibit secretion. Western blot analysis of the lysates from transfected cells revealed a immunoreactive band that was absent from mock-transfected cells or cells transfected with the empty pNUT vector; the band was bigger (~45-48 kDa) than what would be expected given the number of missing amino acids. However, lysates from the wild type TAFI-expressing cells contained both 60 kDa and ~48 kDa bands. Therefore, we propose that the variants encoded by alternatively spliced transcripts are aberrantly folded and do not leave the endoplasmic reticulum (ER). As such, they do not undergo normal addition of N-linked glycans, the bulk of which are added in the ER. The 48 kDa

immunoreactive band likely corresponds to the unglycosylated form of TAFI, which is also detected in wild-type TAFI-expressing cells as an intermediate in the secretory pathway. Further experiments using pulse-chase methods will be required to assess whether they are retained in the ER or targeted for degradation.

It should also be noted that the proteolytic activity of the "brain-TAFI" observed by Matsumoto and coworkers (4) was in the zymogen form. Even though the potential truncated TAFI bands in the lysate sample cannot be activated by IIa/TM, it does not rule out their potential functionalities, particularly the β-secretase-like activity for TAFI-Δ6+10 variant. It would be of interest to test whether the lysate samples from the alternatively spliced TAFI lines, especially the TAFI-Δ6+10, possess proteolytic activity towards APP.

Concerning carboxypeptidase activities of the alternatively spliced TAFI, our preliminary TAFIa assay results failed to detect TAFIa activity on the part of any of the variants encoded by alternatively spliced transcripts (Fig. 23). Importantly, our assay was able to readily detect TAFIa activity in the lysates of cells expressing wild-type TAFI. The probable cause of the lack of TAFIa activity, for the spliced variants, is that none of the variants seems activatable by thrombin-thrombomodulin. The non-activatable nature of the alternatively spliced TAFI protein may be partially explained by a recent study reporting that two adjacent lysine residues Lys-211 and Lys-212, both located in exon 6, are important for TAFI activation by IIa/TM (36). Based on the crystal structure of TAFI, it has been speculated that deletions of a β-sheet followed by an α-helix encoded by exon 6 may affect the intrinsic instability of the enzyme and resulted in a protein with different biochemical properties (64). In addition, the 52- base deletion in exon 10 contains Glu 363, a residue that plays a critical role in breaking the scissile bond of the substrate (10). The 52-base deletion in exon 10 also resulted in a removal of a flexible loop connecting a β-

sheet to an α-helix (16). All together, these deletions, either alone or in combinations can cause major structural changes to the protein that most likely resulted in retention in the ER, loss of function towards TAFI substrates and, consequently, may be subjected to degradation. A structure of recombinant TAFI with the residues encoded by exon 6 and exon 10 of the *CPB2* mRNA is depicted in Figure 24. It is very interesting to note, however, that Matsumoto and coworkers detected TAFI in the brain as intracellular, within the ER, using immunocytochemistry (125).

At this point, we cannot rule out that TAFI-Δ6+10 possesses potential β-secretase-like activity that forms β-amyloid from its precursor APP. Although it would require an entirely new arrangement of catalytic residues as this variant would retain residues that specifically serve to bind the terminal carboxylate group of peptide or protein substrates but would lack the residue critical for nucleophilic catalysis (Glu363). Matsumoto detected peptidase activity using "human brain carboxypeptidase B (HBCPB)" purified from human hippocampus as well as in PC12 cells stably transfected with an expression plasmid for the Δ6+Δ10 variant. Therefore, another potential function for TAFI-Δ6+10 is that it could act as an ER chaperone for the presumptive peptidase that actually acts on amyloid precursor protein. Matsumoto and coworkers transfected cell results could be explained by the acquiring by the cells of the necessary chaperone activity upon ectopic expression of TAFIΔ6+Δ10 (4). The peptidase activity found in the purified brain TAFI sample, from the Matsumoto group, could be explained by contaminating peptidase which would, after all, have a strong affinity for Δ6+Δ10 if the latter was indeed a chaperone for the former.

On the other hand, we observed that alternatively-spliced TAFI variants show (i) low abundance in alternatively-spliced *CPB2* mRNA expressions (less than 1% of the total for all cell

types measured and 5% of the total in HepG2), (ii) potential accumulation inside the cells, (iii) inability to be activated by IIa/TM, hence, (iv) no TAFIa activity observed, lead us to hypothesize that the alternative splicing events for *CPB2* mRNA is a way for cells to down-regulate *CPB2* gene expression by producing non-functional, mis-folded proteins. These proteins are then possibly held inside the cells; either they acquire new functions or are subjected to further degradation. The observations described above agree with the idea that Δ6 spliced variant is produced by balancing selection to maintain genome diversity (64). It must not be neglected that our data could fit with the theory that most alternatively spliced mRNA are of stochastic noise (118).

In summary, we have discovered that exon skipping and alternative splicing of *CPB2* transcripts is a considerably more widespread phenomenon than previously appreciated. Our findings imply the presence of variant forms of *CPB2* transcripts in a variety of different cell types beyond the brain, including liver, which is the organ that secretes the plasma pool of TAFI. Moreover, the brain appears to express intact, full-length *CPB2* transcripts in addition to the previously-described Δ6+Δ10 variant, the latter of which we have shown to be non-secretable and lacking TAFIa activity. Thus, TAFI joins the list of proteins, including tPA and plasminogen, that are produced in brain, as well as in other sites more consistent with their respective fibrinolytic roles. It will be fascinating to uncover the possible role of TAFI in neurophysiology.

4.7 Acknowledgement

We thank Nicole Feric at Queen's University, and Tanya Marar at University of Windsor for preparing the Fluo-plasminogen and purified recombinant TAFI, respectively, used for TAFIa

assay. Anastassia Filipieva for her participation in the initial cloning of alternatively spliced CPB2 cDNA into pBluescript SK+ vector.

Table 4. Primer sequences for RT-PCR analyses

Primer Name	Sequence (5' → 3')	Size of Amplicon
Δ6-5'	GTGGTTCATAGGCCATAATCG	651 bp
Δ6-3' (TAFI-6)	CAATGATTTGGTCTTGCTGG	
Δ6+7-5'	GGTTCATAGGCCATAGGAAG	556 bp
Δ6+7-3' (TAFI-6)	CAATGATTTGGTCTTGCTGG	

Table 5. Primer and probe sequence for quantitative RT-PCR analysis

Name	Sequence (5' → 3')
total-hTAFI-5'	[a](+)CGACAATGTGAAAGCCAATTT
total-hTAFI-3'	[b](−)CACGTCTGCCAGCAAGACA
total-hTAFI probe	[c]6FAM−ATGTGAGCGGAATTC−MGBNFQ
qΔ6-5'	[a](+)TCCTGCTTTCTGGTGGTT
qΔ6-3'	[b](−)CGCATAGAAAGAACGGTTCTTTC
qΔ6 probe	[c]6FAM−CATAGGCCATAATCGATTGT−MGBNFQ

[a](+), forward primer; [b](-), reverse primer; [c]6FAM-MGBNFQ probes: 6FAM(6-carboxyfluorescein), the 5'-end reporter dye; MGBNFQ (minor groove binder nonfluorescent quencher), the 3'-end nonfluorescent quencher.

A

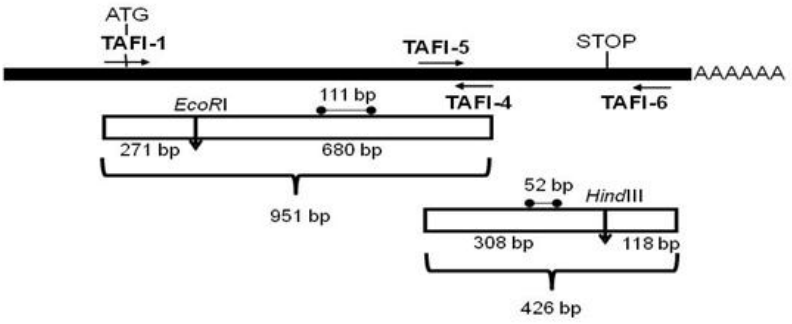
ATG
TAFI-1
TAFI-5
STOP
AAAAAA
EcoRI
111 bp
TAFI-4
TAFI-6
271 bp
680 bp
951 bp
52 bp
HindIII
308 bp
118 bp
426 bp

B

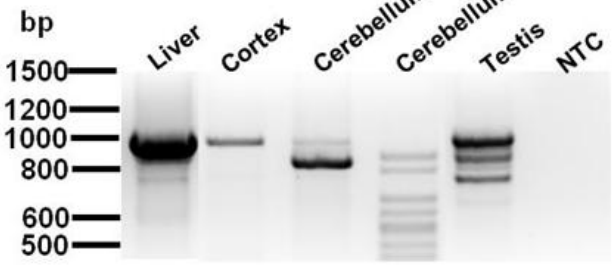
bp
Liver
Cortex
Cerebellum #1
Cerebellum #2
Testis
NTC
1500
1200
1000
800
600
500

C

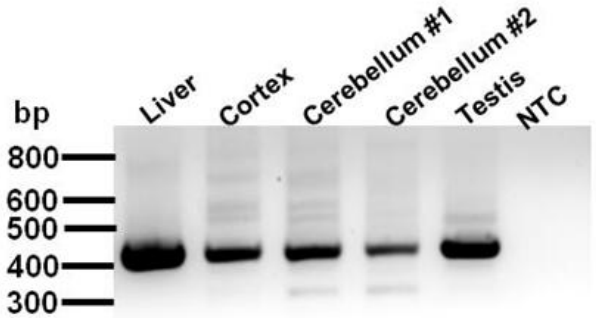
bp
Liver
Cortex
Cerebellum #1
Cerebellum #2
Testis
NTC
800
600
500
400
300

D

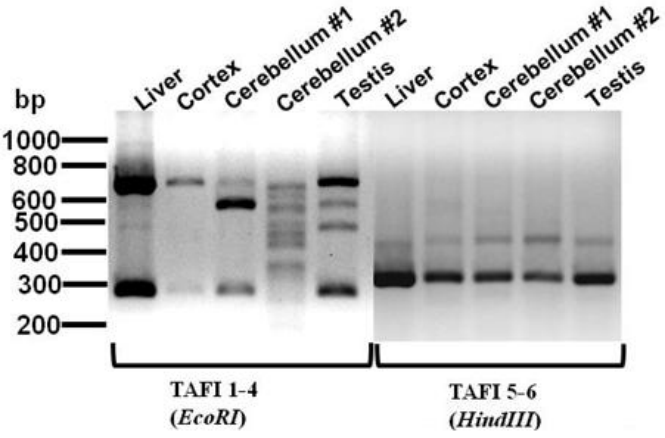
bp
Liver
Cortex
Cerebellum #1
Cerebellum #2
Testis
1000
800
600
500
400
300
200
TAFI 1-4
(EcoRI)
TAFI 5-6
(HindIII)

Figure 17. Detection of alternative *CPB2* mRNA splicing pattern in human tissue samples. **A.** Scheme for amplifications of the entire *CPB2* open reading fram encoding TAFI using primer sets TAFI 1-4 and TAFI 5-6, which resulted in a fragment of 951bp and 426bp, respectively, from full-length *CPB2* mRNA. ●—● indicates the position of reported deletions (not to scale) (4), 111 bp representing exon 6 and 52 bp delection in exon 10, relative to the indicated restriction enzyme cutting site. **B.** RT-PCR with primer set TAFI 1-4. **C.** RT-PCR with primer set TAFI 5-6. The RT-PCR experiments were performed using 1 µg of total RNA isolated from the indicated human tissue samples. **D.** Subsequently, 10 µL of the respective PCR product was subjected to digestion with restriction enzyme *Eco*RI or *Hind*III; the digested products were then resolved on a 2 % agarose gel.

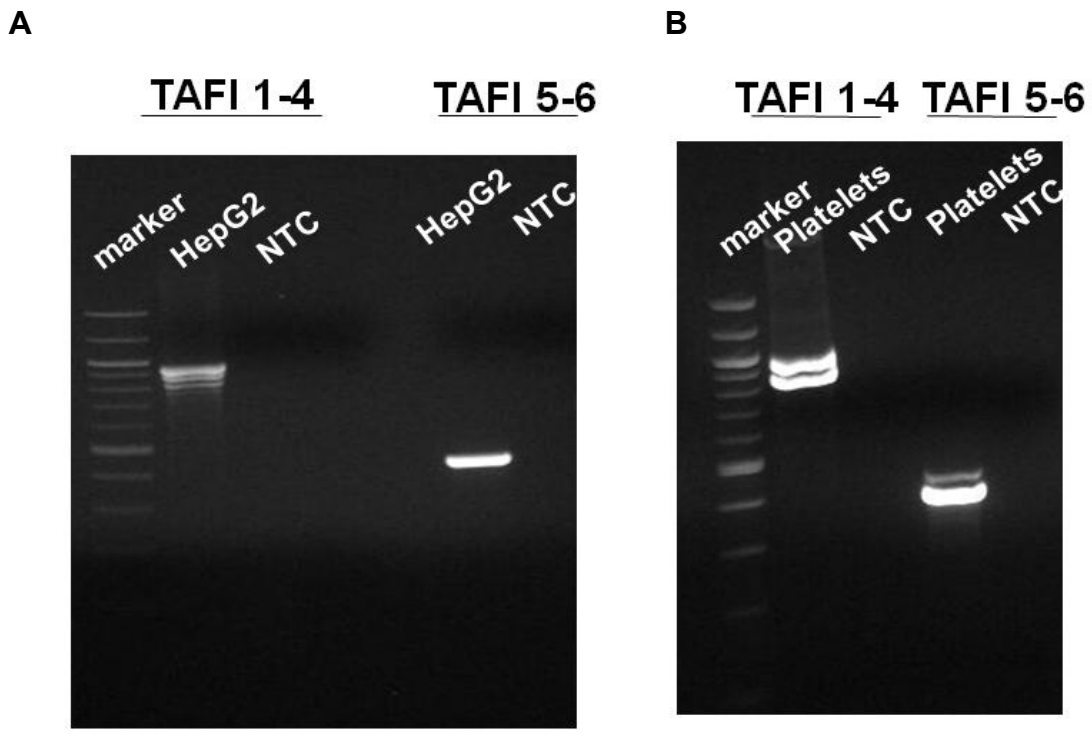

Figure 18. Detection of alternative *CPB2* mRNA splicing pattern in HepG2 cells and human platelets. The presence of alternatively spliced *CPB2* transcripts in HepG2 cells (**A**) and platelets (**B**) was evaluated using RT-PCR. The RT-PCR experiments were performed from 1.0 µg of total RNA isolated from HepG2 and human platelets. A reaction without any RNA template (NTC) was also included as a negative control. Primer sets TAFI 1-4 and TAFI 5-6 were used to amplify the open reading fram encoding TAFI.

Table 6. Presence of alternatively spliced *CPB2* transcripts, as assessed by molecular cloning and nucleotide sequence analysis.

Primer Set	Types	HepG2	Platelets
TAFI 1-4	WT	+	+
	△6	+	+
	△6+7	+	--
TAFI 5-6	WT	+	+
	△10	--	+
TAFI 1-6	WT	+	N/D
	△6+10	--	+

"+", *CPB2* cDNA sequence detected." --", *CPB2* cDNA sequence not detected. "N/D", not determinded.

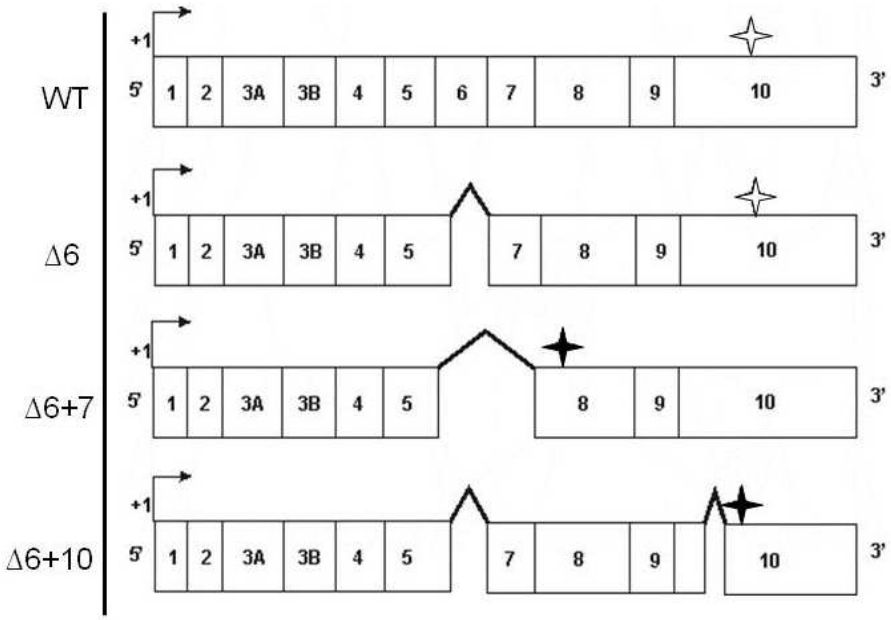

Figure 19. Schematic representation of the *CPB2* mRNA and of its splicing variants. Boxes represent exons. Hatched lines represent alternative splicing events. Hollow stars represent physiologic stop codons; solid starts represent out-of-frame splicing events leading to the introduction of premature stop codons. Exon numbering is as described by Boffa and coworkers (12).

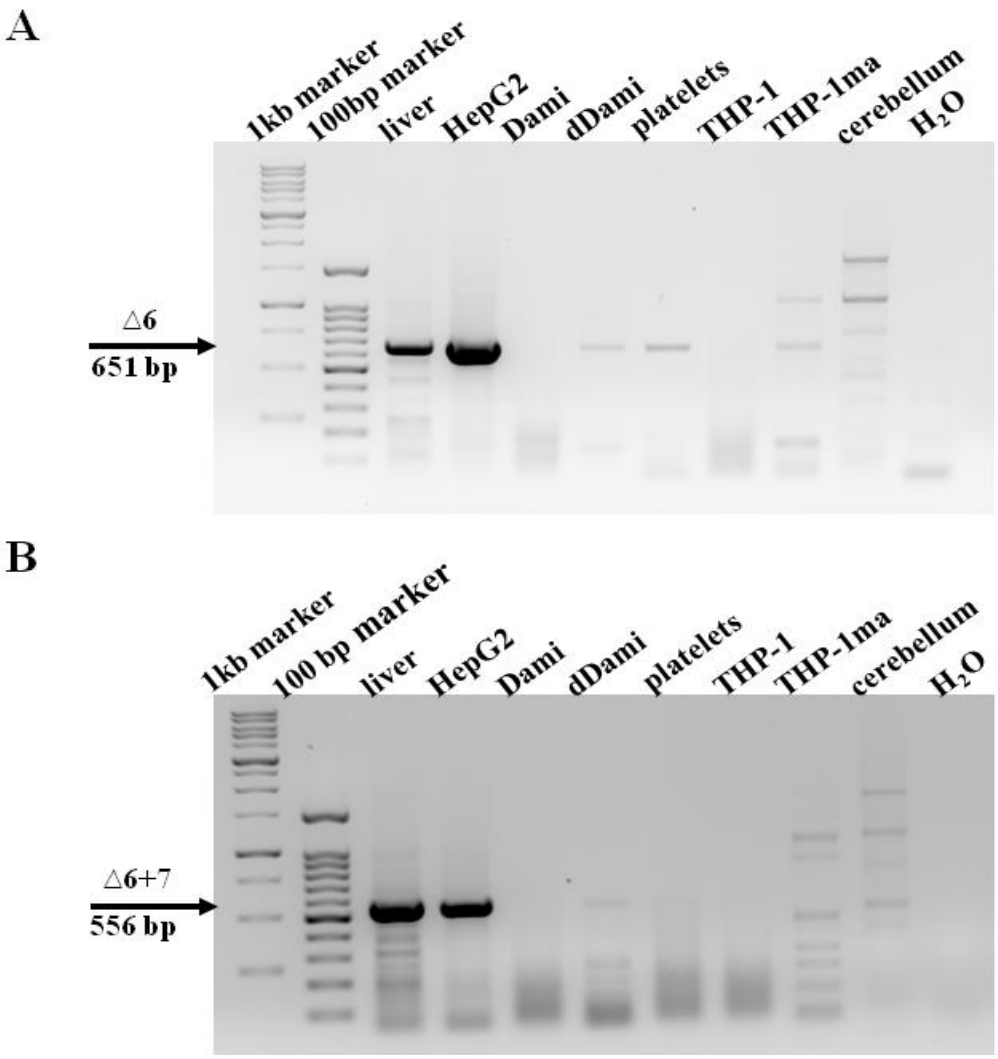

Figure 20. Detection of altrnatively spliced *CPB2* mRNA in various cell and tissue types using RT-PCR. RT-PCR was performed using 1.0 µg of total RNA isolated from the following cell and tissue types: human liver, HepG2, Dami cells, Dami cells differentiated using PMA (dDami), platelets, THP-1 cells, THP-1 cells differentiated using PMA (THP-1ma), and human cerebellum. The primer sets specifically amplify *CPB2* mRNA lacking exon 6 (Δ6) (**A**) or exon 6 and 7 (Δ6+7) (**B**) and produce a 651 bp or a 556 bp fragment, respectively. The RT-PCR products were resolved on 1.2% agarose gels; arrows indicates the expected amplification products. Exon numbering is as described by Boffa and coworkers (12).

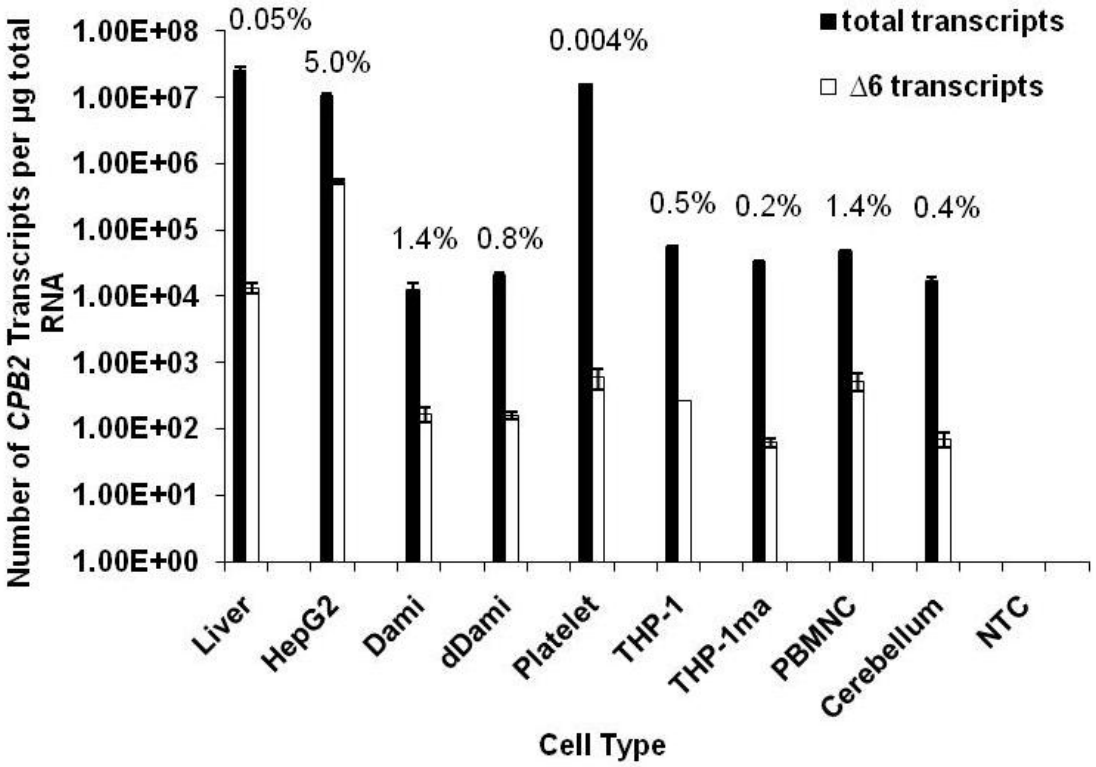

Figure 21. Quantitative analysis of alternativly spliced *CPB2* transcript lacking exon 6 in various human tissue and cell tyeps. The quantification of total and Δ6 *CPB2* transcripts in human liver, HepG2 cells, Dami cells, Dami cells differentiated using PMA (dDami), platelets, THP-1 cells, THP-1 cells differentiated using PMA (THP-1ma), human periferal blood mononuclear cells (PBMNC) and human cerebellum, was performed using quantitative real-time RT-PCR experiments using 1 µg of total RNA, with primer and probe sets specifict for the *CPB2* mRNA variant lacking exon 6 (Δ6). A primers-probe set that lies outside the alternatively spliced regions was also used to quantify total TAFI mRNA abundance. Absolute quantifications for each primers-prob set was based on respective *in vitro* transcribed human *CPB2* mRNA standards for both species; unknown quantities were interpolated from the stand curve. The data shown are the means of one to five independent experiments performed in triplicate. The error bars represent the standard error of the mean. NTC, no template control. % represents the quantity of Δ6 spliced transcripts detected divied by the quantity of total *CPB2* transcripts measured for each cell/tissue type.

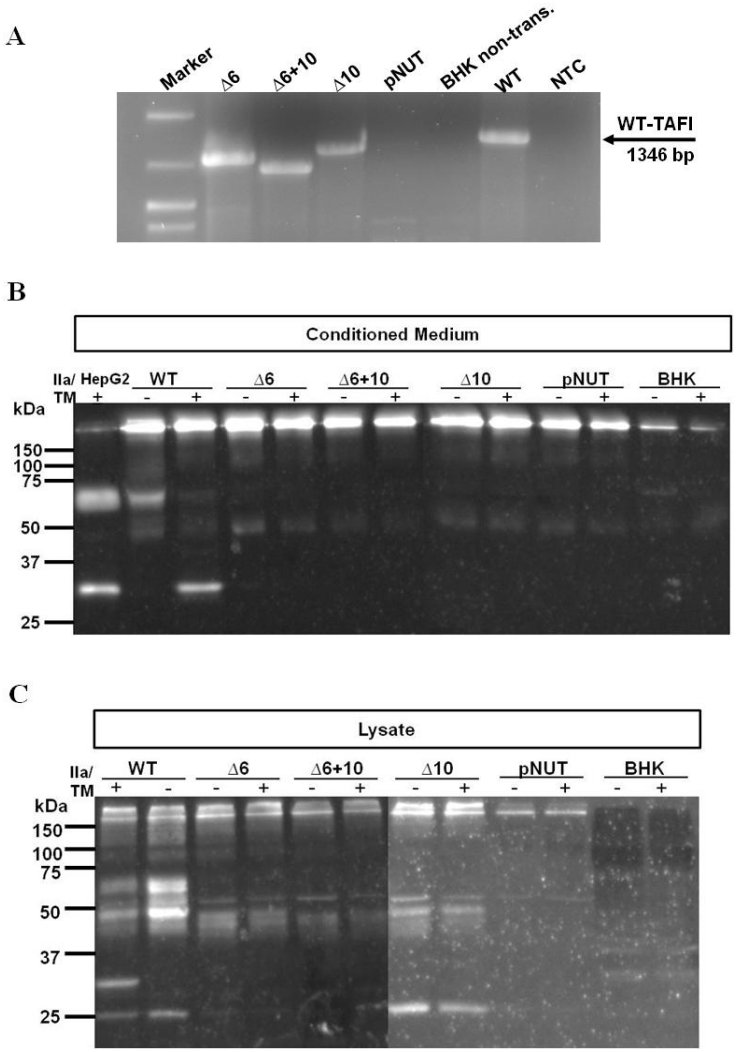

Figure 22. *In vitro* expression of TAFI variants encoded by alternatively spliced *CPB2* mRNA species. BHK cells were stablely stransfected with the expression plasmids TAFI-pNUT (WT), Δ6-pNUT (Δ6), Δ6+10-pNUT (Δ6+10), Δ10-pNUT (Δ10) or empty pNUT vector (pNUT). **A.** RT-PCR with primers TAFI-1 and TAFI-6 (16) was performed using 1.0 µg of total RNA isolated from the indicated cell lines. Reactions with total RNA harvested from untransfected BHK cells as well as a reaction without any RNA template (NTC) were included as negative controls. Primer set TAFI 1-6 amplifies a fragment of 1235 bp, 1183 bp, 1294 bp, and 1346 bp for Δ6, Δ6+10, Δ10 and WT, respectively. **B.** Conditioned midea were harvested from the indicated lines and concentrated approximately 60-fold using centricons followed by western blot analysis using polyclonal anti-TAFI antibodes. **C.** Lysate samples from indicated lines were harvested by applying six freeze/thaw cycles in phosphate-buffered saline (PBS) buffer. Where indicated, thrombin (25 nM final) and thrombomodulin (100 nM final) (IIa/TM) were added to activate potential TAFI in the sample. Samples were then subjected to western blot analysis using polyclonal anti-TAFI antibody.

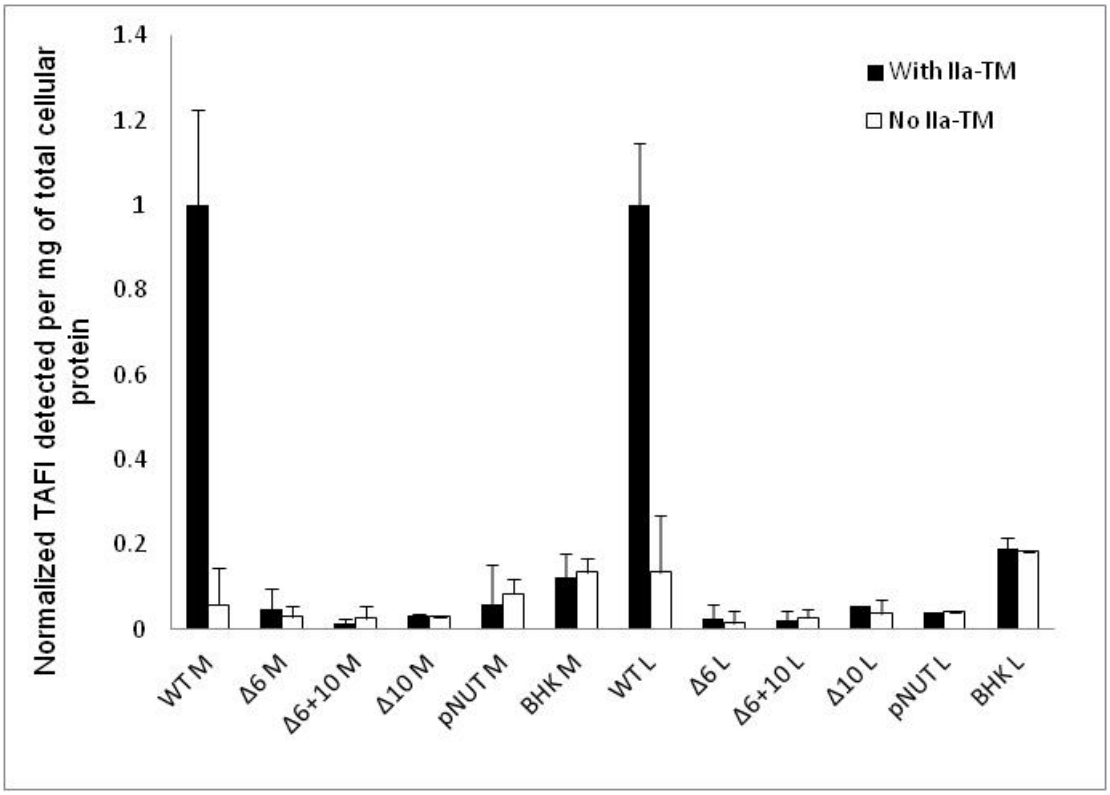

Figure 23. Quantification of the expression of TAFI protein variants from alternatively spliced transcripts. BHK cells were stablely stransfected with the expression plasmids TAFI-pNut (WT), Δ6-pNUT (Δ6), Δ6+10-pNUT (Δ6+10), Δ10-pNUT (Δ10) or empty pNUT vector (pNUT). Conditioned midea (M) were harvested from the indicated lines and concentrated approximately 60-fold using centricons. Lysate samples (L) from indicated lines were harvested by applying six freeze/thaw cycles in phosphate-buffered saline (PBS) buffer. Concentrations of recombinant TAFI variants were measured using a functional assay for TAFIa. Where indicated, thrombin (25 nM final) and thrombomodulin (100 nM final) (IIa/TM) were added to activate the TAFI varient. Then, samples were subjected to a quantitative TAFIa assay in which the concentration of TAFIa is determined from a standard curve. The data shown are the results of one experiment. Total cellular protein concentration from the respective lysates was used to account for the differences in protein content. Results were then normalized to the TAFIa level detected in the wild-type sample.

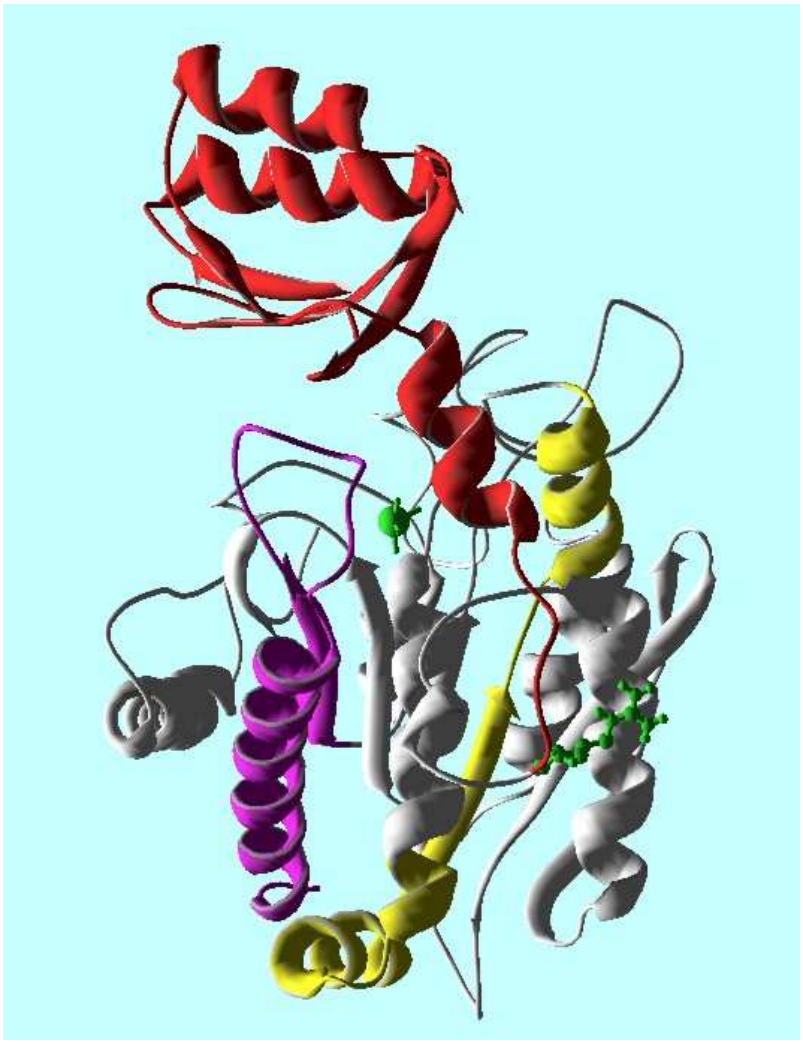

Figure 24. The structure of TAFI with emphasis on the location of amino acids coded by the exon 6 and exon 10 of *CPB2* mRNA. Based on the structure of TAFI by Marx and coworkers (16), the image represents the crystal structure of recombinant human TAFI. The backbone is represented as a ribbon trace, with the activation peptide in red and the catalytic domain in grey. The residues encoded by the exon 6 of *CPB2* mRNA are in yellow and span part of two helices, and internal beta strand and connecting loops. The residues in the carboxyl-terminal replaced as a result of alternative splicing in exon 10 are shown in purple, and consist of an internal beta-strand, a connecting loop, and the carboxyl-terminal alpha helix. Also shown, in green, is the Zn^{2+} atom in the active site as well as the side chain of Arg 92 at the activating cleavage site. Glu 363 is located near the carboxyl-terminus of the beta strand deleted in delta 10. In concert with the $Zn^{2+,}$ Glu 363 activates a water moledule that performs nucleophilic attack on the carbonyl carbon of the scissile bond.

Chapter 5: General Discussion

5.1 Detection of TAFI in non-hepatic cell types

5.1.1 The origin of platelet TAFI

Although the liver is the main source of plasma TAFI, a platelet pool of TAFI has been identified by Mosnier and coworkers (5). However, the source of the platelet TAFI remains to be definitively established. The authors reported that platelet TAFI showed smaller apparent molecular mass when compared to that of plasma TAFI, an observation they attributed to a different glycosylation pattern between the two species because deglycosylated plasma and platelet TAFI had identical electrophoretic mobilities. Furthermore, *CPB2* mRNA was detected in the megakaryocytic cell lines Dami and CHRF, but not MEG-01. Given this evidence, the authors postulated that platelet TAFI is synthesized in megakaryocytes rather than acquired by uptake from the plasma.

To further investigate the origin of platelet TAFI, we first used RT-PCR to detect *CPB2* mRNA in megakaryocytic cell lines MEG-01 and Dami cells, and we detected *CPB2* mRNA expression in both MEG-01 and Dami cells (76). Our MEG-01 RT-PCR results do not contradict what was reported by Mosnier *et al.* (5) as we also could not detect *CPB2* mRNA signal from MEG-01 when the RT-PCR experiments were broken down into a two-step process: cDNA synthesis followed by PCR reaction, a method of lower detection sensitivity (data not shown). We detected *CPB2* mRNA in MEG-01 cells using an RT-PCR protocol in which the reverse transcriptase and *Taq* polymerase enzymes were present in a single reaction mixture. The traditional method of RT-PCR is only semi-quantitative at best; thus, real-time RT-PCR analyses as used to obtain a rigorously quantitative measure of the expression of *CPB2* mRNA in MEG-01

and Dami cells. HepG2 cells showed at least 100-fold higher number of TAFI transcripts than any of the non-hepatic cell types investigated (Fig. 5). This result is plausible because liver is the main source for the circulating plasma TAFI. In addition, the amount of *CPB2* mRNA detected in MEG-01 cells, MEG-01 cells differentiated further along the megakaryocyte lineage by PMA, Dami cells, and Dami differentiated by PMA showed an overall increasing trend (Fig. 5). This observation agrees with the literature that MEG-01 and Dami represent the early and intermediate stages, respectively, of megakaryocyte development (90;91;95). As is the case with many other megakaryocyte genes, the expression of *CPB2* is observed to increase as megakarycoytes become more fully differentiated.

In addition to *CPB2* mRNA, we also reported the detection of TAFI protein in the megakaryocytic cell lines MEG-01 and Dami using western blot and a highly sensitive functional TAFIa assay (76). Interestingly, the conditioned medium of differentiated Dami cells showed the highest TAFI concentration for non-hepatic cell types, suggested that TAFI may be constitutively secreted from megakaryocytes as they mature, mostly likely due to immature granulation (90;91;95). A study by Briquet-Laugier and coworkers (98) reported that thrombopoietin (TPO), a cytokine that is commonly used in megakaryocyte differentiation, is capable of inducing α-granule biogenesis in PMA-treated Dami cells. It will be interesting to see whether or not TPO treatment can increase TAFI storage in differenciated Dami cells. Further analysis of *CPB2* mRNA and protein expression in megakaryocytes isolated from bone marrow could serve to definitively prove megakaryocyte expression of *CPB2*, which has, to this point, only been assessed in detail in megakaryoblastic cell lines derived from patients with leukemia. These experiments are challenging because megakaryocytes are in low abundance in bone marrow. However, we have undertaken some preliminary immunohistochemistry experiments with a

monoclonal antibody against TAFI and human bone marrow, and have found cells that stained positive for TAFI and the megakaryocyte marker CD41. We could not assess whether or not these cells are the multinucleate, mature megakaryocytes thus, further immunohistochemistry experiments are required. Furthermore, a model of human pro-platelet formation from hematopoietic $CD34^+$ progenitor cells that mimics the *in vivo* process has recently been developed (120). A change in *CPB2* gene expression as well as a change in TAFI secretion and packaging in the granules observed using this model will further enhance our understanding of platelet TAFI gene regulation.

It is important to stress that our data are fully consistent with those of Mosnier and coworkers that TAFI is an α-granule protein in platelets (5). Mosnier showed using fluorescence microscopy that TAFI is observed in a granular pattern in resting platelets, although co-localization with established α-granule proteins like von Willebrand factor or factor V was not performed. Furthermore, Mosnier demonstrated that platelet TAFI could be released by a variety of platelet agonists including thrombin, thrombin-receptor activating peptide, ADP, or collagen. In our own experiments, we showed that platelet TAFI was released from thrombin-activated platelets in a manner identical to the granular proteins von Willebrand factor and platelet factor 4 (Fig.11,12).

At this point, platelet TAFI as a result of uptake from plasma cannot be definitively ruled out because plasma-derived proteins can be internalized and packaged into α-granules by megakaryocytes. For example, the uptake of factor V occurs via clathrin-dependent endocytosis (126). A more detailed study examining incorporation of the circulating TAFI into megakaryocyte and platelet granules is needed to firmly address the origin of platelet TAFI. One approach to answer this question could be bone marrow transplantation between normal mice and

mice in which the gene encoding TAFI has been knocked out by homologous recombination. If platelet TAFI is derived solely from megakaryocyte expression, platelet TAFI should be absent in normal mice who have received bone marrow from TAFI$^{-/-}$ mice. Unfortunately, while analogous studies in mice of factor V expression demonstrated that platelet factor V was derived entirely from megakaryocyte expression, studies in human patients who had undergone liver transplantation showed that platelet factor V was entirely derived from endocytosis from plasma (127). As the human population contains variants of TAFI that differ in amino acid sequence and functional properties (the Thr/Ile polymorphism at position 325), perhaps analogous studies on human liver transplantation patients could be performed.

5.1.2 TAFI in monocyte and macrophages

Monocytes and macrophages play a central role in the host inflammatory response to bacterial infection; macrophages also accumulate in the vessel wall and sustain the inflammatory response as seen in atherosclerosis. We report for the first time the detection of *CPB2* mRNA in THP-1 and PMA-treated THP-1 (THP-1ma) cells using RT-PCR and qRT-PCR (Fig. 4-5) (76). Further examination revealed a 74% decrease in *CPB2* mRNA abundance when THP-1 was differentiated to THP-1ma after PMA treatment (Fig. 5). Although no *CPB2* mRNA was detected in atherosclerotic plaques using 2-step RT-PCR experiments (69), we have provided evidence for *CPB2* mRNA expression in PBMNCs. It will be interesting to revisit the study using more sensitive methods such as One-Step RT-PCR and qRT-PCT. Furthermore, it will be interesting to examine the change in *CPB2* gene expression, consequently, the underlying mechanism, using the well established THP-1 macrophage foam cell formation model (128;129).

Unlike the expression of *CPB2* mRNA, TAFI protein was detected in the medium of THP-1 macrophages, but not in the medium or lysate of undifferentiated THP-1 cells (Fig 9), suggested a potential increase in TAFI production and secretion upon differentiation. Studies with attempt to correlate mRNA expression and protein levels have found various degree of success: a yeast transcriptomic and proteomic comparison concluded that transcript level is insufficient in predicting the corresponding protein level (130). A recent study demonstrated a range of 46%- 68% correlation between gene and protein expressions depending on cell types (131). Therefore, it is not surprising to find that TAFI protein is not detected in undifferentiated THP-1 cells even though comparable TAFI transcript abundances are observed between undifferentiated THP-1 and differentiated Dami cells (Fig. 5). Thus, it is also not surprising to detect TAFI protein in THP-1 macrophages but not undifferentiated THP-1 cells when a decrease in TAFI mRNA was observed upon differentiation. It is possible that some blockage to translation of the *CPB2* mRNA is relieved when THP-1 cells differentiate; this topic will be the definite focus of future studies in our laboratory.

The apparent upregulation of TAFI production when monocytes differentiate into macrophages might reflect a role for TAFI in supporting the role of the latter cell type in fighting bacterial infection. Production and secretion of TAFI from macrophages may be a way to help contain bacteria at the site of injury. Monocytes have the ability to specifically invade tissues at sites of infection/inflammation and differentiate into macrophages. The expression of TAFI by macrophages would allow for an endogenous and/or sustained pool of TAFI at these sites, even in the absence of blood. It has been hypothesized that by stabilizing fibrin, TAFI may have a protective effect by isolating regions of severe infection. A study found that after 6 hours of abdominal *E. coli* injection, TAFI-deficient mice showed more bacteria in their peritoneal lavage

fluid and blood than the wild-type mice (132). It will be interesting to see if an increase in TAFI secretion can also be observed upon differentiation of PBMNCs. Based on the data from differentiated Dami cells and THP-1 macrophages (Fig. 9A), it seems that PMA treatment triggers TAFI translation and, hence, secretion. More studies are needed to elucidate the potential roles of monocyte/macrophage-derived TAFI during inflammation. A model for the function of macrophage-derived TAFI is depicted in Figure 25.

5.1.3 TAFI in vascular endothelial and smooth muscle cells.

Even though *CPB2* mRNA is detected in both HUVECs and HCAECs, no TAFI protein expression is observed in these cells (76). All experimental methods used in this study failed to detect *CPB2* mRNA from SMCs, suggesting that neither vascular endothelial cells nor SMCs are likely to be significant sources of TAFI *in vivo*. However, it cannot be ruled out that *CPB2* gene expression and protein translation may be inducible by unknown stimuli.

5.2 Cell type specific regulation of *CPB2* gene

Adding to the accumulating evidence that TAFI is expressed in cell types other then hepatocytes, we confirmed *CPB2* gene expression in the megakaryocytic cell lines MEG-01 and Dami, as well as the monocytic cell line THP-1 (76). We also demonstrated TAFI expression in CD41+ and CD163+ cells from human bone marrow, where CD41 and CD163 are the markers for megakaryocytes and mature monocytes, respectively (107-109). The platelet-derived TAFI provides an additional source of TAFI to modulate fibrinolysis while TAFI expression in

macrophages affords a mechanism to deliver TAFI to the extra-vascular compartment in the absence of a frank breach of the vasculature.

Bone marrow is found within barrier blood vessels inside of the bones. In large bones, bone marrow contains hematopoietic stem cells that give rise to new blood cells, including red and white blood cells as well as platelets. The blood vessels act as a barrier for immature blood cells to enter the blood stream and only the mature cells that contain membrane proteins can attach and pass the endothelium of the blood vessels. CD41, also known as integrin αIIb or platelet glycoprotein IIb (GPIIb), is a well-documented marker of the megakaryocytic lineage (108;109). GPIIb forms a heterodimer with GPIIIa (or CD61) to become GPIIb-IIIa (or $\alpha_{IIb}\beta_3$). On activated platelets, GPIIb-IIIa binds to fibrinogen and von Willebrand factor and plays important roles in enhancing cell adhesion and platelet aggregation (133). Recent studies found that microparticles generated from megakaryocytes and platelets also stained positive for CD41 (134;135).

Monocytes are generated in the bone marrow from common myeloid stem cells. CD163 is a marker that is specific for the mononuclear lineage, and is expressed in high quantity in most subpopulations of mature monocytes/macrophages including blood monocytes as well as resident mature bone marrow macrophages (107). CD163 is a member of the scavenger receptor cysteine-rich (SRCR) superfamily and has been suggested to function as an anti-inflammatory protein and plays a role in the clearance of damaged cells (107).

Using immunohistochemistry techniques, we showed for the first time the co-localization of TAFI with CD163+ and CD41+ cells in human bone marrow (Fig. 10), providing new physiological evidence for TAFI expression in monocytes and megakaryocytes, respectively. We

also found cells that stained positive for TAFI that stained for neither CD163 nor CD41. These findings indicate that additional cell types in the bone marrow (and, possibly, the blood) express TAFI. Candidates include neutrophils, basophils and eosinophils (which are also of the myeloid lineage), as well as cells of the lymphoid lineage including B- and T-lymphocytes, as well as progenitor cells in the respective lineage. Additional immunohistochemical investigations with a wider array of markers are required to complete these analyses.

Hepatic expression is the main source for the plasma pool of TAFI. Transcription factors are key regulatory proteins for the development of cell specificity and for transmitting modulation of gene expression by external stimuli. Molecular analysis of the human *CPB2* proximal promoter (up to nucleotide -425) using *in vitro* footprinting experiments revealed ten potential liver transcription factor binding sites denoted site A to J (Fig. 3). Transcription factors CCAAT/enhancer-binding protein (C/EBP), nuclear factor-Y (NF-Y), and glucocorticoid receptor (GR) bind to sites A, B, and C respectively, with hepatic nuclear factor-1 (HNF-1) binding between sites B and C (14). Quantitative analysis revealed that HepG2 cell expression of *CPB2* mRNA (which is on par with that in human liver) is more than 100-fold higher than that of Dami or THP-1 cells (76). Interestingly, HepG2 and THP-1 cells showed similar promoter activity profiles. Both showed high luciferase activity with the longest reporter construct (-2699-Luc); the promoter continued to stay active with the progressive 5'-deletion of *CPB2* sequences in the reporter constructs until sequences between -110 and -73 were deleted, at which point the reporter plasmid -73-Luc resulted in the same luciferase activity as the promoterless luciferase reporter vector pGL3 Basic ((12) and Fig.13). On the other hand, the promoter activity profile for Dami cells is very different. Transfection of Dami cells of the longest constructs (from -2699-Luc to -620-Luc) resulted in luciferase activities below the level seen with pGL3 Basic (Fig. 13).

Clearly, the *CPB2* gene is transcriptionally active in Dami cells, as we could readily detect endogenous expression of *CPB2* mRNA. It is possible that the sequences in the reporter plasmids between -2699 and -620 bind a transcriptional repressor that is not normally bound to this region in the context of native chromatin.

At the promoter level, one potential explanation for the high *CPB2* mRNA abundance observed in HepG2 compared to that of THP-1 or Dami cells is the presence of liver specific transcription factor such as HNF-1α. To our current knowledge, HNF-1α expression in megakaryocytes and monocytes has not yet been reported. Data from our laboratory demonstrated that the binding of HNF-1α is essential for *CPB2* promoter activity in HepG2 cells (14). It has been shown that HNF-1α synergizes with C/EBPα, another liver-enriched transcription factor, to increase the transcriptional activity of the human albumin gene, the promoter of which similar to that of *CPB2* in that both contain C/EBP, NF-Y, and HNF-1 binding sites within a 60 bp segment of their proximal promoters (136).

In the case of Dami cells, neither HNF-1 nor C/EBPε is expressed in megakaryocytes (137). The transcription factors that are essential for megakaryocyte differentiation and thrombopoiesis are GATA-1, its co-factor FOG-1 (Friend of GATA-1), and NF-E2 (138). GATA-1 is a zinc finger transcription factor that is expressed in erythroid cells and megakaryocytes that targets functional GATA elements ((A/T)GATA(A/G)) in the proximal promoters of erythroid- and megakaryocyte-restricted genes (139). Enforced GATA-1 expression has been shown to convert granulocyte/macrophage precursors into megakaryocyte/erythrocyte precursors, and to inhibit the formation of granulocytes and macrophages (140). A scan of the *CPB2* proximal promoter (up to nucleotide -620) revealed a potential GATA-1 binding site AGATAG 228 bp upstream of the transcriptional start site (+1). It has been shown that GATA-1

can interact with NF-Y to activate the gene encoding FcγRIIa in megakaryocytic cells (141). Hence, it is tempting to speculate that NF-Y binding to Site B of the *CPB2* promoter can allow interaction with GATA-1/Fog-1 and can contribute to the megakaryocyte-specific expression of *CPB2*. NF-Y has also been reported to act as both enhancer and a repressor. NF-Y was found to be an activator when it interacts with the upstream CCAAT element that is required for vWf promoter activation, but can also act as a repressor when interacts with the CCAAT element located in exon 1 of the vWf gene (142). It will be interesting to investigate how these transcription factors including GATA-1 and NF-Y play a role, if any, in *CPB2* gene regulation in Dami cells, particularly, in the context of chromatin.

Concerning monocytes, C/EBPα expression is essential to direct monocytic commitment of primary myeloid progenitors (143). In fact, a study found that when fibroblast cells (NIH 3T3) were over-expressing transcription factors PU.1 and C/EBPα, cells showed up-regulation of macrophage-restricted genes as well as expression of cell surface antigen markers that resemble those of macrophages. At the same time, down-regulation of fibroblast-associated genes was observed (144). While PU.1 and C/EBPα are important for the commitment to form monocytes precursors, PU.1, C/EBPβ and NF-Y have been shown to be important for the differentiation of monocytes to become tissue macrophages (145). In addition, various C/EBP isoforms are known to synergize with NF-Y to activate variety of genes in different tissues, including amelogenin gene in ameloblast-like cell line (146) and adiponectin in adipocytes (147). It is reasonable to propose that C/EBP and NF-Y bind to site A and B of the *CPB2* promoter, respectively, and interact with each other to activate the *CPB2* promoter in THP-1 cells. Further experiments such as *in vitro* and *in vivo* footprinting analyses and electrophoretic mobility shift assays (EMSA) using nuclear extracts from Dami and THP-1 cells will help identify cell-specific transcription

factors that direct *CPB2* gene express in these cells. As the steady-state abundance of the mRNA is dependent on its rate of synthesis and decay, other regulatory mechanisms such as control of mRNA stability may also contribute to the steady-state of *CPB2* mRNA level in Dami and THP-1 cells.

5.3 The role of alternatively spliced *CPB2* mRNA and TAFI variants

TAFI is a carboxypeptidase precursor that, once activated, functions as a carboypeptidase B-like enzyme and removes carboxyl-terminal arginine and lysine residues from proteins and peptide substrates (2). Full-length TAFI is composed of 401 amino acids with a theoretical molecular mass of 48 kDa that migrates on a SDS-PAGE with apparent molecular mass of 60 kDa due to glycosylation modification of the amino-terminal activation domain (2). Upon activation, TAFIa migrates on SDS-PAGE with a molecular mass of 35 kDa due to the loss of this amino-terminal domain containing four *N*-linked oligosaccharides (23). Although liver has been long thought to be the main source of plasma TAFI, TAFI has also been identified in PMA-treated megakaryocytic-cell line Dami, PMA-treated monocytic cell line THP-1, and platelets (5;76). In addition to these TAFI pools, Matsumoto and coworkers described a form of TAFI encoded by an alternatively spliced *CPB2* transcript in the human brain that lacks exon 6 and a 52-base deletion in exon 10 of *CPB2* mRNA (Δ6+10) (4). The later deletion results in a frame-shift and the replacement of the carboxyl-terminal 42 residues of TAFI with a unique 14 amino acid sequence (4). Two forms of brain TAFI seems to co-exist naturally: a 40 kDa TAFI "zymogen" and a 30 kDa "enzyme". Both forms were found to be stored inside the human hippocampus tissue as well as to be constitutively secreted into blood and cerebrospinal fluid

(4;66). They seemed to function as secretase-like proteins that cleave β-amyloid precursor protein (APP) to generate β-amyloid, a process that has implications in Alzheimer's disease (4;66). As outlined in Chapter 4, there are several experimental differences between our system and that of Matsumoto group, difference which will be discussed further below.

Matsumoto and coworkers also reported that the Δ6+10 species was the only one present in human hippocampus RNA. This conclusion is very much at odds with our own findings using quantitative RT-PCR, in which *CPB2* transcripts lacking exon 6 were a very minor component of the total *CPB2* transcripts in brain (Fig. 21). In fact, inspection of Figure 3C of the Matsumoto group's 2000 paper (4) reveals the basis of this contention: a band from RT-PCR that they claim migrates as 1077 bp but in fact appears to be considerably larger (midway between the 1000 bp and 1500 bp markers; the full-length TAFI ORF is almost 1400 bp). It remains possible, however, that alternatively-spliced *CPB2* transcripts predominate specifically in hippocampus, if not in the cerebral cortex as a whole.

Our findings using recombinant expression of TAFI variants encoded by cDNA's representing alternatively spliced mRNA's clearly show that none of the shorter TAFI variants can be secreted by cells. We attribute this to aberrant folding of the shorter variants such that they cannot exit the ER. Indeed, the apparent size of the intracellular variant TAFI species was 45 – 48 kDa, consistent with incomplete glycosylation as would be expected from proteins that did not proceed to the Golgi apparatus. Because glycosylation has been suggested to increase stability of TAFI zymogen (16) and may also affect the folding as well as the function of the protein (34), it is possible that within the environment of the brain cells, brain-TAFI is folded differently and can be activated via auto-activation or other unknown mechanism that is brain specific; consequently, brain-TAFI would acquire a secretase-like activity. Matsumoto and coworkers reported the

secretion of variant TAFI into blood and cerebrospinal fluid (66). However, this contention was based only on immunoreactivity in western blots against poorly characterized antibodies raised against a synthetic peptide encompassing the unique carboxyl-terminus encoded by the Δ10 variant or against a comparatively crude "brain TAFI" preparation.

As we speculate in Chapter 4, it is possible that TAFI variants generated by alternative splicing could act as chaperones, at least for the endopeptidase that degrades APP. In cases where alternatively spliced transcripts are more abundant (such as in HepG2 cells), alternative splicing of the *CPB2* mRNA would serve to limit the secretion of functional TAFI. It is interesting to note that a *CPB2* haplotype associated with an increased extent of exon 6 skipping (H_{B2}) compared to another haplotype (H_A) (64) is associated with an increased chance of a G at position +505, encoding Ala at position 147 (rs3742264). In turn, the Ala/Ala147 genotype is associated with a lower plasma TAFI concentration than the Thr/Thr/147 genotype (148). It is tempting to speculate that the greater extent of exon 6 skipping observed with the +505G (Ala147) allele accounts for this association.

Other potential attempts to define the role of alternative splicing of *CPB2* are more closely related to the basic purpose of the cell to generate a transcript. In general, the role of alternative splicing is to increase the proteome's ability to generate a wide range of proteins with limited genomic information and to increase the proteome's ability to adapt to environmental changes. The alternatively spliced mRNA species have several potential outcomes: (i) produce a novel protein sequence due to frame-shift, thus generate new functionality or characteristics (4;149); (ii) produce a premature stop codon and target the transcript for nonsense-mediated decay (119) (an effect we failed to observe for the Δ6+7 variant); (iii) produce a non-functional protein (119); (iv) are the result of stochastic noise or splicing "error" in the splicing process

(118). Criteria for acceptance of the stochastic noise model include: (a) the number of alternative spliced variants increases as the total expression of a gene and number of introns in a gene increases; (b) the alternatively spliced variants do not show clear tissue specificity; (c) the protein product is non-functional; (d) the amount of splicing "error" decreases as the absolute numbers of "correct forms" increase (118).

In Chapter 4, we set out to characterize the expression of alternatively spliced *CPB2* mRNA variants in cell and tissue types that are important in the pathology of cardiovascular diseases including liver, hepatocarcinoma cell line HepG2, megakaryocytic cell line Dami, platelets, monocytic cell line THP-1 and peripheral blood mononuclear cells. Over the course of the project, we found that the cell types with the highest full-length *CPB2* mRNA abundance, for example, HepG2 and platelets, showed the most consistent splicing patterns with different experimental techniques: HepG2 cells contain alternatively spliced *CPB2* mRNA variants Δ6 and Δ6+7 and platelets contains Δ6+10. On the other hand, the profile of alternatively spliced *CPB2* mRNA variants in other cell types such as Dami and THP-1 differs dramatically from sample to sample. With the exception of full-length *CPB2* cDNA, RT-PCR experiments using primer sets TAFI 1-4 or TAFI 3-4 shows different splicing patterns within the same cell type over the years (compare Fig. 4A (76) and Appendix A-B, particularly Dami and THP-1 samples). These sample to sample differences may, at least in part, explain the inconsistency observed between RT-PCR and qRT-PCR experiments for Δ6 expression in Dami, THP-1, THP-1ma, and cerebellum (Fig.4, Fig.17, Fig. 19-20). Taken together, these observations fit with the criterion (a) stated above that the number of splicing events increases as the total *CPB2* mRNA abundance increases.

Using qRT-PCR, we detected the expression of Δ6 mRNA variants in all the tissue/cell type of interest; quantification analysis also showed that liver and platelets, while expressing the

highest amount of CPB2 mRNA, had the lowest expression of Δ6 variant (in percentage, ~0.05% of the total) compared to the rest of the cell types. On the other hand, the abundance of Δ6 transcript in other cell types seems to be maintained at similar level. Taken together, these observations fit with the criteria (b) and (d) stated above that the Δ6 variant does not show clear cell-type specific preference and that the relative Δ6 expression decreases when the total *CPB2* mRNA abundance increases.

Finally, western blot analysis showed potential accumulation of truncated TAFI inside the cells. These potential TAFI variants cannot be activated with IIa/TM treatment nor have the ability to cleave lysin residues from fibrin degradation products in TAFIa assay, indicating that these proteins have lost their function as TAFI-like carboxypeptidase. Although more experiments are required to further investigate other potential functionality of these TAFI variants, taken together, these observations fits with the criteria (c) stated above, at least for now, that the truncated TAFI variants are non-functional, and that some alternatively spliced *CPB2* mRNA variants detected were the result of stochastic noise in the splicing process.

Importantly, only detailed investigations of the function of TAFI variants derived from alternative splicing, as well as a full enumeration of the relative expression of the different alternatively spliced forms, will allow us to determine whether alternative splicing of *CPB2* mRNA has a definite physiological role.

5.4 Concluding remarks

The analysis of the mechanism of *CPB2* gene expression regulation in non-hepatic cell types presented in this document has three general purposes. First, we explored the *CPB2* gene

expression in non-hepatic cell types that have implication in the pathology of cardiovascular diseases. The detection of TAFI expression in megakaryocytes provided further evidence in addressing the origin of platelet-derived TAFI, while the confirmation of platelet TAFI pool provides new insight on how TAFI pathway affects the clot formation and breakdown. The detection of TAFI expression in monocytes/macrophages suggests novel functions for TAFI in addition to controlling clot lysis; indeed, such roles are beginning to emerge from animal model experiments (49). Second, we initiated the investigation of cell-type specific *CPB2* gene regulation by dissecting proximal *CPB2* promoter in a cell-type specific manner. Continuation of the study will provide new knowledge on how *CPB2* gene is regulated in different cell type and environment and its respond to external stimuli. Third, we discovered alternatively spliced *CPB2* mRNA in several additional cell types to those reported. Alternative splicing may provide another way to regulate the *CPB2* gene expression. The study of alternatively spliced *CPB2* mRNA expressions and the functionality of the protein variants will advance our general knowledge in the molecular basis of *CPB2* gene regulation.

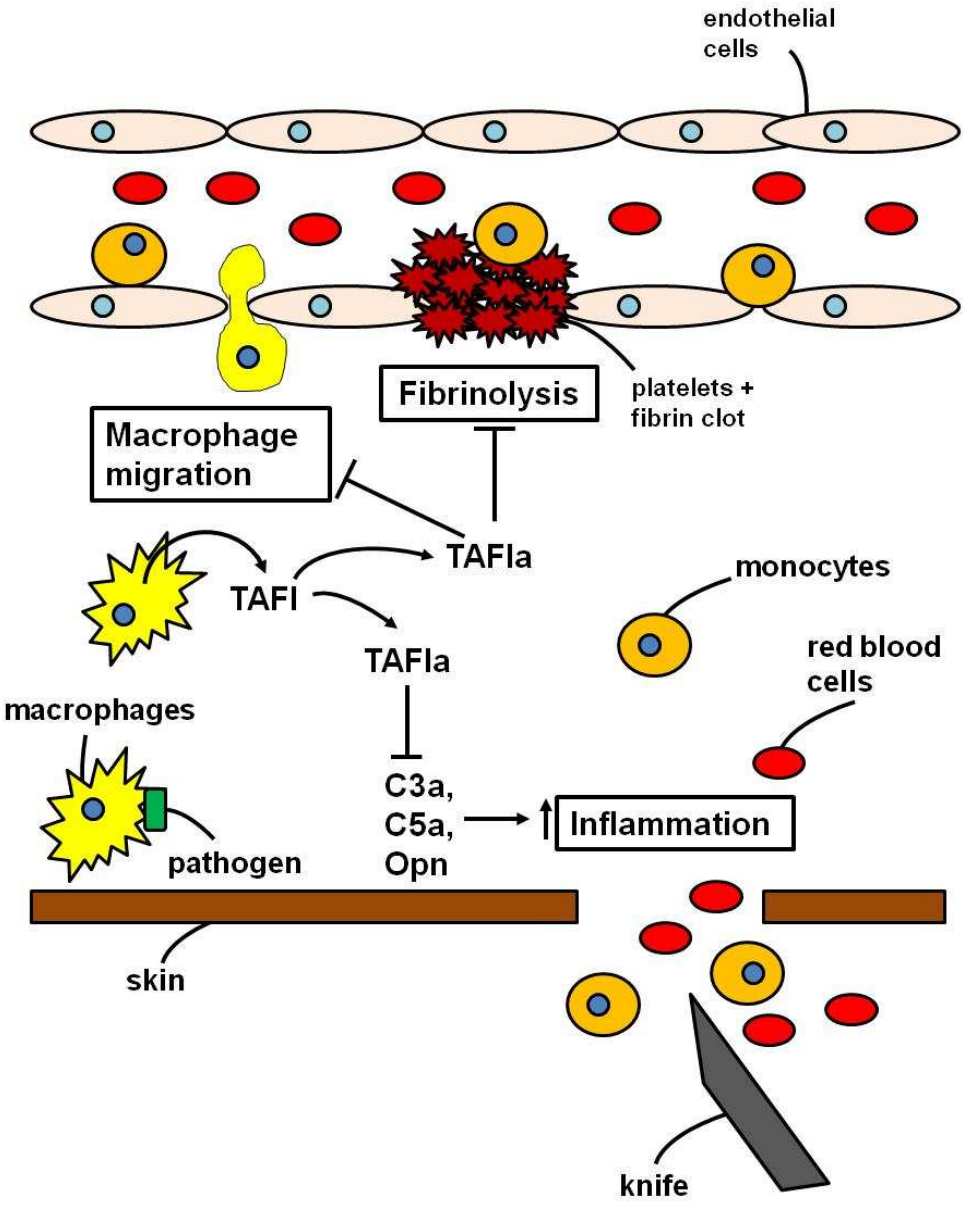

Figure 25. Model for the potential functions of macrophage-derived TAFI. In addition to the balancing between coagulation and fibrinolysis, macrophage-derived TAFI may also contribute to anti-inflammation in site specific manner. In addition to Lysin residue from degraded fibrin, TAFIa inhibit C3a, C5a and thrombin-cleaved osteopontin (Opn) activity by cleaving Arginine from their carboxyl-termini. By inhibiting plasmin function, TAFIa can also slow down macrophage migration as well as to help contain bacteria at the site of injury.

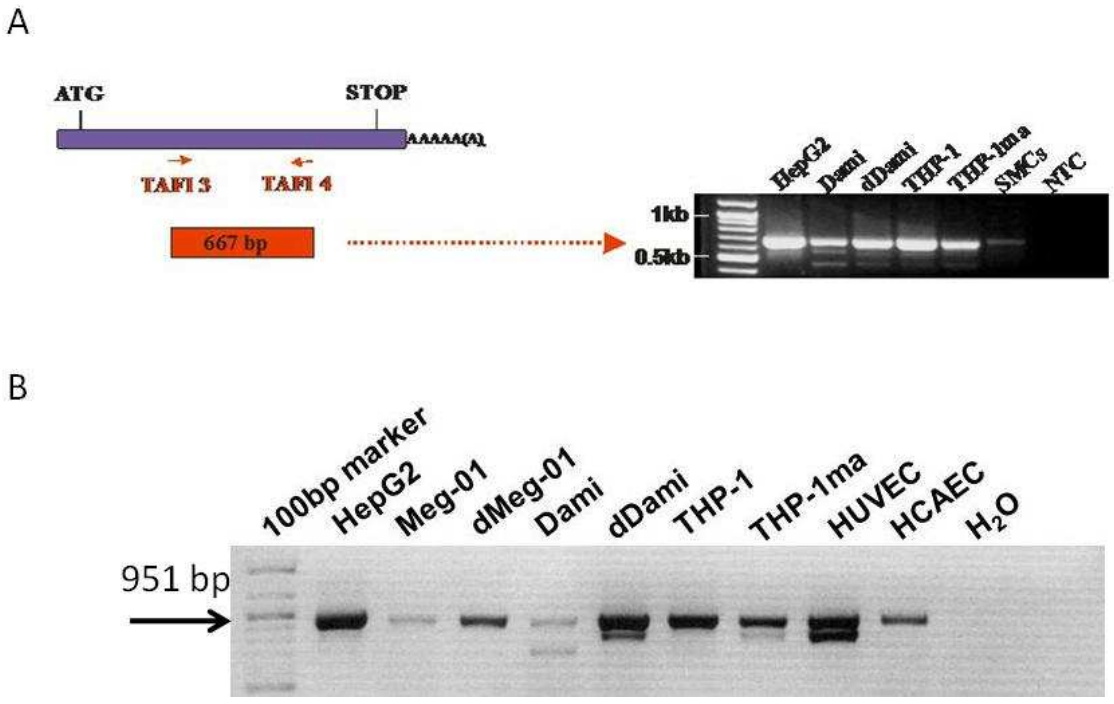

Appendix. Detection of alternative *CPB2* mRNA splicing pattern in various cell types. RT-PCR experiments with two different primer sets were performed using total RNA from the indicated cell types. RT-PCR products were resolved on 1.2% gels. **A.** RT-PCR experiment using primer set TAFI 3-4 performed in year 2006. **B.** RT-PCR experiment using primer set TAFI 1-4 performed in year 2008. NTC, no template control. Arrows indicated the expected fragments for full-length *CPB2* cDNA.

Reference

(1) Vine AK. Recent advances in haemostasis and thrombosis. Retina 2009;29:1-7.

(2) Nesheim M. Thrombin and fibrinolysis. Chest 2003;124:33S-9S.

(3) Frere C, Morange PE, Saut N, Tregouet DA, Grosley M, Beltran J, et al. Quantification of thrombin activatable fibrinolysis inhibitor (TAFI) gene polymorphism effects on plasma levels of TAFI measured with assays insensitive to isoform-dependent artefact. Thromb Haemost 2005;94:373-9.

(4) Matsumoto A, Itoh K, Matsumoto R. A novel carboxypeptidase B that processes native beta-amyloid precursor protein is present in human hippocampus. Eur J Neurosci 2000;12:227-38.

(5) Mosnier LO, Buijtenhuijs P, Marx PF, Meijers JC, Bouma BN. Identification of thrombin activatable fibrinolysis inhibitor (TAFI) in human platelets. Blood 2003;101:4844-6.

(6) Hori Y, Gabazza EC, Yano Y, Katsuki A, Suzuki K, Adachi Y, et al. Insulin resistance is associated with increased circulating level of thrombin-activatable fibrinolysis inhibitor in type 2 diabetic patients. J Clin Endocrinol Metab 2002;87:660-5.

(7) Qu Z, Chaikof EL. Interface between hemostasis and adaptive immunity. Curr Opin Immunol 2010;22:634-42.

(8) Hoffman M. Remodeling the blood coagulation cascade. J Thromb Thrombolysis 2003;16:17-20.

(9) Nesheim M, Bajzar L. The discovery of TAFI. J Thromb Haemost 2005;3:2139-46.

(10) Boffa MB, Nesheim ME, Koschinsky ML. Thrombin activable fibrinolysis inhibitor (TAFI): molecular genetics of an emerging potential risk factor for thrombotic disorders. Curr Drug Targets Cardiovasc Haematol Disord 2001;1:59-74.

(11) Vanhoof G, Wauters J, Schatteman K, Hendriks D, Goossens F, Bossuyt P, et al. The gene for human carboxypeptidase U (CPU)--a proposed novel regulator of plasminogen activation--maps to 13q14.11. Genomics 1996;38:454-5.

(12) Boffa MB, Reid TS, Joo E, Nesheim ME, Koschinsky ML. Characterization of the gene encoding human TAFI (thrombin-activable fibrinolysis inhibitor; plasma procarboxypeptidase B). Biochemistry 1999;38:6547-58.

(13) Boffa MB, Maret D, Hamill JD, Bastajian N, Crainich P, Jenny NS, et al. Effect of single nucleotide polymorphisms on expression of the gene encoding thrombin-activatable fibrinolysis inhibitor: a functional analysis. Blood 2008;111:183-9.

(14) Garand M, Bastajian N, Nesheim ME, Boffa MB, Koschinsky ML. Molecular analysis of the human thrombin-activatable fibrinolysis inhibitor gene promoter. Br J Haematol 2007;138:231-44.

(15) Eaton DL, Malloy BE, Tsai SP, Henzel W, Drayna D. Isolation, molecular cloning, and partial characterization of a novel carboxypeptidase B from human plasma. J Biol Chem 1991;266:21833-8.

(16) Marx PF, Brondijk TH, Plug T, Romijn RA, Hemrika W, Meijers JC, et al. Crystal structures of TAFI elucidate the inactivation mechanism of activated TAFI: a novel mechanism for enzyme autoregulation. Blood 2008;112:2803-9.

(17) Bajzar L, Manuel R, Nesheim ME. Purification and characterization of TAFI, a thrombin-activable fibrinolysis inhibitor. J Biol Chem 1995;270:14477-84.

(18) Campbell W, Okada H. An arginine specific carboxypeptidase generated in blood during coagulation or inflammation which is unrelated to carboxypeptidase N or its subunits. Biochem Biophys Res Commun 1989;162:933-9.

(19) Wang W, Hendriks DF, Scharpe SS. Carboxypeptidase U, a plasma carboxypeptidase with high affinity for plasminogen. J Biol Chem 1994;269:15937-44.

(20) Valnickova Z, Thogersen IB, Potempa J, Enghild JJ. Thrombin-activable fibrinolysis inhibitor (TAFI) zymogen is an active carboxypeptidase. J Biol Chem 2007;282:3066-76.

(21) Foley JH, Kim P, Nesheim ME. Thrombin-activable fibrinolysis inhibitor zymogen does not play a significant role in the attenuation of fibrinolysis. J Biol Chem 2008;283:8863-7.

(22) Kim PY, Foley J, Hsu G, Kim PY, Nesheim ME. An assay for measuring functional activated thrombin-activatable fibrinolysis inhibitor in plasma. Anal Biochem 2008;372:32-40.

(23) Valnickova Z, Christensen T, Skottrup P, Thogersen IB, Hojrup P, Enghild JJ. Post-translational modifications of human thrombin-activatable fibrinolysis inhibitor (TAFI): evidence for a large shift in the isoelectric point and reduced solubility upon activation. Biochemistry 2006;45:1525-35.

(24) Song EY, Kang SK, Lee YC, Park YG, Chung TH, Kwon DH, et al. Expression of bisecting N-acetylglucosaminyltransferase-III in human hepatocarcinoma tissues, fetal liver tissues, and hepatoma cell lines of Hep3B and HepG2. Cancer Invest 2001;19:799-807.

(25) Bajzar L, Morser J, Nesheim M. TAFI, or plasma procarboxypeptidase B, couples the coagulation and fibrinolytic cascades through the thrombin-thrombomodulin complex. J Biol Chem 1996;271:16603-8.

(26) Boffa MB, Koschinsky ML. Curiouser and curiouser: recent advances in measurement of thrombin-activatable fibrinolysis inhibitor (TAFI) and in understanding its molecular genetics, gene regulation, and biological roles. Clin Biochem 2007;40:431-42.

(27) Boffa MB, Wang W, Bajzar L, Nesheim ME. Plasma and recombinant thrombin-activable fibrinolysis inhibitor (TAFI) and activated TAFI compared with respect to glycosylation, thrombin/thrombomodulin-dependent activation, thermal stability, and enzymatic properties. J Biol Chem 1998;273:2127-35.

(28) Anand K, Pallares I, Valnickova Z, Christensen T, Vendrell J, Wendt KU, et al. The crystal structure of thrombin-activable fibrinolysis inhibitor (TAFI) provides the structural basis for its intrinsic activity and the short half-life of TAFIa. J Biol Chem 2008;283:29416-23.

(29) Boffa MB, Bell R, Stevens WK, Nesheim ME. Roles of thermal instability and proteolytic cleavage in regulation of activated thrombin-activable fibrinolysis inhibitor. J Biol Chem 2000;275:12868-78.

(30) Schneider M, Boffa M, Stewart R, Rahman M, Koschinsky M, Nesheim M. Two naturally occurring variants of TAFI (Thr-325 and Ile-325) differ substantially with respect to thermal stability and antifibrinolytic activity of the enzyme. J Biol Chem 2002;277:1021-30.

(31) Marx PF, Havik SR, Marquart JA, Bouma BN, Meijers JC. Generation and characterization of a highly stable form of activated thrombin-activable fibrinolysis inhibitor. J Biol Chem 2004;279:6620-8.

(32) Jia Z. TAFI: structured for self-destruction. Blood 2008;112:2597-8.

(33) Marx PF, Plug T, Havik SR, Morgelin M, Meijers JC. The activation peptide of thrombin-activatable fibrinolysis inhibitor: a role in activity and stability of the enzyme? J Thromb Haemost 2009;7:445-52.

(34) Biscetti F. Glycosylation of thrombin activatable fibrinolysis inhibitor: why is it so important? Circ Res 2008;102:278-9.

(35) Buelens K, Hillmayer K, Compernolle G, Declerck PJ, Gils A. Biochemical importance of glycosylation in thrombin activatable fibrinolysis inhibitor. Circ Res 2008;102:295-301.

(36) Wu C, Kim PY, Manuel R, Seto M, Whitlow M, Nagashima M, et al. The roles of selected arginine and lysine residues of TAFI (Pro-CPU) in its activation to TAFIa by the thrombin-thrombomodulin complex. J Biol Chem 2009;284:7059-67.

(37) van Tilburg NH, Rosendaal FR, Bertina RM. Thrombin activatable fibrinolysis inhibitor and the risk for deep vein thrombosis. Blood 2000;95:2855-9.

(38) Eichinger S, Schonauer V, Weltermann A, Minar E, Bialonczyk C, Hirschl M, et al. Thrombin-activatable fibrinolysis inhibitor and the risk for recurrent venous thromboembolism. Blood 2004;103:3773-6.

(39) Leebeek FW, Goor MP, Guimaraes AH, Brouwers GJ, Maat MP, Dippel DW, et al. High functional levels of thrombin-activatable fibrinolysis inhibitor are associated with an increased risk of first ischemic stroke. J Thromb Haemost 2005;3:2211-8.

(40) Santamaria A, Oliver A, Borrell M, Mateo J, Belvis R, Marti-Fabregas J, et al. Risk of ischemic stroke associated with functional thrombin-activatable fibrinolysis inhibitor plasma levels. Stroke 2003;34:2387-91.

(41) Santamaria A, Martinez-Rubio A, Borrell M, Mateo J, Ortin R, Fontcuberta J. Risk of acute coronary artery disease associated with functional thrombin activatable fibrinolysis inhibitor plasma level. Haematologica 2004;89:880-1.

(42) Juhan-Vague I, Morange PE, Aubert H, Henry M, Aillaud MF, Alessi MC, et al. Plasma thrombin-activatable fibrinolysis inhibitor antigen concentration and genotype in relation to myocardial infarction in the north and south of Europe. Arterioscler Thromb Vasc Biol 2002;22:867-73.

(43) Broze GJ, Jr., Higuchi DA. Coagulation-dependent inhibition of fibrinolysis: role of carboxypeptidase-U and the premature lysis of clots from hemophilic plasma. Blood 1996;88:3815-23.

(44) Foley JH, Nesheim ME. Soluble thrombomodulin partially corrects the premature lysis defect in FVIII-deficient plasma by stimulating the activation of thrombin activatable fibrinolysis inhibitor. J Thromb Haemost 2009;7:453-9.

(45) Campbell WD, Lazoura E, Okada N, Okada H. Inactivation of C3a and C5a octapeptides by carboxypeptidase R and carboxypeptidase N. Microbiol Immunol 2002;46:131-4.

(46) Myles T, Nishimura T, Yun TH, Nagashima M, Morser J, Patterson AJ, et al. Thrombin activatable fibrinolysis inhibitor, a potential regulator of vascular inflammation. J Biol Chem 2003;278:51059-67.

(47) Asai S, Sato T, Tada T, Miyamoto T, Kimbara N, Motoyama N, et al. Absence of procarboxypeptidase R induces complement-mediated lethal inflammation in lipopolysaccharide-primed mice. J Immunol 2004;173:4669-74.

(48) Leung LL, Nishimura T, Myles T. Regulation of tissue inflammation by thrombin-activatable carboxypeptidase B (or TAFI). Adv Exp Med Biol 2008;632:61-9.

(49) Morser J, Gabazza EC, Myles T, Leung LL. What has been learnt from the thrombin-activatable fibrinolysis inhibitor-deficient mouse? J Thromb Haemost 2010;8:868-76.

(50) Du XY, Zabel BA, Myles T, Allen SJ, Handel TM, Lee PP, et al. Regulation of chemerin bioactivity by plasma carboxypeptidase N, carboxypeptidase B (activated thrombin-activable fibrinolysis inhibitor), and platelets. J Biol Chem 2009;284:751-8.

(51) Luangsay S, Wittamer V, Bondue B, De HO, Rouger L, Brait M, et al. Mouse ChemR23 is expressed in dendritic cell subsets and macrophages, and mediates an anti-inflammatory activity of chemerin in a lung disease model. J Immunol 2009;183:6489-99.

(52) Sato T, Miwa T, Akatsu H, Matsukawa N, Obata K, Okada N, et al. Pro-carboxypeptidase R is an acute phase protein in the mouse, whereas carboxypeptidase N is not. J Immunol 2000;165:1053-8.

(53) van Gorp EC, Minnema MC, Suharti C, Mairuhu AT, Brandjes DP, ten CH, et al. Activation of coagulation factor XI, without detectable contact activation in dengue haemorrhagic fever. Br J Haematol 2001;113:94-9.

(54) Watanabe R, Wada H, Watanabe Y, Sakakura M, Nakasaki T, Mori Y, et al. Activity and antigen levels of thrombin-activatable fibrinolysis inhibitor in plasma of patients with disseminated intravascular coagulation. Thromb Res 2001;104:1-6.

(55) Zeerleder S, Schroeder V, Hack CE, Kohler HP, Wuillemin WA. TAFI and PAI-1 levels in human sepsis. Thromb Res 2006;118:205-12.

(56) Verbon A, Meijers JC, Spek CA, Hack CE, Pribble JP, Turner T, et al. Effects of IC14, an anti-CD14 antibody, on coagulation and fibrinolysis during low-grade endotoxemia in humans. J Infect Dis 2003;187:55-61.

(57) Boffa MB, Hamill JD, Maret D, Brown D, Scott ML, Nesheim ME, et al. Acute phase mediators modulate thrombin-activable fibrinolysis inhibitor (TAFI) gene expression in HepG2 cells. J Biol Chem 2003;278:9250-7.

(58) So AK, Varisco PA, Kemkes-Matthes B, Herkenne-Morard C, Chobaz-Peclat V, Gerster JC, et al. Arthritis is linked to local and systemic activation of coagulation and fibrinolysis pathways. J Thromb Haemost 2003;1:2510-5.

(59) te Velde EA, Wagenaar GT, Reijerkerk A, Roose-Girma M, Borel Rinkes IH, Voest EE, et al. Impaired healing of cutaneous wounds and colonic anastomoses in mice lacking thrombin-activatable fibrinolysis inhibitor. J Thromb Haemost 2003;1:2087-96.

(60) Swaisgood CM, Aronica MA, Swaidani S, Plow EF. Plasminogen is an important regulator in the pathogenesis of a murine model of asthma. Am J Respir Crit Care Med 2007;176:333-42.

(61) Boffa MB. TAFI and wound healing: closing a knowledge gap. J Thromb Haemost 2003;1:2075-7.

(62) Maret D, Boffa MB, Brien DF, Nesheim ME, Koschinsky ML. Role of mRNA transcript stability in modulation of expression of the gene encoding thrombin activable fibrinolysis inhibitor. J Thromb Haemost 2004;2:1969-79.

(63) Boffa MB, Hamill JD, Bastajian N, Dillon R, Nesheim ME, Koschinsky ML. A role for CCAAT/enhancer-binding protein in hepatic expression of thrombin-activable fibrinolysis inhibitor. J Biol Chem 2002;277:25329-36.

(64) Cagliani R, Fumagalli M, Riva S, Pozzoli U, Fracassetti M, Bresolin N, et al. Polymorphisms in the CPB2 gene are maintained by balancing selection and result in haplotype-preferential splicing of exon 7. Mol Biol Evol 2010;27:1945-54.

(65) Ballard C, Gauthier S, Corbett A, Brayne C, Aarsland D, Jones E. Alzheimer's disease. Lancet 2011;377:1019-31.

(66) Matsumoto A, Motozaki K, Seki T, Sasaki R, Kawabe T. Expression of human brain carboxypeptidase B, a possible cleaving enzyme for beta-amyloid precursor protein, in peripheral fluids. Neurosci Res 2001;39:313-7.

(67) Yano Y, Kitagawa N, Gabazza EC, Morioka K, Urakawa H, Tanaka T, et al. Increased plasma thrombin-activatable fibrinolysis inhibitor levels in normotensive type 2 diabetic patients with microalbuminuria. J Clin Endocrinol Metab 2003;88:736-41.

(68) Chudy P, Kotulicova D, Stasko J, Kubisz P. The relationship among TAFI, t-PA, PAI-1 and F1 + 2 in type 2 diabetic patients with normoalbuminuria and microalbuminuria. Blood Coagul Fibrinolysis 2011.

(69) Aubert H, Frere C, Aillaud MF, Morange PE, Juhan-Vague I, Alessi MC. Weak and non-independent association between plasma TAFI antigen levels and the insulin resistance syndrome. J Thromb Haemost 2003;1:791-7.

(70) Hori Y, Nakatani K, Morioka K, Katsuki A, Gabazza EC, Yano Y, et al. Insulin enhanced thrombin-activable fibrinolysis inhibitor expression through PI3 kinase/Akt pathway. Int J Mol Med 2005;15:265-8.

(71) Schadinger SL, Lin JH, Garand M, Boffa MB. Secretion and antifibrinolytic function of thrombin-activatable fibrinolysis inhibitor from human platelets. J Thromb Haemost 2010;8:2523-9.

(72) Fairchild KD, Singh IS, Carter HC, Hester L, Hasday JD. Hypothermia enhances phosphorylation of I{kappa}B kinase and prolongs nuclear localization of NF-{kappa}B in lipopolysaccharide-activated macrophages. Am J Physiol Cell Physiol 2005;289:C1114-C1121.

(73) Stoll G, Bendszus M. Inflammation and atherosclerosis: novel insights into plaque formation and destabilization. Stroke 2006;37:1923-32.

(74) Miura H, Liu Y, Gutterman DD. Human coronary arteriolar dilation to bradykinin depends on membrane hyperpolarization: contribution of nitric oxide and Ca2+-activated K+ channels. Circulation 1999;99:3132-8.

(75) Owens GK, Kumar MS, Wamhoff BR. Molecular regulation of vascular smooth muscle cell differentiation in development and disease. Physiol Rev 2004;84:767-801.

(76) Lin JH, Garand M, Zagorac B, Schadinger SL, Scipione C, Koschinsky ML, et al. Identification of human thrombin-activatable fibrinolysis inhibitor in vascular and inflammatory cells. Thromb Haemost 2011;105:999-1009.

(77) Mao SS, Cooper CM, Wood T, Shafer JA, Gardell SJ. Characterization of plasmin-mediated activation of plasma procarboxypeptidase B. Modulation by glycosaminoglycans. J Biol Chem 1999;274:35046-52.

(78) Wang W, Boffa MB, Bajzar L, Walker JB, Nesheim ME. A study of the mechanism of inhibition of fibrinolysis by activated thrombin-activable fibrinolysis inhibitor. J Biol Chem 1998;273:27176-81.

(79) Hendriks D, Scharpe S, van SM, Lommaert MP. Characterisation of a carboxypeptidase in human serum distinct from carboxypeptidase N. J Clin Chem Clin Biochem 1989;27:277-85.

(80) Schneider M, Nesheim M. A study of the protection of plasmin from antiplasmin inhibition within an intact fibrin clot during the course of clot lysis. J Biol Chem 2004;279:13333-9.

(81) Schneider M, Brufatto N, Neill E, Nesheim M. Activated thrombin-activatable fibrinolysis inhibitor reduces the ability of high molecular weight fibrin degradation products to protect plasmin from antiplasmin. J Biol Chem 2004;279:13340-5.

(82) Meltzer ME, Lisman T, DE Groot PG, Meijers JC, le CS, Doggen CJ, et al. Venous thrombosis risk associated with plasma hypofibrinolysis is explained by elevated plasma levels of TAFI and PAI-1. Blood 2010;116:113-21.

(83) Rooth E, Wallen H, Antovic A, von AM, Kaponides G, Wahlgren N, et al. Thrombin activatable fibrinolysis inhibitor and its relationship to fibrinolysis and inflammation during the acute and convalescent phase of ischemic stroke. Blood Coagul Fibrinolysis 2007;18:365-70.

(84) Ladenvall C, Gils A, Jood K, Blomstrand C, Declerck PJ, Jern C. Thrombin activatable fibrinolysis inhibitor activation peptide shows association with all major subtypes of ischemic stroke and with TAFI gene variation. Arterioscler Thromb Vasc Biol 2007;27:955-62.

(85) de Bruijne EL, Gils A, Guimaraes AH, Dippel DW, Deckers JW, van den Meiracker AH, et al. The role of thrombin activatable fibrinolysis inhibitor in arterial thrombosis at a young age: the ATTAC study. J Thromb Haemost 2009;7:919-27.

(86) Tregouet DA, Schnabel R, Alessi MC, Godefroy T, Declerck PJ, Nicaud V, et al. Activated thrombin activatable fibrinolysis inhibitor levels are associated with the risk of cardiovascular death in patients with coronary artery disease: the AtheroGene study. J Thromb Haemost 2009;7:49-57.

(87) Hendriks D, Wang W, van SM, Scharpe S. Human serum carboxypeptidase U: a new kininase? Agents Actions Suppl 1992;38 (Pt 1):407-13.

(88) Van Thiel DH, George M, Fareed J. Low levels of thrombin activatable fibrinolysis inhibitor (TAFI) in patients with chronic liver disease. Thromb Haemost 2001;85:667-70.

(89) Knowles BB, Howe CC, Aden DP. Human hepatocellular carcinoma cell lines secrete the major plasma proteins and hepatitis B surface antigen. Science 1980;209:497-9.

(90) Ogura M, Morishima Y, Ohno R, Kato Y, Hirabayashi N, Nagura H, et al. Establishment of a novel human megakaryoblastic leukemia cell line, MEG-01, with positive Philadelphia chromosome. Blood 1985;66:1384-92.

(91) Greenberg SM, Rosenthal DS, Greeley TA, Tantravahi R, Handin RI. Characterization of a new megakaryocytic cell line: the Dami cell. Blood 1988;72:1968-77.

(92) Tsuchiya S, Yamabe M, Yamaguchi Y, Kobayashi Y, Konno T, Tada K. Establishment and characterization of a human acute monocytic leukemia cell line (THP-1). Int J Cancer 1980;26:171-6.

(93) Zhao SP, Deng P, Huang HG, Xu ZM, Dai HY, Hong SC, et al. Expression of COX-2 mRNA in peripheral blood monocytes from patients with acute myocardial infarction and its significance. Clin Chem 2005;51:2170-3.

(94) Gils A, Alessi MC, Brouwers E, Peeters M, Marx P, Leurs J, et al. Development of a genotype 325-specific proCPU/TAFI ELISA. Arterioscler Thromb Vasc Biol 2003;23:1122-7.

(95) Isakari Y, Sogo S, Ishida T, Kawakami T, Ono T, Taki T, et al. Gene expression analysis during platelet-like particle production in phorbol myristate acetate-treated MEG-01 cells. Biol Pharm Bull 2009;32:354-8.

(96) Perez A, Thuillard JL, Bentzen CL, Niesor EJ. Expression of nuclear receptors and apo E secretion during the differentiation of monocytic THP-1 cells into macrophages. Cell Biol Toxicol 2003;19:95-105.

(97) Fugman DA, Witte DP, Jones CL, Aronow BJ, Lieberman MA. In vitro establishment and characterization of a human megakaryoblastic cell line. Blood 1990;75:1252-61.

(98) Briquet-Laugier V, El GN, Nurden P, Lavenu-Bombled C, Dubart-Kupperschmitt A, Nurden A, et al. Thrombopoietin-induced Dami cells as a model for alpha-granule biogenesis. Platelets 2004;15:341-4.

(99) Auwerx J. The human leukemia cell line, THP-1: a multifacetted model for the study of monocyte-macrophage differentiation. Experientia 1991;47:22-31.

(100) Swaisgood CM, Schmitt D, Eaton D, Plow EF. In vivo regulation of plasminogen function by plasma carboxypeptidase B. J Clin Invest 2002;110:1275-82.

(101) Emonts M, de Bruijne EL, Guimaraes AH, Declerck PJ, Leebeek FW, de Maat MP, et al. Thrombin-activatable fibrinolysis inhibitor is associated with severity and outcome of severe meningococcal infection in children. J Thromb Haemost 2008;6:268-76.

(102) Bengtson SH, Sanden C, Morgelin M, Marx PF, Olin AI, Leeb-Lundberg LM, et al. Activation of TAFI on the surface of Streptococcus pyogenes evokes inflammatory reactions by modulating the kallikrein/kinin system. J Innate Immun 2008;1:18-28.

(103) Wohner N. Role of cellular elements in thrombus formation and dissolution. Cardiovasc Hematol Agents Med Chem 2008;6:224-8.

(104) Weisel JW. Structure of fibrin: impact on clot stability. J Thromb Haemost 2007;5 Suppl 1:116-24.

(105) Kolev K, Longstaff C, Machovich R. Fibrinolysis at the fluid-solid interface of thrombi. Curr Med Chem Cardiovasc Hematol Agents 2005;3:341-55.

(106) Shantsila E, Lip GY. The role of monocytes in thrombotic disorders. Insights from tissue factor, monocyte-platelet aggregates and novel mechanisms. Thromb Haemost 2009;102:916-24.

(107) Fabriek BO, Polfliet MM, Vloet RP, van der Schors RC, Ligtenberg AJ, Weaver LK, et al. The macrophage CD163 surface glycoprotein is an erythroblast adhesion receptor. Blood 2007;109:5223-9.

(108) Murphy GJ, Leavitt AD. A model for studying megakaryocyte development and biology. Proc Natl Acad Sci U S A 1999;96:3065-70.

(109) Wang J, Yi Z, Wang S, Li Z. The effect of decitabine on megakaryocyte maturation and platelet release. Thromb Haemost 2011;106:337-43.

(110) Mutch NJ, Moore NR, Wang E, Booth NA. Thrombus lysis by uPA, scuPA and tPA is regulated by plasma TAFI. J Thromb Haemost 2003;1:2000-7.

(111) Cassel DL, Subudhi SK, Surrey S, McKenzie SE. GATA and NF-Y participate in transcriptional regulation of FcgammaRIIA in megakaryocytic cells. Blood Cells Mol Dis 2000;26:587-97.

(112) Marziali G, Perrotti E, Ilari R, Coccia EM, Mantovani R, Testa U, et al. The activity of the CCAAT-box binding factor NF-Y is modulated through the regulated expression of its A subunit during monocyte to macrophage differentiation: regulation of tissue-specific genes through a ubiquitous transcription factor. Blood 1999;93:519-26.

(113) Koenig RJ. Thyroid hormone receptor coactivators and corepressors. Thyroid 1998;8:703-13.

(114) Belakavadi M, Dell J, Grover GJ, Fondell JD. Thyroid hormone suppression of beta-amyloid precursor protein gene expression in the brain involves multiple epigenetic regulatory events. Mol Cell Endocrinol 2011;339:72-80.

(115) Semeraro F, Ammollo CT, Semeraro N, Colucci M. Tissue factor-expressing monocytes inhibit fibrinolysis through a TAFI-mediated mechanism, and make clots resistant to heparins. Haematologica 2009;94:819-26.

(116) Pan Q, Shai O, Lee LJ, Frey BJ, Blencowe BJ. Deep surveying of alternative splicing complexity in the human transcriptome by high-throughput sequencing. Nat Genet 2008;40:1413-5.

(117) Sorek R, Shamir R, Ast G. How prevalent is functional alternative splicing in the human genome? Trends Genet 2004;20:68-71.

(118) Melamud E, Moult J. Stochastic noise in splicing machinery. Nucleic Acids Res 2009;37:4873-86.

(119) Asselta R, Rimoldi V, Guella I, Solda G, De CR, Peyvandi F, et al. Molecular characterization of in-frame and out-of-frame alternative splicings in coagulation factor XI pre-mRNA. Blood 2010;115:2065-72.

(120) Denis MM, Tolley ND, Bunting M, Schwertz H, Jiang H, Lindemann S, et al. Escaping the nuclear confines: signal-dependent pre-mRNA splicing in anucleate platelets. Cell 2005;122:379-91.

(121) Carter MS, Doskow J, Morris P, Li S, Nhim RP, Sandstedt S, et al. A regulatory mechanism that detects premature nonsense codons in T-cell receptor transcripts in vivo is reversed by protein synthesis inhibitors in vitro. J Biol Chem 1995;270:28995-9003.

(122) Pan Q, Saltzman AL, Kim YK, Misquitta C, Shai O, Maquat LE, et al. Quantitative microarray profiling provides evidence against widespread coupling of alternative splicing with nonsense-mediated mRNA decay to control gene expression. Genes Dev 2006;20:153-8.

(123) Schwertz H, Tolley ND, Foulks JM, Denis MM, Risenmay BW, Buerke M, et al. Signal-dependent splicing of tissue factor pre-mRNA modulates the thrombogenicity of human platelets. J Exp Med 2006;203:2433-40.

(124) Drummond DA, Bloom JD, Adami C, Wilke CO, Arnold FH. Why highly expressed proteins evolve slowly. Proc Natl Acad Sci U S A 2005;102:14338-43.

(125) Matsumoto A, Itoh K, Seki T, Motozaki K, Matsuyama S. Human brain carboxypeptidase B, which cleaves beta-amyloid peptides in vitro, is expressed in the endoplasmic reticulum of neurons. Eur J Neurosci 2001;13:1653-7.

(126) Bouchard BA, Williams JL, Meisler NT, Long MW, Tracy PB. Endocytosis of plasma-derived factor V by megakaryocytes occurs via a clathrin-dependent, specific membrane binding event. J Thromb Haemost 2005;3:541-51.

(127) Hoffman M. One more way that mice and men are different. J Thromb Haemost 2005;3:448-9.

(128) Lloyd EE, Gaubatz JW, Burns AR, Pownall HJ. Sustained elevations in NEFA induce cyclooxygenase-2 activity and potentiate THP-1 macrophage foam cell formation. Atherosclerosis 2007;192:49-55.

(129) McLaren JE, Michael DR, Salter RC, Ashlin TG, Calder CJ, Miller AM, et al. IL-33 reduces macrophage foam cell formation. J Immunol 2010;185:1222-9.

(130) Gygi SP, Rochon Y, Franza BR, Aebersold R. Correlation between protein and mRNA abundance in yeast. Mol Cell Biol 1999;19:1720-30.

(131) Pascal LE, True LD, Campbell DS, Deutsch EW, Risk M, Coleman IM, et al. Correlation of mRNA and protein levels: cell type-specific gene expression of cluster designation antigens in the prostate. BMC Genomics 2008;9:246.

(132) Renckens R, Roelofs JJ, ter Horst SA, van ', V, Havik SR, Florquin S, et al. Absence of thrombin-activatable fibrinolysis inhibitor protects against sepsis-induced liver injury in mice. J Immunol 2005;175:6764-71.

(133) Phillips DR, Charo IF, Parise LV, Fitzgerald LA. The platelet membrane glycoprotein IIb-IIIa complex. Blood 1988;71:831-43.

(134) Flaumenhaft R, Dilks JR, Richardson J, Alden E, Patel-Hett SR, Battinelli E, et al. Megakaryocyte-derived microparticles: direct visualization and distinction from platelet-derived microparticles. Blood 2009;113:1112-21.

(135) Italiano JE, Jr., Mairuhu AT, Flaumenhaft R. Clinical relevance of microparticles from platelets and megakaryocytes. Curr Opin Hematol 2010;17:578-84.

(136) Wu KJ, Wilson DR, Shih C, Darlington GJ. The transcription factor HNF1 acts with C/EBP alpha to synergistically activate the human albumin promoter through a novel domain. J Biol Chem 1994;269:1177-82.

(137) Morosetti R, Park DJ, Chumakov AM, Grillier I, Shiohara M, Gombart AF, et al. A novel, myeloid transcription factor, C/EBP epsilon, is upregulated during granulocytic, but not monocytic, differentiation. Blood 1997;90:2591-600.

(138) Shivdasani RA. Molecular and transcriptional regulation of megakaryocyte differentiation. Stem Cells 2001;19:397-407.

(139) Wang X, Crispino JD, Letting DL, Nakazawa M, Poncz M, Blobel GA. Control of megakaryocyte-specific gene expression by GATA-1 and FOG-1: role of Ets transcription factors. EMBO J 2002;21:5225-34.

(140) Iwasaki H, Mizuno S, Wells RA, Cantor AB, Watanabe S, Akashi K. GATA-1 converts lymphoid and myelomonocytic progenitors into the megakaryocyte/erythrocyte lineages. Immunity 2003;19:451-62.

(141) Cassel DL, Subudhi SK, Surrey S, McKenzie SE. GATA and NF-Y participate in transcriptional regulation of FcgammaRIIA in megakaryocytic cells. Blood Cells Mol Dis 2000;26:587-97.

(142) Peng Y, Jahroudi N. The NFY transcription factor functions as a repressor and activator of the von Willebrand factor promoter. Blood 2002;99:2408-17.

(143) Wang D, D'Costa J, Civin CI, Friedman AD. C/EBPalpha directs monocytic commitment of primary myeloid progenitors. Blood 2006;108:1223-9.

(144) Feng R, Desbordes SC, Xie H, Tillo ES, Pixley F, Stanley ER, et al. PU.1 and C/EBPalpha/beta convert fibroblasts into macrophage-like cells. Proc Natl Acad Sci U S A 2008;105:6057-62.

(145) Valledor AF, Borras FE, Cullell-Young M, Celada A. Transcription factors that regulate monocyte/macrophage differentiation. J Leukoc Biol 1998;63:405-17.

(146) Xu Y, Zhou YL, Luo W, Zhu QS, Levy D, MacDougald OA, et al. NF-Y and CCAAT/enhancer-binding protein alpha synergistically activate the mouse amelogenin gene. J Biol Chem 2006;281:16090-8.

(147) Park SK, Oh SY, Lee MY, Yoon S, Kim KS, Kim JW. CCAAT/enhancer binding protein and nuclear factor-Y regulate adiponectin gene expression in adipose tissue. Diabetes 2004;53:2757-66.

(148) Henry M, Aubert H, Morange PE, Nanni I, Alessi MC, Tiret L, et al. Identification of polymorphisms in the promoter and the 3' region of the TAFI gene: evidence that plasma TAFI antigen levels are strongly genetically controlled. Blood 2001;97:2053-8.

(149) Bogdanov VY, Balasubramanian V, Hathcock J, Vele O, Lieb M, Nemerson Y. Alternatively spliced human tissue factor: a circulating, soluble, thrombogenic protein. Nat Med 2003;9:458-62.